Gypsic Soils on the Kane Alluvial Fans, Big Horn County, Wyoming

U.S. GEOLOGICAL SURVEY BULLETIN 1590–C

Gypsic Soils on the Kane Alluvial Fans, Big Horn County, Wyoming

By MARITH C. REHEIS

U.S. GEOLOGICAL SURVEY BULLETIN 1590–C

SOIL CHRONOSEQUENCES IN THE WESTERN UNITED STATES

DEPARTMENT OF THE INTERIOR
DONALD PAUL HODEL, Secretary

U.S. GEOLOGICAL SURVEY
Dallas L. Peck, Director

UNITED STATES GOVERNMENT PRINTING OFFICE, WASHINGTON : 1987

For sale by the
Books and Open-File Reports Section
U.S. Geological Survey
Federal Center, Box 25425
Denver, CO 80225

Library of Congress Cataloging-in-Publication Data

Reheis, Marith C.
Gypsic soils on the Kane alluvial fans, Big Horn County, Wyoming.

(Soil chronosequences in the western United States)
(U.S. Geological Survey Bulletin 1590-C)
Bibliography
Supt. of Docs. No.: I 19.3:1590-C
1. Soils—Wyoming—Big Horn County—Gypsum content. 2. Soils—Gypsum content. 3. Soil formation—Wyoming—Big Horn County. 4. Soil chronosequences—Wyoming—Big Horn County. 5. Geology—Wyoming—Big Horn County. I. Title. II. Title: Kane alluvial fans, Big Horn County, Wyoming. III. Series. IV. Series: U.S. Geological Survey Bulletin 1590-C.
QE75.B9 No. 1590-C 557.3 86-600172
[S599.W8] [631.4'7'78733]

FOREWORD

This series of reports, "Soil Chronosequences in the Western United States," attempts to integrate studies of different earth-science disciplines, including pedology, geomorphology, stratigraphy, and Quaternary geology in general. Each discipline provides information important to the others. From geomorphic relations we can determine the relative ages of deposits and soils; from stratigraphy we can place age constraints on the soils. Field investigations and mineralogic and sedimentologic studies provide information on the nature and types of deposits in which soils form. As a result of our work, we have estimated rates of soil formation, inferred processes of soil formation from trends in soil development with increasing age, and obtained information on the types of weathering that occur in various areas. In return, soil development and soil genesis have provided data on the age of landforms, the timing and duration of sedimentation, and, in some cases, the history of climatic fluctuations.

Between 1978 and 1983, a coordinated and systematic study was conducted on soil development in different types of geologic deposits in the Western United States. The goals of this project, led by the late D.E. Marchand and subsequently by M.N. Machette, were to learn whether rates of chemical, physical, and mineralogic transformations could be determined from soil chronosequences; how these rates vary in different mineralogic and climatic environments; and how accurately soils can be used for such problems as estimating the ages of deposits, periods of landscape stability, and timing of fault movements. This series of reports presents data from several soil chronosequences of that project.

More than 100 analyses on more than 1,000 samples were performed on soils collected in the Western United States. Some results have appeared in various books, journals, and maps (for example, Harden and Marchand, 1977, 1980; Burke and Birkeland, 1979; Dethier and Bethel, 1981; Marchand and Allwardt, 1981; Meixner and Singer, 1981; Busacca, 1982; Harden, 1982a, b; Harden and Taylor, 1983; Machette, 1983; Machette and Steven, 1983; Busacca and others, 1984; Machette and others, 1984; Reheis, 1984). In the reports in this series, the basic field information, geologic background, and analytical data are presented for each chronosequence, as well as some results additional to the previous publications.

One of the most significant aspects of these chronosequence studies is that in every study area, many soil parameters change systematically over time, or with the age of deposits. As Deming (1943) emphasized, it is this recurrence of correlation in such different conditions that is most significant to geologic and pedologic studies. In relatively moist areas, such as coastal and central California, such soil properties as percent clay or reddening of soil colors change most systematically over time. In more arid regions, such as in the Bighorn Basin of Wyoming, calcium carbonate and gypsum contents best reflect the relative ages of the deposits. A few parameters—for example, elemental composition of sands or clays—appear to be comparable between areas so diverse in climatic setting.

Numeric age control has enabled us to estimate rates of soil development. In some places, we have been able to compare rates between different areas. For example, in central California, rates of clay accumulation were found to be most rapid during the initial stages of soil development; these rates declined with increasing age. The straightest lines for regression were on a log-log scale. In coastal California, rates of clay accumulation appeared to be much higher than in central California. This difference in rates could be due to parent material (the coastal soils that we studied were formed on reworked shale and sandstone, whereas central California soils were developed in granitic alluvium), and (or) the differences in rates could be due to eolian additions of clay. In the Bighorn Basin of Wyoming, rates of clay accumulation, as well as most other soil properties, increased linearly over time, with no apparent decrease in initial rates.

The data we present here suggest many opportunities for further interpretation. For example, we may learn how climate, vegetation, and mineralogy affect the rates of clay formation or organic-matter accumulation. In some study areas, we present data for rare-earth elements, which could be used to examine how each element reacts in different weathering environments. These examples are only a fraction of the possible future studies that could be conducted on the data presented here.

J.W. Harden
Editor

CONTENTS

FIGURES

TABLES

SUPPLEMENTARY TABLES

Gypsic Soils on the Kane Alluvial Fans, Big Horn County, Wyoming

By Marith C. Reheis

ABSTRACT

Soils on the Kane alluvial fans, in the northeastern Bighorn Basin near Lovell, Wyo., accumulate gypsum ($CaSO_4 \cdot 2H_2O$) over time. This gypsum is added chiefly as eolian dust derived from both local and long-range sources. The arid but cool climate has permitted gypsum to accumulate continuously for the past 600 ka (thousands of years). The linear increase in pedogenic gypsum with time suggests that effective moisture in the Kane area has never increased substantially in the past 600 ka. The dates when the fan surfaces stabilized and, thus, the times when the soils began to form are estimated by various dating methods, including tephrochronology, paleontology, and stream-incision rates.

The gypsum content influences the development of other soil properties. At the Kane fans, pedogenic or secondary gypsum has accumulated at annual rates of 1.1 X 10^{-6} to 120 X 10^{-6} g/cm^2; modern aerosolic gypsum measured in dust traps is being added at annual rates of 26 X 10^{-6} to 60 X 10^{-6} g/cm^2. Secondary calcium carbonate ($CaCO_3$) does not increase in soils older than 100 ka, despite the availability of $CaCO_3$ in eolian dust and in the parent material, probably because gypsum suppresses the solubility of $CaCO_3$. Total texture (a measure of pedogenic silt and clay) and pH increase over time in soils younger than 300 ka, but decrease or show irregular trends in older soils because of large accumulations of pedogenic gypsum. In contrast to soils in most environments, rubification (reddening and brightening of soil colors) in the study area increases with depth. Gypsum also causes physical disintegration of gravel clasts in the soils by crystallizing in cracks and along grain boundaries.

Depth to gypsum in soils on the Kane fans is controlled by climate, soil age, and the hygroscopic properties of gypsum. The youngest soil containing visible gypsum and those soils older than 100 ka have their maximum gypsum accumulations at the average depth (2.6 cm) to which the modern precipitation moistens the soil. The 100-ka-old soils have their maximum gypsum accumulations at a greater depth (more than 5.5 cm). This disparity between gypsum depths probably reflects both differences in climate and the near-surface accumulation of gypsum during interglacial periods. Buildup of pedogenic gypsum at shallower depth during interglacials may have hindered subsequent leaching and reprecipitation of gypsum at greater depth during glacial periods of increased soil moisture, because the gypsum can hygroscopically hold the increased moisture. Thus, the near-surface accumulations of gypsum in soils older than 100 ka mainly reflect interglacial wetting depths.

INTRODUCTION

Studies of soils formed on the Kane alluvial fans[1], on the northeastern margin of the Bighorn Basin, yield valuable information on the processes and rates of soil development in a cool, arid climate. This study assesses the effects of time on soil development in a chronologic sequence of soils. To ascribe the characteristics of soils to their ages, it is necessary to demonstrate conclusively that the other four important soil-forming factors—parent material, topography, vegetation, and modern climate, as defined by Jenny (1941)—are constant or have little effect on these characteristics.

Many studies of aridic soils in the southwestern United States (for example, Gile and others, 1966; Gardner, 1972; Bachman and Machette, 1977; Shlemon, 1978; Machette, 1985) have demonstrated that the dominant pedogenic process in that region is the accumulation of calcium carbonate ($CaCO_3$), most of which is derived from dust and rainfall. In contrast, gypsum ($CaSO_4 \cdot 2H_2O$) accumulates in soils in the arid environment of the Kane fans, and secondary $CaCO_3$ is negligible. Accumulation of soluble salts characterizes hot desert soils (Watson, 1979) and polar desert soils (Bockheim, 1980a), but gypsic soils have been little studied in the United States (Nettleton and others, 1982). There are few studies of soils in arid parts of the intermontane basins of the northern Rocky Mountains (for example, Reider and others, 1974, in the Laramie Basin, Wyo.). Information on the soils formed on the Kane fan may help to link soil-forming processes in warm deserts and polar deserts.

Interpretations in this paper rely chiefly on field data and gypsum analyses. Some particle-size and chemical data are used to discuss the parent material. Reheis (1984) discussed other laboratory data, including particle size and chemical and mineralogic analyses.

Acknowledgments.—My greatest appreciation goes to P. W. Birkeland, who critically read most of this manuscript, for discussion and thoughtful evaluation of many ideas. K. L. Pierce, D. W. Moore, and L. D. McFadden also contributed valuable perspectives. The late D. E. Marchand coerced me into studying gypsic soils. Able field assistance was provided by Kim Jones.

[1]The Kane alluvial fans are informally named for an abandoned railway station across the Bighorn River, which also gives its name to the Kane, Wyo., 7 1/2-minute quadrangle within which the fans lie.

GEOMORPHIC AND CLIMATIC SETTING

Geomorphic Setting

The Kane fans are alluvial fan deposits of Cottonwood Creek, an ephemeral stream draining a 45-km^2 catchment basin on the west front of the Bighorn Mountains. The fans are sandwiched between the mountain front and the confluence of the Bighorn and Shoshone Rivers (figs. 1, 2). Lovell, the nearest town, is situated on the Shoshone River about 20 km upstream from the fans.

The relation of fan deposition to fluvial-terrace deposition in the study area must be understood in order to constrain the ages of the fan surfaces. Only two dates have been obtained from materials within the fan deposits. However, the fan and underlying Bighorn River deposits are related to regional glacial-interglacial climatic fluctuations that provide a chronologic framework for these deposits. The gradient and depositional regime of the unglaciated Cottonwood Creek has been controlled by the positions of the Bighorn and Shoshone Rivers. The Bighorn River is the master stream in the Bighorn basin. It drains the glaciated Wind River Range southwest of the study area, and is fed by streams draining the west flank of the Bighorn Mountains and glaciated areas of the Absaroka Range. The Shoshone River heads in the Absaroka Mountains to the west (fig. 1).

The formation of the Shoshone River terraces has long been argued. Mackin (1937) believed that the terraces were formed by lateral planation of the Shoshone River and were not of glaciofluvial origin. On the Shoshone River, John Moss (Moss and Bonini, 1961; Moss and Whitney, 1971; Moss, 1974) later demonstrated that deposits of the lowest major terrace (Cody terrace of Mackin, 1937), and possibly the next higher terrace (Powell terrace of Mackin, 1937), can be traced upvalley into moraines and constitute fill terraces near the front of the Absaroka Range. Downstream, these are strath terraces comprised of about 5 m of gravel overlying bedrock surfaces. Moss (1974) believed that the spreading of gravel into the basin, whether deposited as fill or as strath terraces, accompanied or slightly postdated a maximum glacial advance in the Absaroka Range, and that subsequent incision was associated with deglaciation and interglacial conditions. Palmquist (1983) suggested, however, that incision episodes of the Bighorn River are out of phase with episodes on its tributaries; for example, the Bighorn may incise during glaciations even as the Shoshone River aggrades. Some terraces may have formed by capture. Recently, Ritter and Kaufman (1983) demonstrated that the Powell terrace as previously mapped below the town of Powell is younger than the Powell terrace above the town, and was formed by capture.

The regime of the Bighorn River is probably controlled by climate. Near the headwaters area of the Bighorn (Wind) River, an outwash terrace sequence suggests eight major glacial advances (Richmond, 1976).

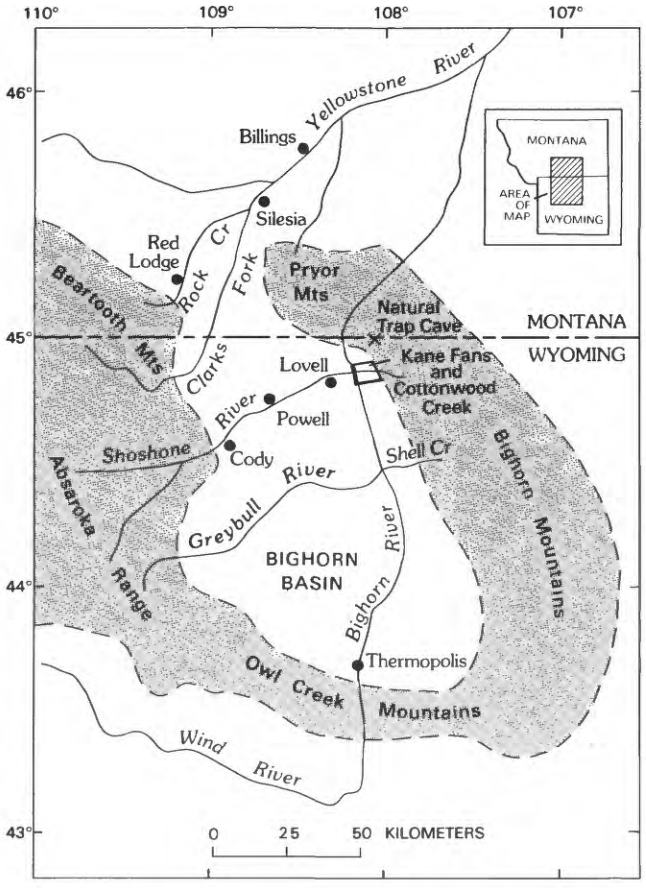

Figure 1. Location of study area in the northern Bighorn Basin (modified from Mackin, 1937).

Modern Climate and Vegetation

Climate is one of the most important factors that govern soil development. Weather data from Lovell, Wyo. (National Climatic Center, 1976), and data from soil temperature probes planted at the study site, represent the present climatic regime near the Kane fans (table 1). Although the fans are about 20 km from Lovell, the climate of the study area is probably similar to that of Lovell because the vegetation is similar. At the Kane fans, sagebrush, pricklypear cactus, and bunchgrass are the dominant species. Scrub juniper occurs on the mountain footslopes above the fans, and cottonwoods grow along the Bighorn and Shoshone Rivers.

Judging from the vegetation, all soil sites have about the same climate. Rainfall generally increases with elevation (orographic effect), but the distribution of deposits and limited land access did not permit all sample sites to be at the same elevation. Soil sites on the younger fans (fig. 2) are lower and farther from the mountain front, and these sites, therefore, may be slightly drier than those on the older, higher fans (lowest soil site is B-5 on fan 2 at 1,117 m; highest site is B-19 on fan 7 at 1,275 m).

The Lovell area (table 1) has an aridic soil-moisture regime and a mesic soil-temperature

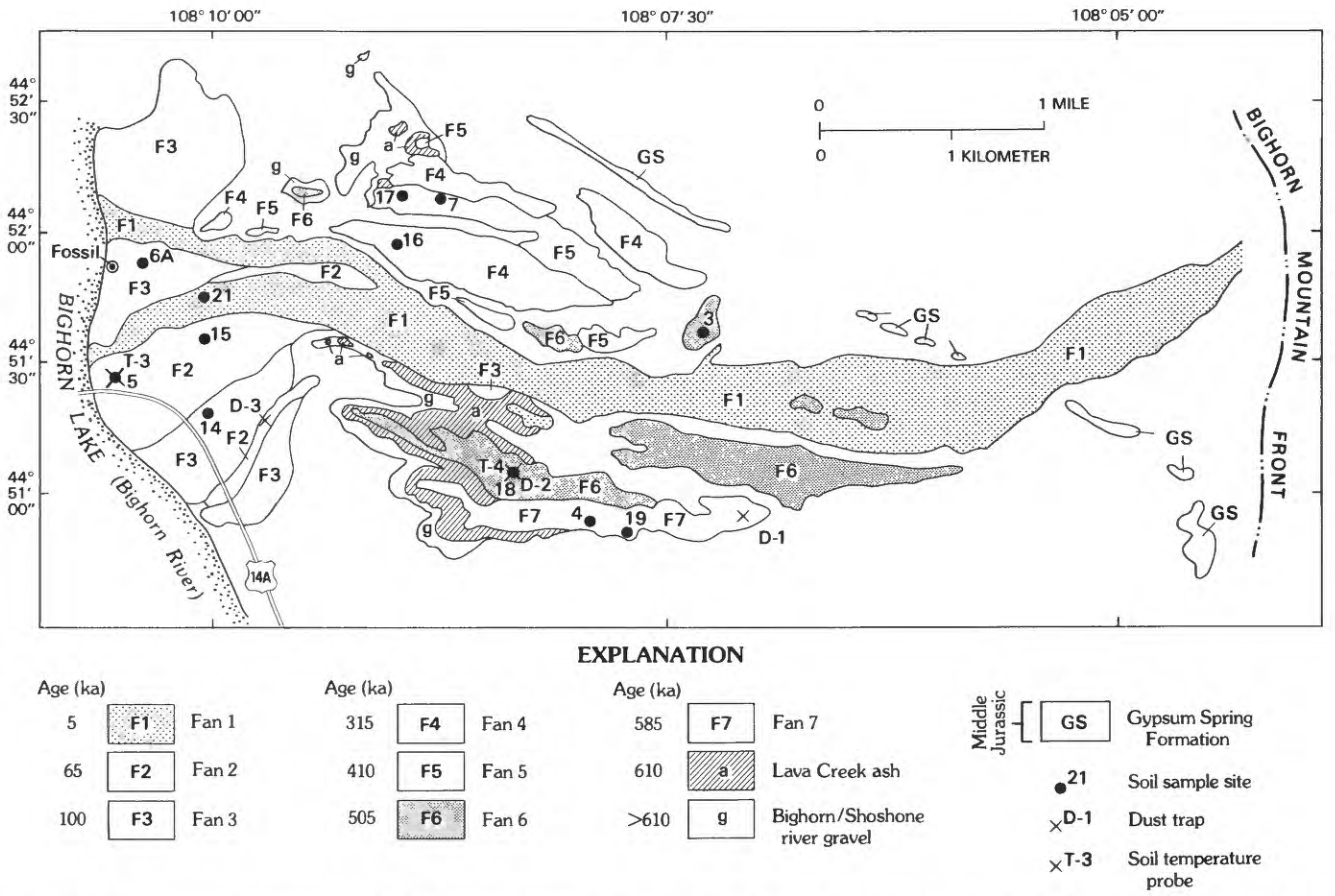

Figure 2. Generalized map of the Kane alluvial fan gravels of Cottonwood Creek and fluvial deposits of the Bighorn and Shoshone Rivers. Outcrop of gypsum beds of the Middle Jurassic Gypsum Spring Formation is also shown. Map unit F1 includes the modern channel and flood plain of Cottonwood Creek. Fluvial gravels under fan 3 not shown because they are exposed in vertical cliffs. Soil site numbers correspond to those preceded by "B-" in text.

regime. Soil temperature was estimated from the mean annual temperature (Soil Survey Staff, 1975, p. 61) and also measured by soil temperature probes. The estimated soil temperature of 8.2° C is near the boundary between the mesic and frigid temperature regimes. The soil temperature probes, probably affected by local conditions,[2] recorded temperatures about 4° C warmer than the estimated soil temperature (Trembour and others, 1986).

Near Lovell, much of the moisture falls in late spring and early summer and is ineffective in weathering or solution of salts, because evapotranspiration rates are high at these times. Using Arkley's (1963) leaching index for Lovell, only 26 mm of water is available to wet the soil from November to March (fig. 3). Thus, in the average year, only the surface of the soil is ever wet; insufficient water percolates through the soils to remove soluble salts and other weathering products.

[2]Temperatures measured by soil - temperature probes can be affected by local conditions, such as the yearly range of temperatures, or air pockets left along the probe when refilling the probe hole.

Paleoclimate

Characterization of the modern climate adequately describes the general climate of the Holocene but fails to describe the climate during glacial periods. More moist glacial periods probably had important effects on soil development at the Kane fans, so it is important to discuss the available evidence concerning paleoclimate.

Sediments at Natural Trap Cave, 10 km north of and 350 m higher than the Kane fans (fig. 1), contain opal phytoliths of tall prairie grass (Gilbert and others, 1980). The modern vegetation around Natural Trap Cave consists of short grasses and cactus; tall prairie grass commonly occurs at elevations 300 m higher than the cave. The tall-grass phytoliths span the period from 110 thousand to 12 thousand years before present (ka) and indicate increased moisture during that time. Tundra phytoliths near the top of the sedimentary section suggest an episode of cold dry climate from 17 to 14 ka. Environmental reconstructions based on faunas from several Wisconsin-aged sites in Wyoming (summarized in Walker, 1982) and the presence of a musk-ox vertebra (discussed below) in the Kane fans indicate that a cold, dry arctic steppe/savannah biome existed on the basin floor.

Table 1. Climatic data for Lovell, Wyo., for 1951 to 1974, and postulated climatic parameters for the last glaciation

	Modern	Glacial
Mean annual precipitation	16.5 cm	16.5 cm
Mean annual air temperature	7.2°C	-2.8°C
Mean July air temperature	22.1°C	9.1°C
Mean January air temperature	-7.9°C	-12.9°C
Mean annual soil temperature from probes at Kane fans, 1980-82:		
at 0.5 m depth	12.1°C	
at 1.0 m depth	12.6°C	
Mean annual soil temperature, Soil Survey Staff calculation:	8.2°C	
Leaching index	2.6 cm	8.2 cm

This climatic reconstruction is supported by other work. Recent studies of relict ice and sand wedges in Quaternary deposits in the intermontane basins of Wyoming (Mears, 1981) indicate that the climate during the last glaciation was dry and cold; mean annual temperatures may have been 10-13° C colder than at present. This estimate of cooler temperature is compatible with glacial to present snowline changes if the effect of altitudinal gradients of precipitation is considered (Pierce, 1982). Gates's (1976) model of global ice-age climate suggests that mean July temperature decreased by 13°C near the Bighorn Basin, and that precipitable moisture decreased 35 percent in the northern hemisphere.

A plausible reconstruction of climate during the last glaciation can be made for the Lovell area, assuming that (1) the mean annual temperature was 10° C lower than present, (2) the mean July temperature was 13° C lower, and (3) the mean January temperature was 5° C lower (table 1). No evidence is available concerning glacial winter temperature, but some lowering probably occurred. For the reconstruction, temperatures for other months are adjusted to fit the postulated changes of mean annual, July, and January temperatures. No moisture decrease is postulated in this reconstruction, in order to avoid extrapolation of hypothetical moisture changes in the northern hemisphere (Gates, 1976) to the study area. Evapotranspiration is calculated from monthly temperature data using van Hylckama's (1959) method. Diagrams of soil-temperature and soil-moisture balance compare glacial with modern conditions (fig. 3).

In the climate reconstruction (table 1 and fig. 3), the glacial soil-moisture regime probably was aridic and the soil-temperature regime pergelic (modern pergelic regimes correspond to permafrost zones; terms defined in Soil Survey Staff, 1975). The estimated glacial leaching index (method of Arkley, 1963) increases to 8.2 cm from the modern level of 2.6 cm because evapotranspiration is lower. Some of the additional available moisture may not have been utilized in leaching because more precipitation would have fallen as snow. If snowfall from November to March did not contribute to soil moisture, the glacial leaching index was 5.3 cm. Gates's (1976) climatic model also suggests that the glacial leaching index was lower than 8.2 cm. The presence of a large stable high-pressure zone over the continental ice sheet 350 km northwest of the study area probably would have caused a year-round dominance of dry northerly air flow, whereas the present southerly air flow in spring and summer delivers moisture from the Gulf of Mexico.

GEOLOGIC SETTING AND CHRONOLOGY

Previous Work

Andrews and others (1947) were the first to map the Kane fans, but called them pediment surfaces. Birdseye (1980, 1983) described the alluvial fans of Five Springs Creek, 5 km south of the Kane fans, and has mapped the Kane fans as well (written commun., 1982). Palmquist (1978, 1983) used the Lava Creek ash bed (Izett and Wilcox, 1982) that underlies the Kane fan gravels to date terraces along the Bighorn River. Bedrock geology near the Kane fans was described by Darton (1906) and later by Rioux (1958) and Pierce (1978).

Source of Deposits

Bedrock units in the Cottonwood Creek drainage basin range in age from Cambrian to Cretaceous and include marine shale and sandstone, evaporites,

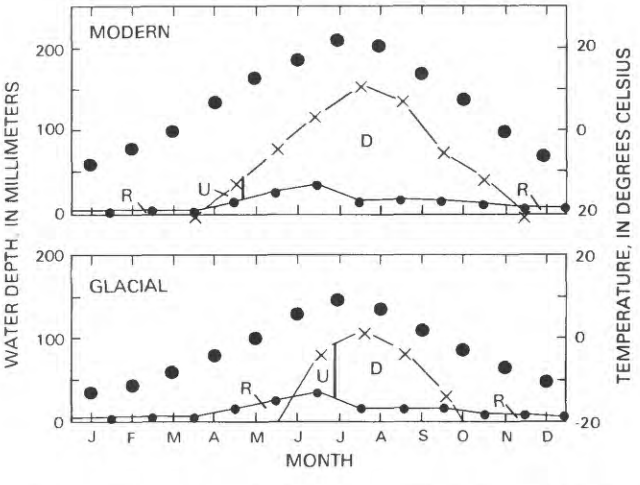

Figure 3. Modern (24-year record) and last-glacial climate and soil-water balance for Lovell, Wyo. Reconstruction of glacial temperature described in text. No surplus water available during either period. Large dots are air temperatures, small dots are precipitation, and X's are inferred evapotranspiration. Soil AWC (available water-holding capacity) of 110 mm is average for Kane fan soils; young soils have lower AWCs, older soils have higher AWCs. R denotes period of recharge of soil water when precipitation exceeds evapotranspiration; U denotes period of utilization of stored soil water when soil is dry in some part, because evapotranspiration exceeds precipitation; D denotes deficit period when soil-moisture control section is dry.

redbeds, limestone, and dolomite (Pierce, 1978). The Kane fan deposits overlie Cretaceous sandstone and shale but contain little debris from these formations. Continental redbed and evaporite deposits of Mesozoic age constitute 40 percent of the local sedimentary section. The Middle Jurassic Gypsum Spring Formation has up to 50 percent by volume of lenticular gypsum beds and crops out just upslope from the fan deposits (fig. 2). Little or no gypsum was deposited in the fans, however (table 2 and supplementary table 3). Paleozoic limestone and dolomite account for another 40 percent of the section. Because these latter rocks are resistant to weathering and mechanical abrasion, they constitute the majority of the fan material.

A second component of the fan deposits is andesitic sand and gravel, which was deposited by the Bighorn and (or) Shoshone Rivers and was incorporated into the fans by reworking.

Parent Material—Nature and Variability

The parent material is another important factor in soil development. If the parent materials of the soils on the Kane fans are different, then differences in the soils cannot be ascribed to either time or climate. Thus, it is critical to compare stable chemical and physical properties of the various alluvia.

The parent material among all soils examined on the Kane fans is compositionally similar (table 2). By visual estimate, the gravel consists of about 90 percent limestone and dolomite, 5 percent andesite, and 5 percent sandstone, siltstone, and chert. Carbonates usually compose about 50 percent of the unweathered <2-mm fraction (supplementary table 3). Soils on fan 5 deposits have slightly greater proportions of igneous detritus, because they contain more reworked river gravel and volcanic ash.

Fresh fan deposits in the Kane area typically have 80 percent gravel, but the upper 20-75 cm of the soils is less gravelly. Deposits in the youngest fan are very gravelly up to 5 cm below the surface. The thickness of the less gravelly layer roughly increases with fan age (supplementary tables 1 and 2). This trend suggests that the finer material at the surface is a result of soil-forming processes rather than deposition.

Chemical uniformity of parent material both within and between soil profiles was examined using titanium-oxide to zirconium-oxide ratios of the silt-plus-clay fraction (TiO_2/ZrO_2; data in supplementary table 5). Titanium and zirconium are primarily contained within the minerals rutile and zircon, which are very resistant to weathering (zircon is most resistant). Generally, the proportion of TiO_2 to ZrO_2 should reflect the composition of the parent material; thus abrupt changes in the TiO_2/ZrO_2 ratio with depth probably reflect changes in the parent material chemistry rather than changes due to weathering (Chapman and Horn, 1968; Smeck and Wilding, 1980).

TiO_2/ZrO_2 ratios for all horizons of four profiles (B-21, B-14, B-17, and B-19; fans 1, 3, 5, and 7 respectively) range from 5.1 to 11.9, with a mean ($\underline{x}$) of 8.9 and standard deviation ($\underline{s}$) of 2.0 (table 3). No ratios exceed $2\underline{s}$ from the mean, and only six ratios ($\underline{N}$ = 24) exceed $1\underline{s}$. Relative variability among different groups is examined by the coefficient of variability ($\underline{s}/\underline{x}$), which for TiO_2/ZrO_2 ratios of all horizons is 23 percent. Because Ti does weather, some of this variation may be caused by soil-forming processes (Chapman and Horn, 1968; Wilding and others, 1971). If only C-horizon TiO_2/ZrO_2 ratios are considered, the mean ratio is 10.1 and the standard deviation is 1.6, for a between-profile variability of 16 percent. Within-profile variability ranges from 11 to 25 percent, averaging 19 percent. These ratios show that the between-profile variability is similar to the within-profile variability. TiO_2/ZrO_2 ratios tend to be larger at depth, but the increase is not uniform and the changes are gradual. Because ratios for all horizons fall within $2\underline{s}$ of the mean ratio, the variation is considered normal for the population, which suggests that the soils are chemically similar.

Textural variability is estimated by calculating ratios of coarse to very coarse sand (C/VC) and medium to coarse plus very coarse sand (M/C+VC) for C horizons. Near-surface sand fractions of Kane fan soils tend to be distinctly coarser than sands in the B and upper C horizons, especially in older soils (data not shown). In contrast to the sand fractions, the gravel clasts do not increase in size in the near-surface horizons. Deflation of surface fines is an unlikely cause of the near-surface coarseness of the sand fractions, because the thickness of the less gravelly surface layer increases with time (supplementary tables 1 and 2), suggesting that fines are accumulating. Because the inverse grading of sand grains seems most marked in older soils, the surface material may be more coarse than deeper sediments due to the breakdown of sand grains by gypsum accumulation at depth (discussed below). Because the B-horizon sand fractions appear to have been affected by weathering, only sand fractions from C horizons are compared.

The sand-fraction ratios in most cases are based on measurements after removal of carbonates (including parent material) and gypsum. This step should result in greater uniformity in the ratios than in untreated soils (table 3). Sand-fraction ratios for four profiles (B-5, B-7, B-3, and B-4) are more variable among C horizons with carbonates (80 percent for C/VC and 76 percent for M/C+VC) than among C horizons without carbonates (38 percent and 53 percent respectively, table 3). Remarkably, within-profile variability is the same for both sets of profiles.

Of the 39 C horizons in 13 profiles examined, none have C/VC or M/C+VC ratios that exceed $2\underline{s}$ from the mean ratio; eight horizons exceed $1\underline{s}$ from the mean ratio for either C/VC or M/C+VC, but not both. These horizons are considered to lie within the range of normal variability for this population. Considering the textural variation that is possible on alluvial fans, the sand fractions are unusually uniform both with depth and with distance from the mountain front (variability about 40-80 percent). For comparison, Merced River soils (Harden, 1982a) average 44 percent for within-profile variability of both sand-fraction ratios, whereas between-profile variability is 114 percent for M/C+VC and 96 percent for C/VC ratios.

In summary, the fan alluvia are chemically and lithologically similar, but do vary somewhat in grain

Table 2. Field description of Kane fan deposits relative to distance from fan head

[Proximal is nearest remnant to fan head, distal is farthest remnant from fan head. Refer to figure 2 and to U.S.G.S. 7-1/2-minute Kane and Cottonwood Canyon, Wyo., quadrangles for approximate locations. Percent lithologies and mean clast diameters were visually estimated; maximum clast diameters were measured. Mean diameters are not given for poorly exposed sites. No proximal exposures are available for fans 2, 3, and 4]

Fan number	Description of exposure	Estimated thickness (m)	Mean clast diameter (cm)	Maximum clast diameter (cm)	Gypsum stage
	Proximal deposits				
1	Arroyo, NW/4SW/4SW/4 sec. 6, T. 56 N., R. 93 W; poor exposure. Crude bedding, poorly sorted. 95 percent carbonates (carb.), 5 percent other sedimentary (sed.) rocks.	2	10	70	0
5	SE/4NE/4NE/4 sec. 2, T. 56 N., R. 94 W.; poor exposure. Gravel overlies shale. No bedding visible; poorly sorted, gravelly, 90 percent carb., 10 percent other sed. rocks. Gypsum decreases with depth.	3	--	60	II-III
6	SW/4SE/4SW/4 sec. 6, T. 56 N., R. 93 W.; poor exposure. No bedding visible; poorly sorted, gravelly. 95 percent carb., 5 percent other sed. rocks. No visible gypsum at base of gravel.	15	--	100	0-IV
7	Poor exposure, at soil site B-19. Gravel overlies shale. No bedding visible; poorly sorted, gravelly. 95 percent carb., 5 percent other sed. rocks. No visible gypsum at base of gravel.	10	--	150	0-IV
	Distal deposits				
1	0.2 km north of Kane highway bridge. Crudely bedded; some 10-cm-thick lenses of sand and silt intercalated with poorly sorted, imbricated gravel. 85 percent carb., 10 percent other sed. rocks, 5 percent andesites (and.).	>3	15	45	0
2	Low river bluff 0.1 km north of bridge; gravel overlies shale. Crudely bedded; discontinuous 5-cm-thick lenses of sand and silt intercalated with poorly sorted imbricated gravel lenses. 85 percent carb., 10 percent other sed. rocks, 5 percent and.	5	10	45	0
3	High river bluff 0.8 km north of bridge; fan gravel overlies 1 m of fluvial gravel above shale. Crudely bedded; lenses of finer material up to 50 cm thick intercalated with poorly sorted imbricated gravel. 85 percent carb, 10 percent other sed. rocks, 5 percent and. Gypsum decreases with depth.	5	5	25	0-I
4	Poor exposure, NW/4NW/4 sec. 3, T. 56 N., R. 94 W.; gravel overlies shale. No bedding visible; poorly sorted, gravelly. 90 percent carb., 10 percent and. Gypsum decreases with depth.	4	--	80	0-II
5	Poor exposure, NE/4NW/4 sec. 3, T. 56 N., R.94 W.; gravel overlies shale. No bedding visible; poorly sorted, gravelly 90 percent carb., 10 percent and. Gypsum decreases with depth.	4	--	--	0-III
6	Poor exposure, NE/4NW/4 sec. 3, T. 56 N., R. 94 W.; fan gravel overlies thin fluvial gravel over shale. No bedding visible; poorly sorted, gravelly. 90 percent carb., 10 percent and. Gypsum decreases with depth.	4	--	--	0-IV
7	Corner secs. 2, 3, 10, 11, T. 56 N., R. 94 W.; fan gravel overlies 30 m of ash. Crudely bedded; 25-cm-thick lenses of fine material intercalated with poorly sorted imbricated gravel. 90 percent carb., 10 percent and. Gypsum decreases with depth.	15	15	50	0-IV

size. Textural variability is greater than chemical variability due to the nature of fluvial processes, assuming that different size fractions have similar chemical compositions. Hence, differences among the soils developed on the Kane fan surfaces reflect differences in age and paleoclimate.

Table 3. Parent-material variability within and among soils of the Kane fans

[N, number of cases; $\bar{x}$, mean; s, standard deviation; s/x, relative variability in percent. M, medium sand; C, coarse sand; VC, very coarse sand. Sand ratios are given both for samples with carbonate and without carbonate (gypsum was removed from all samples)]

Variability	N	$\bar{x}$	s	s/x(percent)
Samples without carbonates				
Among profiles:				
C/VC, C horizons	39	1.2	0.5	38
M/C+VC, C horizons	38	.8	.5	53
Within profiles:				
mean of s/x for C/VC	13	--	--	47±25 (1s)
mean of s/x for M/C+VC	13	--	--	51±21 (1s)
Samples with carbonates				
Among profiles:				
TiO_2/ZrO_2, all horizons	24	8.9	2.0	23
TiO_2/ZrO_2, C horizons	12	10.1	1.6	16
C/VC, C horizons	12	1.9	1.5	80
M/C+VC, C horizons	12	.77	.59	76
Within profiles:				
mean of s/x for TiO_2/ZrO_2	4	--	--	19± 6 (1s)
mean of s/x for C/VC	4	--	--	48±14 (1s)
mean of s/x for M/C+VC	4	--	--	49±24 (1s)

Stratigraphic Units

I recognize seven prominent surfaces that are developed on the Kane fans (figs. 2 and 4). The surfaces are numbered 1 to 7 from youngest to oldest. For brevity, these surfaces will henceforth be referred to as fan 1, fan 2, and so forth. Other minor surfaces and deposits occur in the area but are omitted from this study. Correlation of discontinuous deposits was based on both height above Cottonwood Creek and stratigraphic relations. Each fan surface overlies gravel beds resting either on a bedrock surface or on pre-existing fan or other fluvial deposits. Because the Bighorn River is the local base level for Cottonwood Creek, the fan surfaces probably are graded to former levels of the Bighorn-Shoshone river system.

A schematic cross section (fig. 4) sketches the relations of the fan deposits. The fan deposits are 5-15 m thick near the Bighorn River; exposures on fans 6 and 7 nearest the mountain front indicate little thinning toward the mountains (table 2). The deposits underlying fans 2, 4, and probably 1 rest on cut surfaces of Cretaceous shale and sandstone. The deposits underlying fans 3, 6, and 7 grade into the underlying fluvial deposits of the Bighorn-Shoshone river system. Where exposed, andesitic river gravel grades upward, over a 1- to 3-m interval, into calcareous fan deposits. The oldest fan deposits

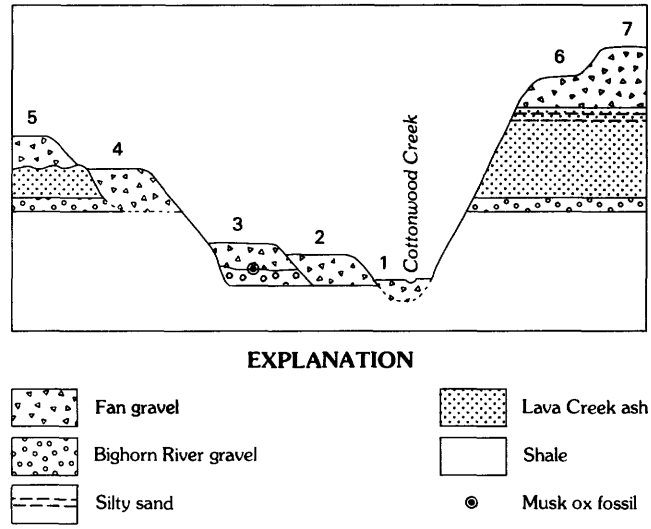

Figure 4. Schematic cross section showing relationships of Quaternary deposits. Thickness of deposits not to scale; maximum thickness of Quaternary deposits under fan 7 is 55 m, including 15 m fan gravel, 35 m ash, and 5 m river gravel. Cottonwood Creek is presently incised about 13 m below the base of the ash.

conformably overlie fluvially deposited Lava Creek volcanic ash that was erupted from the Yellowstone National Park area (Izett and Wilcox, 1982). The crossbedded ash and pumice deposits, as much as 35 m thick, overlie and are interbedded with andesitic river-channel gravel (Birdseye, 1983). Remnants of the channel gravel and overlying ash extend north from fan 7 to fan 5 but pinch out toward the mountain front (fig. 2), suggesting that the Bighorn River formerly flowed about 2-3 km east of its present course. Fan 5 gravel unconformably overlies the fluvial ash and gravel on the north side of the study area, hence this fan gravel postdates the deposition of the material composing fans 6 and 7.

The Kane fan gravels consist of crudely bedded lenses of sand and silt intercalated with imbricated, poorly sorted gravel lenses (table 2). Vertical exposures of fans 1, 2, 3, and 7, near the Bighorn River, reveal that visible gypsum decreases from the surface downward and does not occur at the base of the gravels. Gypsum does occur at the base of the thin (3-5 m) gravel deposits of fans 4 and 5 but is less abundant in the lower parts. Maximum clast size is greater toward the head of each fan (table 2), but little change occurs in gravel thickness, bedding, or sorting.

Geochronology

The difference in age of the fan surfaces, and to some extent paleoclimate, have determined the differences observed among the Kane fan soils. In order to study time-dependent changes in soils on the Kane fans, estimates of the time of stabilization of each surface must be obtained. Tephrochronology, paleontology, and incision rates have been used to estimate the age of the deposits and their surfaces (table 4). The ages of fans 1, 3, and 7 are discussed first because these ages are most closely constrained. From these ages, incision rates are calculated in order to estimate the ages of fans 2, 4, 5, and 6.

Fan 1 is the most recently abandoned surface (figs. 2 and 4) and still exhibits bar-and-swale

Table 4. Stratigraphic units and ages of the Kane fan soil chronosequence

[Height column gives mean and standard deviation (N = 4-7) of height of fan surface above Cottonwood Creek used in figure 5]

Geologic unit	Age control (ka)	Best estimate and range for surface age (ka)	Height (m)	Comments
Fan 1	0 [1]10	5 (0-10)	3.0±0.6	Post-last glaciation.
Fan 2	[2]20 [2]100	[3]65 (20-100)	6.6±0.6	Younger than fan 3, older than fan 1.
Fan 3	[4]70 [5]100 [6]175	100 (70-150)	8.4±2.0	Correlated with Yellowstone-type volcanic ash; musk-ox vertebra in basal fan gravel.
Fan 4	[2]230 [2]400	[3]315 (230-400)	20.8±1.3	Older than fan 3, younger than fan 5.
Fan 5	[2]320 [2]480	[3]410 (320-480)	25.9±1.3	Older than fan 4, younger than fan 6.
Fan 6	[2]415 [2]570 [7]610	[3]505 (415-570)	31.4±1.3	Overlies Lava Creek ash; younger than fan 7.
Fan 7	[8]542 [7]610	585 (540-600)	35.8±1.6	Overlies Lava Creek ash; older than fan 6.

[1]Date from obsidian hydration on Pinedale-age deglacial deposits, West Yellowstone, Montana (Pierce and others, 1976).
[2]Estimated incision rate of Cottonwood Creek, calibrated from fan surfaces 1, 3, and 7 (fig. 5 and text discussion).
[3]Best-estimate age derived from incision-rate calculations as described in text; 5-ka accuracy of the ages is not implied.
[4]Youngest possible ash eruption from Yellowstone area (K.L. Pierce, oral commun., 1984); ash contained in colluvial deposits overlying alluvium correlated to that which underlies fan 3.
[5]Superhydration of volcanic ash (described in 4 above) on Shell Creek, Wyo. (Palmquist, 1983).
[6]Earliest possible arrival of musk ox in North America (C.A. Repenning, written commun., 1982).
[7]Lava Creek ash erupted from Yellowstone Park area (Izett, 1981).
[8]End of interglacial stage following eruption of Lava Creek ash, as determined from marine oxygen-isotope curves (Shackleton and Opdyke, 1976).

morphology. The surface is 3 m above the modern Bighorn River channel. Moss (1974) believed that the Cody terrace of Wisconsin age merges with the Shoshone River floodplain 25 km above its junction with the Bighorn River, but small remnants of this terrace occur 10 km above the junction and are 6 m higher than the river (Mackin, 1937; Ritter and Kauffman, 1983). Because fan 1 is graded to a level only 3 m above the Bighorn River, it probably postdates the last glaciation; hence this surface is of Holocene age, or 5 ± 5 ka (table 4).

The lower age limit of the fan 3 surface is constrained by a musk-ox vertebra (found by Lucy Piety) at the contact between the fan 3 deposits and the underlying river gravel (figs. 2 and 4). C. A. Repenning (U.S. Geological Survey, written commun., 1982) noted that modern musk oxen (genus Ovibos) did not appear in North America before the peak of the Illinoian glaciation (between 130 and 175 ka). Most modern musk-ox fossils (genus Ovibos) in the conterminous United States are considered to be of Wisconsin age, but in two localities, the fossils may be of Illinoian age (Walker, 1982). Thus, the vertebra at Kane constrains the lower age limit of fan 3 to 175 ka.

The lower age limit of the fan 3 surface is also post-Bull Lake glaciation, based on mapping, and on correlation by height above stream level of the underlying river gravel with that along the Bighorn and Shoshone Rivers. The underlying river gravel extends up the Shoshone River to Powell, where it constitutes the sub-Powell terrace of Ritter and Kauffman (1983) (also called the "Intermediate Terrace" by Mackin, 1937). The slightly higher Powell terrace has been traced upstream from Powell to possible moraines west of Cody (Moss, 1974) that are considered to be of Bull Lake age, dated at no younger than 125 ka in West Yellowstone (Pierce and others, 1976).

Fan 3 must be younger than the river gravel on which it lies. Palmquist (1983) estimated the age of the Bighorn River terrace that underlies fan 3 at about 90 ka, using the average incision rate of the Bighorn River for the past 600,000 years.

The upper age limit of fan 3 is further constrained by an ash deposit in sheetwash and colluvium overlying fluvial deposits on Shell Creek (fig. 1). These fluvial deposits were correlated to those underlying the fan 3 gravel by Palmquist (1978, 1983), based on similar heights above the Bighorn River. He assigned a tentative date of 100 ka, based on superhydration of the ash (dated by V. Steen-McIntyre). The ash is not younger than 70 ka, which is the age of the youngest ash eruption from the Yellowstone Park area, and it is probably not older than 150 ka, the inferred age of one of the more widespread young ash eruptions from Yellowstone (K. L. Pierce, oral commun., 1984).

These age constraints indicate that the fan 3 deposits are about 100 ka old, and that the river gravel underlying fan 3 probably is of Bull Lake age. Hence, deposition of the fan gravel may have required about 25,000 years, which is the time interval between the probable youngest age of Bull Lake outwash (Pierce and others, 1976) and the age of the ash on Shell Creek in colluvium that overlies Bull Lake(?) outwash. I estimate the time of stabilization of the fan 3 surface to be 100 $^{+50}_{-30}$ ka (table 4).

Deposits of fan 7 overlie the 610-ka Lava Creek ash (Izett, 1981; Izett and Wilcox, 1982). As neither unconformities nor buried soils were found at this ash-fan gravel contact or within the fan material, the surface of fan 7 is probably not much younger than 600 ka. If aggradation is associated with glacial episodes and incision with deglaciation and interglacials, as Moss (1974) believed, then the fan gravel overlying the ash at Kane must have accumulated rapidly just prior to downcutting by the Bighorn-Shoshone river system. If accumulation of the fan 7 gravel took as long as that of fan 3 gravel, the surface of fan 7 may have been abandoned about 585 ka. Alternatively, if Palmquist's (1983) views are accepted, that the Bighorn River is stable or aggrades during interglacials and incises during glacials, then the fan gravel may have been deposited during an interglacial period. From the marine oxygen-isotope record (Shackleton and Opdyke, 1976), the interglacial that followed 610 ka ended about 540 ka. The fan 7 surface dates from about 585 $^{+15}_{-45}$ ka (table 4).

Age estimates for fans 1, 3, and 7 can be used to estimate ages of stabilization for the remaining fan surfaces (fig. 5 and table 4). The means and standard deviations of the heights above Cottonwood Creek of the three dated fans are plotted against age. The dashed line connecting the three points of known age yields an average stream-incision rate of 5.6 cm/1,000 yr for the past 585,000 years. When the means and standard deviations of heights above the creek of the remaining fan surfaces are plotted on the resultant line, approximate ages and age errors can be derived for the undated surfaces (method from Palmquist, 1979, 1983). The ages are as follows: fan 2, 65±10 ka; fan 4, 315±25 ka; fan 5, 410±25 ka; and fan 6, 505±25 ka. These are minimum age errors because they only

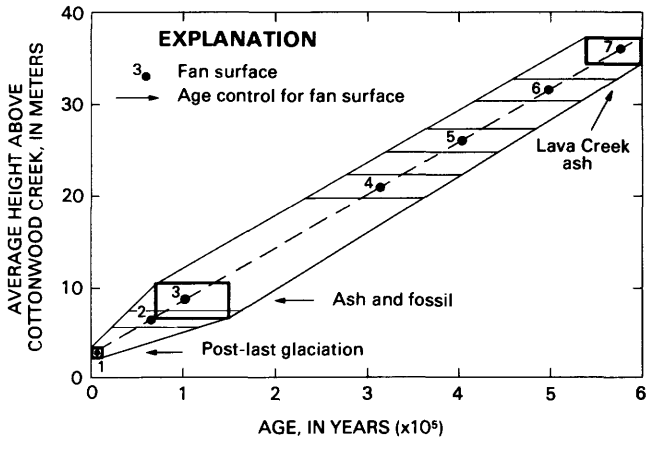

Figure 5. Graph for estimating fan surface ages from average heights above Cottonwood Creek and incision rates (dashed line) derived from ages for fans 1, 3, and 7. Boxes around points for fans 1, 3, and 7 show error limits of age (horizontal) and height (±1 standard deviation, vertical). Lines connecting outermost points of the boxes show the error envelope. Parallelograms show the age errors for other fans, derived by projecting their height errors (±1 standard deviation) horizontally to meet the lines of the error envelope.

include uncertainties in the fan heights above stream level.

The maximum age errors also include uncertainties in the heights and ages of the dated surfaces. The error envelope (fig. 5) permits estimation of the maximum errors on the ages of the undated surfaces. From figure 5, for example, the age of fan 2 is estimated to be 65 ka and to range from 20 ka to 175 ka. However, fan 2 is younger than fan 3, so the lower age limit is probably about 100 ka. The upper age limit of 20 ka for fan 2 is reasonable, because this fan surface is roughly the same height above the Bighorn River as the Cody (Pinedale-aged) terrace is above the Shoshone River. Age errors for fans 4, 5, and 6 can only be evaluated from their relative age order. For example, if the lower age limit of 400 ka for fan 4 is the true age, then the age of fan 5 is older.

Estimates of age based on incision rates involve two major assumptions: first is that the long-term incision rate has remained constant. In the short term, this assumption is false, because terraces and fans are formed during stable or aggrading fluvial conditions and isolated by later incision. The second assumption is that the lateral position of the Bighorn River has either remained stable or has moved in the same direction at a steady rate. If the river has moved irregularly, the fan surface slopes and elevations may vary unpredictably. Fluvial gravels underlying fans 7 and 3 indicate that the Bighorn River has shifted to the west, but whether the shift was gradual or episodic is not known.

SOIL DEVELOPMENT IN THE CHRONOSEQUENCE

The physical appearance or morphology of soils commonly reflects time-dependent soil properties. The Kane fan soils have light-colored, ochric A horizons with vesicular pores and desert pavements; in age sequence the soils progress from having only traces of gypsum, to having gypsic horizons, to having petrogypsic horizons (fig. 6). Soil morphology is commonly described with reference to the U.S. soil classification system (Soil Survey Staff, 1975). Unfortunately, this system does not discriminate the Kane fan soils with respect to their age. These soils have argillic (clay-rich) horizons, and possession of such horizons overrides differences in gypsum content in the process of classification. Translocated clay in Kane fan soils cannot be seen with a hand lens, but such clay surrounds calcite, dolomite, and quartz grains in petrographic thin sections of B horizons. Observations (Nettleton and others, 1969; Holliday, 1982) and experiments (Goss and others, 1973) have shown that clay can be translocated in calcareous soils if pore spaces or cracks are large enough. Thus, all the Kane fan soils are classified as Typic Haplargids (aridic soils with argillic horizons), regardless of their $CaCO_3$ or gypsum content.

Profile Indices

Some soil properties that change with soil age include texture (in this study, determined in the field by hand), rubification (reddening and brightening), and pH. These properties can be described, but in this study they were converted to numerical quantities using Harden's (1982b) soil development index (see "Field Methods and Calculations" section). Some other soil properties did not show consistent age trends. Structure tends to be poorly developed in gravelly desert soils, and in the Kane fan soils is disrupted by gypsum. Organic matter content does not increase consistently with time in desert climates, where organic material is rapidly oxidized. The gradual accumulation of $CaCO_3$ causes soils to whiten with age. Gypsum, rather than $CaCO_3$, increases with age on the Kane fans, and indices for color-paling and color-lightening poorly reflect gypsum accumulation.

This study extrapolates or limits all soil depths to 250 cm when calculating property values using the Harden (1982b) index, in order to minimize the variability caused by different sampling depths in the different excavations. However, total-texture (texture plus wet consistence), pH, and rubification vary with depth (fig. 7). Because these three properties reflect weathering and additions to the soil, they should be most pronounced near the surface, where weathering is most intense. Thus, limiting the calculations to 250 cm should not seriously affect the value of a given property summed for a soil profile. Index values for total-texture are indeed largest in the B horizons, but those for pH increase and rubification are often greatest at depth. Hence, index values for these properties summed over the profile may be minimum values for soil development, especially in the older soils.

Total-texture consistently increases with age for soils on fans 1-4, and is significant at the 0.01 level in distinguishing between these soils (fig. 8). The texture-age correlation is also significant (at the 0.025 level) for all soils, but the r^2 value (coefficient of determination) for this correlation is quite low. Laboratory textural data for these soils cannot be used because in most cases, carbonate parent material was removed along with the gypsum before particle size was determined. Hence texture was determined in the field by hand. Expectably, such a technique reflects the high gypsum content of older soils, for gypsum crystals impart a sandy feel to the soil.

Rubification (both moist and dry colors used) increases consistently with age (fig. 9); the r^2 value is significant at the 0.01 level. If extrapolated values are not used, the correlation is improved from $r^2=0.69$ to $r^2=0.86$. This trend reflects reddening at depth in the profiles, rather than mainly in the B horizons (fig. 7). The most reddened horizons occur at or just below gypsic horizons; this suggests a connection between rubification and gypsum content. This association also appears in gypsic soils developed on similar parent materials in southern Israel (Dan and others, 1981, p. 268-296; Dan and others, 1982).

The patterns of pH change are complex (figs. 7 and 10). Values of pH become more alkaline with depth. When pH index values are extrapolated to depths of 250 cm, anomalously high values of pH change for the young soils are derived (fig. 10). The young soils, especially B-21, B-5, and B-15, were sampled shallowly because they showed no visible evidence of pedogenic alteration at shallow depths. It

A

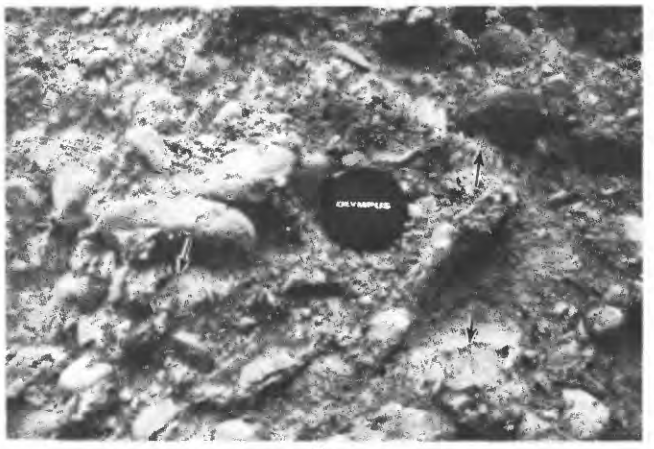

B

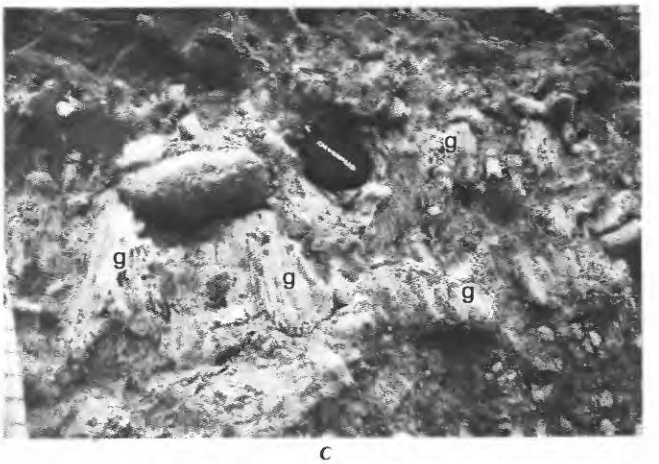

C

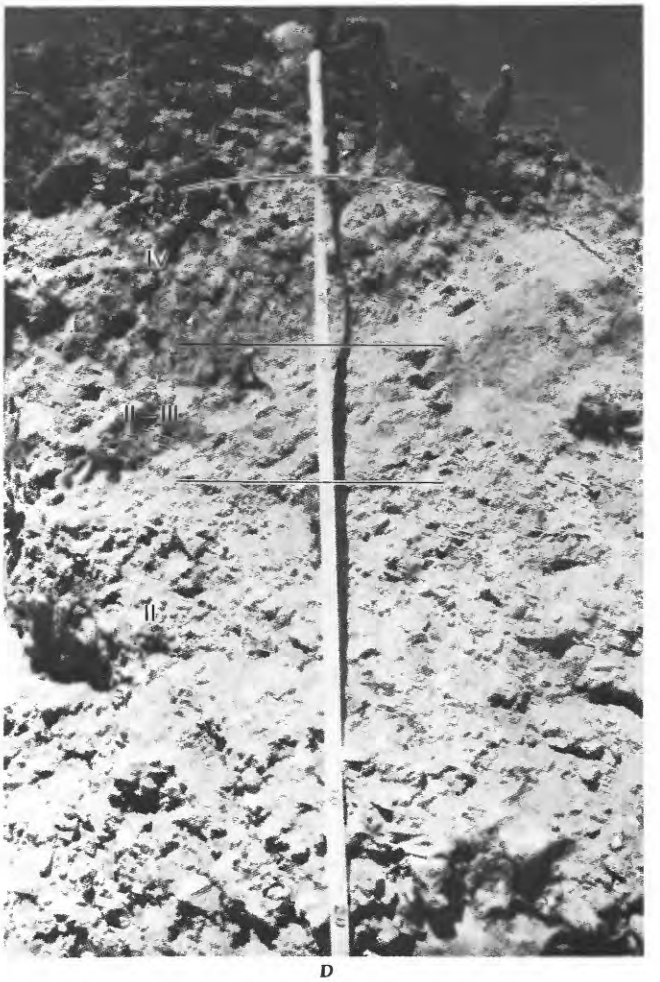

D

Figure 6. Typical appearance in soil profiles of gypsum stages (see "Field Methods and Calculations" section). Gypsum pebble coats and small masses shown by arrows, larger masses indicated by "g." A, Stage I, from the 2C4cs horizon in soil B-17; note gypsum-cracked clast in center. B, Stage II, from the 2C3cs horizon in soil B-17. C, Stage IV, from the 2C1csca horizon in soil B-17; note clasts floating in gypsum matrix. D, Soil B-18B, with stage IV gypsum from 20 to 50 cm, stage II-III gypsum from 50 to 75 cm, and stage II gypsum below 75 cm.

is unrealistic to extrapolate pH values measured at depths of only 100-150 cm to 250 cm (supplementary table 1).

The minimum index values for pH (calculated to the sampling depth for each soil) increase with time for fans 1-4 but decrease in the older fans (fig. 10). This pattern is consistent with probable changes in soil chemistry as interpreted from soil morphology and soluble salts. The amount of secondary $CaCO_3$ increases with time in the young soils (supplementary table 1), which causes an increase in pH. The accumulation of secondary gypsum in older soils (fig. 6) causes a decrease in pH, because the pH of gypsum is 6, as opposed to 8 for $CaCO_3$ (Stevens and Carron, 1948).

The profile index is calculated in two ways. The first (fig. 11A) combined texture, rubification, and pH increase; the second (fig. 11B) used texture and rubification, in order to eliminate the uncertainties in the calculation of index values for pH. Using three properties, correlation of the profile index with age is not significant when the extrapolated maximum values of the index for young soils are used. If the minimum values are used, the correlation is significant at the 0.01 level. The r^2 value of the regression increases from 0.57 to 0.86 by deleting the soils on fan 7 that appear eroded. When pH is excluded, the correlation of the profile index with time is significant at the 0.01 level, and the r^2 value again increases from 0.69 to 0.86 if the soils on fan 7 are deleted. Comparing these methods, correlation using all the soils is better if pH

values are excluded, but there is no difference between the results when soils on fan 7 are excluded.

Linear rates of soil development (figs. 8-11) are contrary to results obtained by workers in warmer, more moist climates (Colman and Pierce, 1981; Harden, 1982a, b; Birkeland, 1984, p. 204 and 225), where rates were found to be logarithmic or exponential in character. Bockheim (1980b) obtained logarithmic trends with time for soils formed in climates ranging from tropical rainy to cold desert; his study, however, used maximum values in each profile, rather than summations over the total profile depth. Muhs (1982) expressed soil properties in an arid xeric climate as profile summations and found linear trends with time; these soils probably received considerable

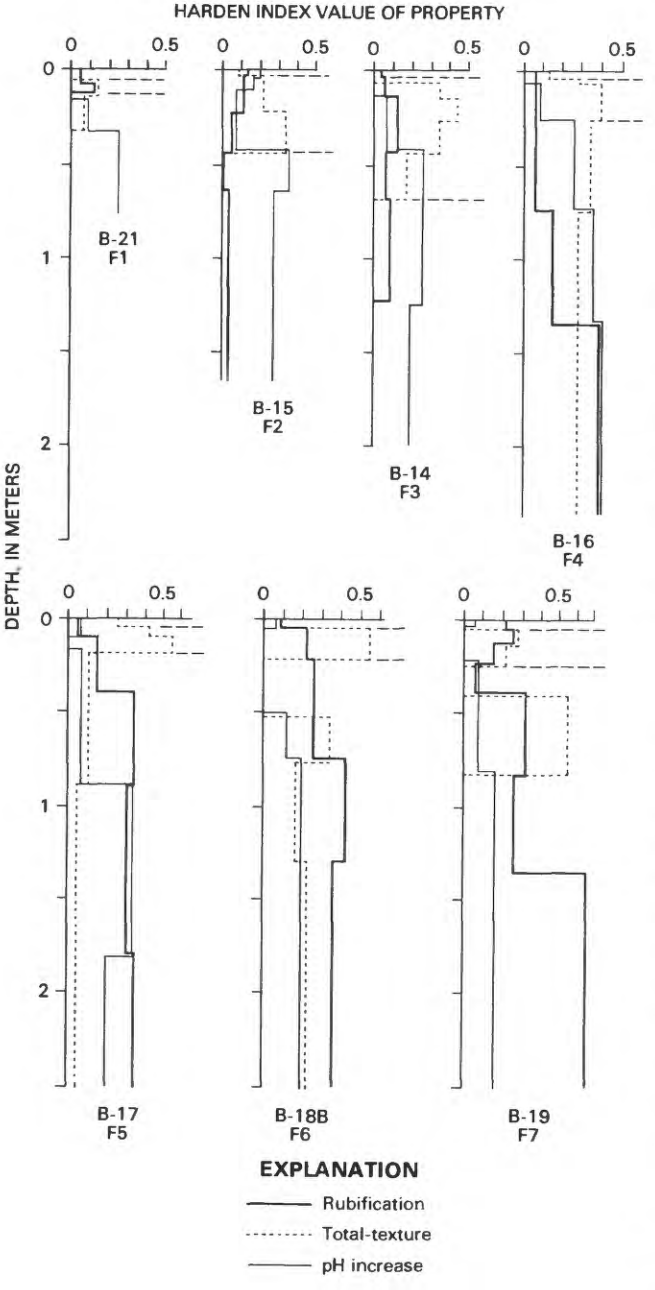

Figure 7. Values of pH, total-texture, and rubification in selected soils (B-numbers) on each fan surface. Note increase of rubification and pH at depth in soils. F1-F7, fan numbers. Horizontal dashes separate A, B, and C horizons.

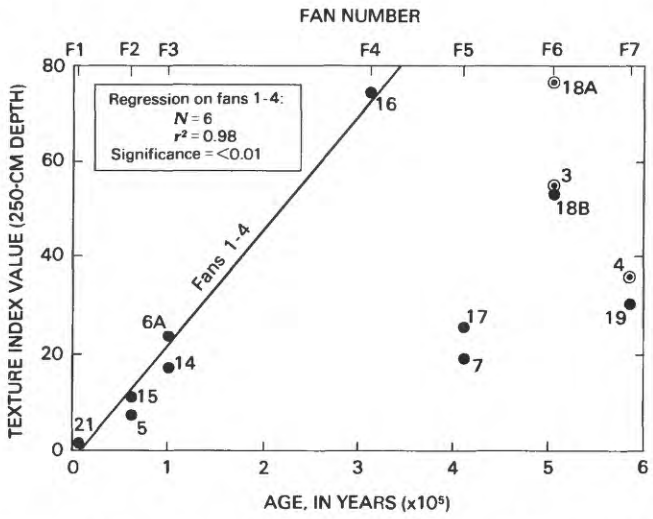

Figure 8. Regression of total-texture (texture + wet consistence) with soil age. Dots are index values for each soil; circled dots are values derived by large extrapolations to 250-cm depth. Numbers correspond to profile numbers without prefix "B-". The r^2 value is for linear regression based on index values for fans 1-4. Index for older soils is nonsystematic in part because of effect of gypsum on field determination of texture and consistence (see text).

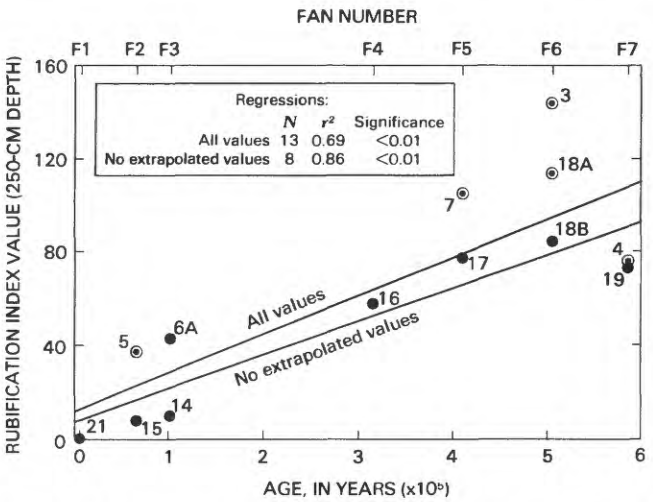

Figure 9. Regression of rubification (based on dry and moist colors) with soil age. Dots are index values for each soil; circled dots represent values derived by large extrapolations to 250-cm depth. Numbers correspond to profile numbers without prefix "B-". The r^2 values are for linear regression based on all index values, and on values excluding those extrapolated. Values for older soils are minimum because calculations are limited to 250-cm depth.

dust influx. Therefore, linear trends with soil age of index values based on field criteria for the Kane fan soils may best be explained, not by weathering phenomena, but by cumulative additions from atmospheric sources to the soil profiles, and by secondary effects of these additions.

Calcium Carbonate and Gypsum

Early in soil development on the Kane fans, $CaCO_3$ is dissolved from the calcareous parent material and from eolian additions, and is reprecipitated lower in the profile mainly as coats and pendants under clasts (supplementary table 1). The depth to and the amount of secondary $CaCO_3$ increase with age in soils on fans 1-3. However, $CaCO_3$ does not increase beyond stage II and, in fact, appears in lesser proportions in the oldest soils, despite the availability of $CaCO_3$ in the parent material and aerosolic dust.

Gypsum first appears in trace amounts in soils on fan 2 and steadily increases in concentration and in thickness with age (fig. 6 and supplementary tables 1 and 3). Petrogypsic horizons first appear in fan 5 soils. Expectably, gypsum accumulates below the first appearance of secondary $CaCO_3$ because gypsum is more soluble. I was not able to find the maximum depth of gypsum accumulation in backhoe pits up to 3 m deep, but observations (table 2) indicate that gypsum amounts decrease with depth and that gypsum does not occur in most of the basal fan gravels.

The composition and amount of dust collected in traps (table 5) suggest that atmospheric additions of silicates, $CaCO_3$, and gypsum determine the development of soils on the Kane fans. The annual infall of mineral particles (non-salt, non-organic fraction) is about 5 X 10^{-4} g/cm^2 (based on one year of data), $CaCO_3$ is added at the annual rate of 2 X 10^{-4} g/cm^2, whereas the gypsum rate is about 0.4 X 10^{-4} g/cm^2.

Eolian silt and clay may compose a large part of the silt and clay in the upper parts of the soils. Continual input of silt and clay through time can account for the linear textural increase seen in the younger soils (fig. 8). Gravelly material makes an effective long-term sediment trap, especially where a desert pavement helps protect the surface from deflation. Eolian dust influx also helps to account for

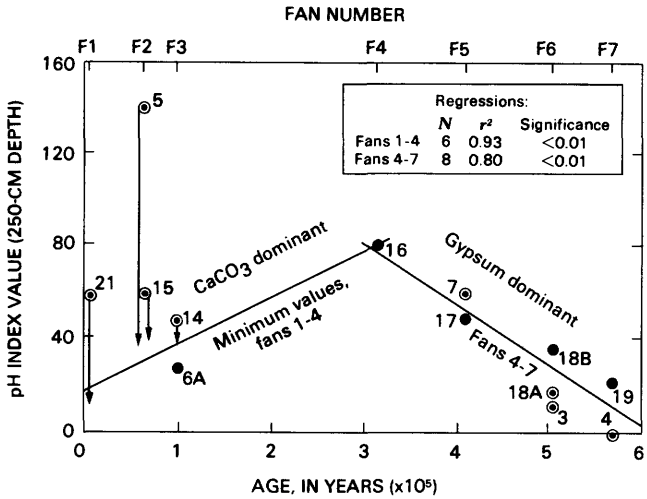

Figure 10. Regression of pH with soil age. Dots are index values for each soil; circled dots are values derived by large extrapolations to 250-cm depth; arrows extend down to minimum index values for young soils. Numbers correspond to profile numbers without prefix "B-". The r^2 value for fans 1-4 is for regression using minimum index values for young soils. Values for older soils are minimum because calculations are limited to 250-cm depth.

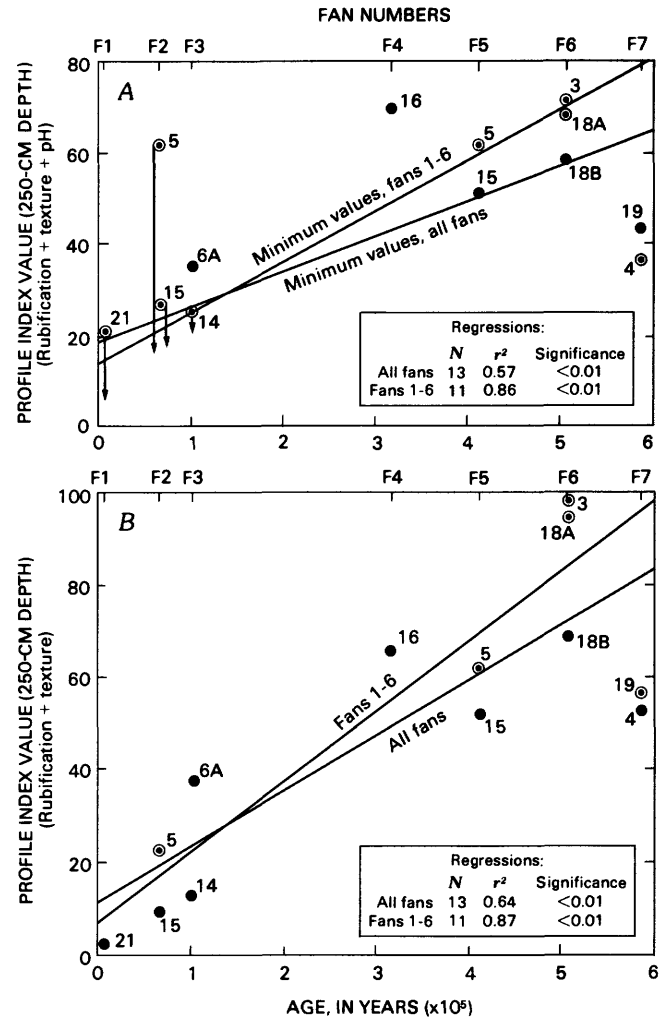

Figure 11. Regression of profile index with soil age. (A, Combined pH, total-texture, and rubification. B, Total-texture and rubification). Dots are index values for each soil; circled dots represent values derived by large extrapolations to 250-cm depth; arrows extend down to minimum index values for young soils. Numbers correspond to profile numbers without prefix "B-". The r^2 values in A are for linear regression using minimum values for young soils. Values for older soils are minimum because calculations are limited to 250-cm depth.

Table 5. Data from dust traps

[Analytical methods are described in text. The first major oxides column gives percent as measured on the nonsalt silt-plus-clay fraction. The second column gives recalculated percent oxides assuming that all $CaCO_3$ and gypsum in the traps were contained in the silt-plus-clay fraction. Oxides were determined on combined samples from D-1 and D-2]

	Trap D-1	Trap D-2
Air-dry weight----	0.6818 g	0.9360 g
Percent of total sample:		
Organics----------	19.3	15.6
$CaCO_3$----------	16.6	22.9
Gypsum----------	3.3	5.6
Mineral matter----	60.8	55.9
Percent of mineral matter fraction:		
Sand----------	4.0	12.0
Silt----------	59.6	54.2
Clay----------	36.3	33.8
Annual flux rates (10^{-4} g/cm^2):		
Mineral matter----	4.8	6.0
$CaCO_3$----------	1.3	2.5
Gypsum----------	.26	.60

Percent major oxides of silt-plus-clay fraction, combined samples:

	Nonsalt	With $CaCO_3$ and gypsum
SiO_2----------	67.	59.
Al_2O_3----------	11.7	10.3
Fe_2O_3----------	4.4	3.9
MgO----------	2.0	1.8
CaO----------	2.0	14.0
Na_2O----------	3.2	2.8
K_2O----------	3.0	2.6
TiO_2----------	.53	.46
MnO----------	.038	.033
ZrO_2----------	.026	.023

the presence of illuvial clay in B horizons of soils that show few signs of weathering (Holliday, 1982).

The $CaCO_3$ dust rate is similar to the Holocene rate calculated by McFadden and Tinsley (1985) for soils in southern California and is slightly higher than modern dustfall rates in the area of Las Cruces, N. Mex. (Gile and Grossman, 1979). Machette (1985) calculated that annual Pleistocene rates of carbonate accumulation were 1.4, 2.2-2.6, and 5.1 X 10^{-4} g/cm^2 for the respective areas of Beaver, Utah, Albuquerque-Las Cruces, N. Mex., and Roswell-Carlsbad, N. Mex. Formation of calcic soils in the United States is commonly attributed to atmospheric additions of $CaCO_3$, including calcareous dust and calcium ions contained in precipitation (for example, Gardner, 1972; Bachman and Machette, 1977; Gile and Grossman, 1979).

If $CaCO_3$ is being added to the Kane fan soils at the rate indicated, the amount of secondary $CaCO_3$ in the older soils should be much greater than the amount actually observed. For example, soils at Las Cruces as young as 25-75 ka have stage III $CaCO_3$ horizons (Gile and others, 1981). At Silesia, Mont., in a climate moister than the Kane area with a smaller carbonate dust flux, 400-ka soils in granitic alluvium have stage III $CaCO_3$ (Reheis, 1984). Some mechanism that diluted or prevented eolian $CaCO_3$ from being added to the older Kane fan soils appears to be required. One possible answer is that $CaCO_3$, much less soluble than gypsum, could have been removed from the fan surfaces by wind before it could be dissolved and moved into the soils.

Potential sources of gypsum in the study area include: (1) local evaporite fragments in the fan detritus, (2) ground water from nearby springs, (3) the past and present base-flow component of runoff within the fan gravels, and (4) upwind dust sources.

Incorporation of gypsum into the fan debris from local bedrock sources is not significant. Analyses of relatively unaltered fan debris from the base of profiles developed on fans 1-3 and from the base of fan 3 deposits (supplementary table 4), plus field observations at depth (table 2), show only trace amounts of gypsum (about 0.07 percent). The bulk density of unweathered fan gravels is about 2.0 g/cm^3 (supplementary table 2). Hence, only 0.0014 g of gypsum can be obtained from a cubic centimeter of parent material. The profile weight of gypsum in a 250-cm thickness of soil on fan 7 is about 43 g/cm^2 (fig. 12). In order to derive all the gypsum in the uppermost 250 cm of fan 7 soils from weathering and solution of the carbonate parent material, about 305 m of deposits above the present land surface would be required. This is extremely unlikely because the fan surfaces are quite well preserved.

A ground water source for the secondary gypsum cannot be dismissed, but several facts argue against it. (1) Analyses (supplementary table 3) and observations (table 2) show that gypsum is concentrated about 0.25-1.0 m below fan surfaces. It decreases with depth and does not visibly occur in basal gravel in most cases, even where the gravel overlies relatively impermeable shale bedrock. Ground water flow would concentrate above such aquacludes, so if the gypsum precipitated out of ground water, it should also concentrate near the base of the gravel. (2) If ground water were the main contributor of gypsum, the observed increase of gypsum with time should not occur. Gypsum would be added only as long as the soil remained within reach of the ground water table. After incision and isolation of the fan surface, gypsum should not continue to accumulate. (3) The vertical distribution of gypsum and carbonate argues against ground water origin. Precipitation of salts from solutions of upward-moving capillary water should result in more soluble salts occurring closer to the surface than less soluble ones, but gypsum-rich horizons in the Kane soils always occur beneath horizons that contain secondary $CaCO_3$. Additionally, with a ground water source, gypsum should occur closer to the surface in younger soils that are near the ground water table; the reverse is true in the study area.

Eolian-derived gypsum (Page, 1972; Watson, 1979) appears to account for most of the observed increase in gypsum content. Profile weights (g/cm^2 in a column of soil) of gypsum (calculated to a depth of 250 cm) increase at a linear rate (fig. 12), and the r^2 value based on nine soils is significant at the 0.01 level

when ages are estimated from the stream-incision rate (table 4 and fig. 5). The r^2 value increases from 0.90 to 0.93 when the soil on fan 7 that appears eroded is excluded from the regression. Annual rates of gypsum accumulation calculated from the profile weights and estimated soil ages vary[3] between 1.1 and 120 X 10^{-6} g/cm^2. Addition of eolian gypsum (table 5) now occurs at annual rates between 26 and 60 X 10^{-6} g/cm^2. Thus, the observed accumulation rate of aerosolic gypsum is enough to account for most of the pedogenic gypsum.

Local and long-range sources of eolian gypsum are abundant. Presently stabilized clay and gypsum dunes (up to 90 percent gypsum) 4 km south of the Kane fans indicate eolian gypsum transport (Birdseye, 1983), and may be a gypsum source for the Kane fan soils. Cretaceous rocks underlying the central part of the Bighorn basin commonly contain gypsum. Gypsum deposits are exposed in the Sheep Mountain anticline to the southwest, on the slopes of the Pryor Mountains to the northwest (Pierce, 1978), and in the Cody area on the west side of the Bighorn Basin (Bullock and Wilson, 1969). At present, prevailing winds in the study area are westerly.

Effects of Gypsum on Other Soil Properties

Depression of $CaCO_3$ solubility

Mobility of $CaCO_3$ in gypsic soils is restricted because of the common ion effect (Krauskopf, 1967, p.17): the solubility of any salt ($CaCO_3$) in equilibrium with a saturated solution is less if an excess of one of its ions (Ca^{+2}) is present. Calculations indicate that the solubility of $CaCO_3$ is depressed by a factor of 64 in the presence of a solution saturated with gypsum at 25°C, assuming that equilibrium conditions are maintained and that the partial pressure of CO_2 is constant (see "Field Methods and Calculations" section). The solubility of $CaCO_3$ may be even further reduced by the low partial pressure of CO_2 in arid soils (modeled growing-season pCO_2 is less than 0.1 percent in arid climates, 0.6-4 percent in semiarid climates; Brook and others, 1983). The reverse is not true; because $CaCO_3$ is much less soluble than gypsum, gypsum solubility remains nearly constant in a $CaCO_3$-saturated solution.

Although trace amounts of gypsum occur in the uppermost soil horizons, gypsum accumulates in horizons lower than the first occurrence of secondary $CaCO_3$ (supplementary table 1). The depths to accumulations of secondary $CaCO_3$ and gypsum in the soils can be compared best by calculating these depths in units of yearly water penetration (Arkley, 1963) based on the estimated available water-holding capacity (AWC) of each horizon (fig. 13). The depths then are plotted on a curve that represents the movement of water calculated for 24 years of Lovell weather data (National Climatic Center, 1976). Theoretically, rainfall will dissolve gypsum and $CaCO_3$ either from eolian dust or parent material and carry the ions downward. As soon as this solution contacts a significant amount of gypsum, the addition of Ca^{+2} and SO_4^{-2} ions to the solution will depress the solubility of $CaCO_3$ and it will precipitate. Thus, the more gypsum that accumulates, the less movement of $CaCO_3$ will occur.

The following method permits estimation of the depth at which gypsum saturation occurs and $CaCO_3$ precipitates for the Kane fan soils (table 6). The amount of water per year that is available to dissolve the gypsum in a 1-cm^2 column through a soil horizon is equal to the yearly amount of water passing through the soil at the base of that horizon (fig. 13), plus the water held within the horizon (AWC, table 6). Finely powdered gypsum is soluble at the rate of 19 X 10^{-4} g/mL H_2O (distilled) at 10°C (Hardie, 1967). The potential amount of gypsum that can be dissolved yearly in a horizon is equal to the gypsum solubility multiplied by the total amount of water held in and passing through that horizon. The amount of gypsum present in a 1-cm^2 horizon column is known (table 6). The percent saturation with gypsum of water percolating down from the base of the soil horizon is equal to the amount of gypsum actually present divided by the amount that could be dissolved, assuming that if sufficient unsaturated water is present, all the gypsum in the horizon will dissolve. The calculation is repeated for each successively lower horizon, except that the capacity of water to dissolve gypsum in each lower horizon is decreased by the percent saturation of the water when it enters that horizon.

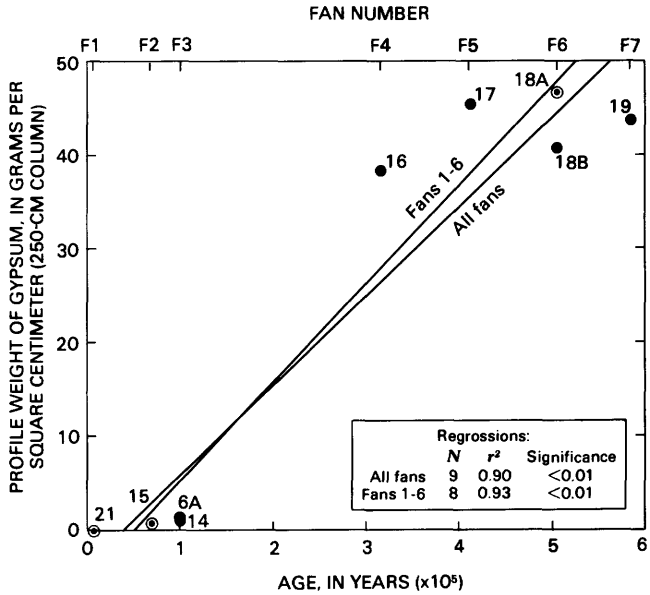

Figure 12. Regression of profile weights of pedogenic gypsum with soil age. Dots are values for each soil; circled dots represent values derived by large extrapolations to 250-cm depth. Numbers correspond to profile numbers without prefix "B-". The r^2 values are for linear regression based on soils for which bulk density is known.

[3]The variation in rates of gypsum accumulation calculated from the soils may be due to episodic solution of gypsum, or to variation in the gypsum dust flux with time.

The gypsum-saturation depth of the normal yearly amount of water occurs within 10 cm of the surface in all the Kane fan soils except B-21 on fan 1 (table 6). In most of the soils, the water becomes saturated with gypsum at or just above the uppermost level of accumulation of $CaCO_3$ (B-14 and B-19, table 6). This observation supports the above hypothesis concerning the inhibition of $CaCO_3$ dissolution by gypsum. In profile B-19, the water percolating through the soil is not saturated with gypsum until it enters the uppermost gypsic horizon, implying ongoing dissolution of gypsum. Field observations of this soil indicate that dissolution is occurring, for the gypsum distribution in the B horizon is patchy and irregular. This is shown by two different lines representing the depths to gypsum accumulation for the soil on fan 7 in figure 13.

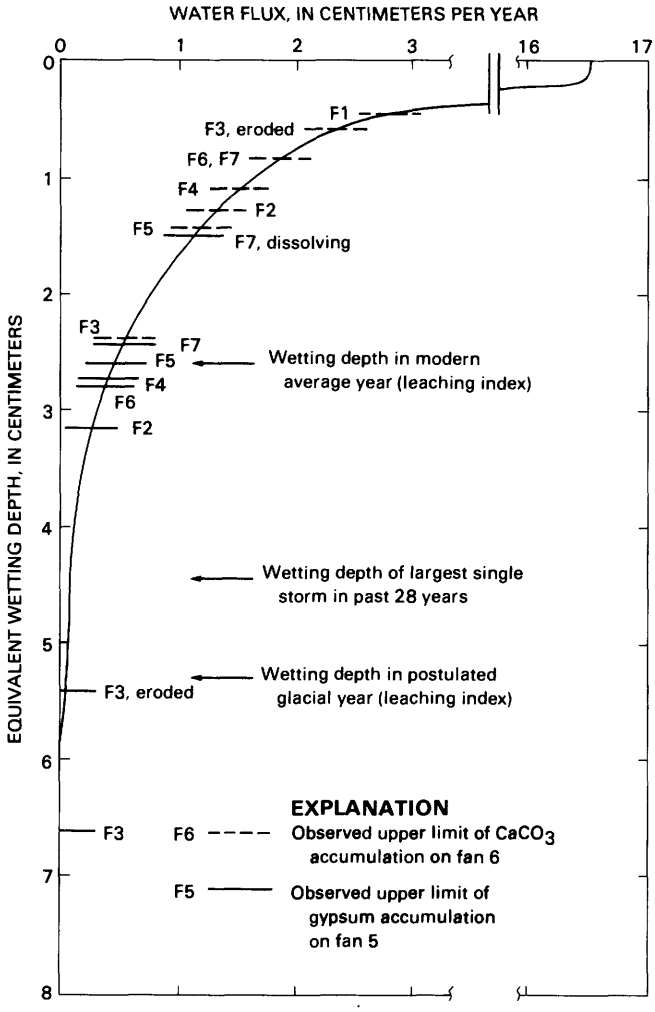

Figure 13. Average yearly water movement (24-year record at Lovell, Wyo.) and relationship to gypsic and calcic horizons using Arkley's (1963) method. Upper limits of gypsum (solid line) and $CaCO_3$ (dashed line) horizons for soils on fans F1-F7; units of depth were calculated by estimating AWC for each horizon from textural data. F1 has no gypsum accumulation in the depth sampled. "F3, eroded" denotes top of carbonate horizon of a stripped soil (there are two F3 soils); "F7, dissolving" is top of gypsic horizon that shows signs of ongoing dissolution. Soil profiles used include: F1 = B-21, F2 = B-14 and B-15, F3 = B-6A, F4 = B-16, F5 = B-17, F6 = B-18A, F-7 = B-19.

Several assumptions are involved in the calculations of gypsum-saturation depths: (1) All of the gypsum in each horizon is dissolved if sufficient unsaturated water is present. This assumption is probably justified for the A and B horizons of the Kane fan soils, because in these horizons, gypsum occurs in such small, disseminated amounts that it is not visible. Gypsum in these horizons is probably finely crystalline and can dissolve rapidly. The assumption is not justified for the horizons with coarsely crystalline gypsum (all those horizons designated "cs" in table 6). (2) The solubility of gypsum is not depressed by a common ion present in a more soluble salt. No other salts were observed in X-ray diffraction analyses of the Kane fan soils. (3) The amount of gypsum calculated in each horizon is reasonably accurate. Horizon weights of gypsum are calculated from the percent gypsum, bulk density, and horizon thickness (supplementary table 7). The total horizon weight includes both pedogenic gypsum and parent-material gypsum, assuming the latter has not been leached out. Due to uncertainties, only the amount of pedogenic gypsum was used to calculate saturation depth of gypsum. Hence, saturation depths in table 6 are probably minimum estimates.

An obvious implication of this work is that, through time, the amount of gypsum in the A and B horizons should decrease and disappear as it is dissolved. That this does not occur is proved by the occurrence of gypsum in small amounts in the upper parts of all soils. Several factors may explain this phenomenon: (1) Small amounts of gypsum are added by dust influx (table 5). This factor is considered unlikely, for present rainfall is more than enough to dissolve the very small amounts of gypsum added ($26\text{-}60 \times 10^{-6}$ g/cm^2 per year). (2) Small amounts of gypsum, if present, may be released from the limestone and dolomite clasts as they weather on and near the ground surface. Most carbonate rocks contain trace amounts of gypsum and other salts (less than 0.1 percent; Lamar and Shrode, 1958). These two factors are incompatible: if percolating water dissolves aerosolic gypsum near the ground surface, then the common ion effect will hinder this water in dissolving carbonate and releasing gypsum from the near-surface clasts. (3) Evaporation of water at the ground surface probably causes upward movement of soil water in the upper, fine-grained parts of the soil (supplementary table 1). Thus, small amounts of gypsum that are dissolved and moved down by a rainfall event may be redistributed upward as evaporation occurs.

Effects on other soil-forming processes

Pedogenic silt and clay shows no increase in soils older than 300 ka (fig. 8); this may be related to the gypsum accumulations in older soils. Gypsum may control the movement of fines in two different ways: First, gypsum is much more soluble than $CaCO_3$; thus it flocculates clay particles more effectively than $CaCO_3$ and can prevent clay from being translocated into the profile. Second, if enough gypsum

Table 6. Estimated depths to saturation of leaching water with gypsum

[Numbers (C1-C6) at top of each column are used to abbreviate equations to calculate the quantities in other columns. Equations are shown in parentheses at the bottoms of column headings. GS, gypsum solubility, 19×10^{-4} g/mL at 10°C (Hardie, 1967). C6, value of column C6 for the next higher horizon]

Fan and profile number,	Horizon thickness	C1 Est. AWC (cm)	C2 Estimated water flux from horizon (mL/yr) (from fig. 13)	C3 Water in or leaving horizon (mL/yr (C1+C2)	C4 Gypsum capacity of water (g) ($C3 \cdot GS \cdot [\frac{100-C6}{100}]$)	C5 Pedogenic gypsum in horizon (g/cm^2) (supp. table 7)	C6 Saturation of water leaving horizon (percent) (C5/C4)
F1 (B-21)							
A	6	0.47	2.9	3.4	0.0065	0	0
2Btca	7	.18	2.3	2.5	.0048	.0002	4
2Cca	20	.52	1.5	2.0	.0036	.0012	33
2Cn	40	.44	1.2	1.6	.0020	.0008	40
F3 (B-14)							
A11	4	.47	3.0	3.5	.0067	0	0
A12	4	.47	1.7	2.2	.0042	.0007	17
B1	9	1.46	.6	2.1	.0033	.0049	100
B21tca	11	1.78	.2	2.0	0	0	100
B22tca	16	2.45	0	.2	0	0	100
2B3tca	26	.57	0	0	0	.0037	100
2Cca	53	1.17	0	0	0	.0935	100
2Cnca	70	1.40	0	0	0	.218	100
F7 (B-19)							
A	6	.86	1.8	2.7	.0051	.0019	37
B21tca	8	.58	1.3	1.9	.0023	.0007	31
B22tcsca	11	.99	.6	1.6	.0021	.509	100
2C1csca	15	1.56	.2	1.8	0	7.13	100
2C2cs	45	3.38	0	.2	0	13.9	100
2C3cs	52	4.06	0	0	0	13.0	100
3C4cs	125	3.25	0	0	0	9.47	100

accumulates, the soil horizon may be plugged, and clay particles physically cannot pass through it. Petrogypsic horizons in soils on fans 5, 6, and 7 might act as barriers to clay movement.

Gypsum appears to cause rapid physical disintegration of gravels (fig. 6). Limestone and dolomite cobbles within gypsic and petrogypsic horizons are commonly split, and gypsum crystals fill the cracks. Gypsum crystallization has apparently split the clasts. Gypsum crystals also have disaggregated andesite clasts along grain boundaries. Such weathering has been reported in other arid regions (Coleman and others, 1966; Dan and others, 1982) and has been duplicated in the laboratory (Goudie and others, 1979). It is commonly attributed to pressures caused by hydration and crystallization.

Rubification may be associated with gypsum in the Kane fan soils. Rubification does not appear to be related to weathering processes in the B horizons of these soils, because it continues to increase with depth in the profile (fig. 7). However, Dan and others (1982) suggested that high salt contents of older desert soils in southern Israel may enhance deep weathering, because the hygroscopic nature of the salts encourages moisture retention in the soils. In addition, gypsum may encourage rubification by disintegrating clasts and mineral grains, which increases the surface area of debris exposed to oxidation. Petrogypsic horizons do not appear most rubified simply because gypsum dilutes the red coloration.

Possible Climatic Implications

Depth to accumulations of secondary $CaCO_3$ and gypsum should bear some relation to climate (Jenny and Leonard, 1939; Arkley, 1963). These relations are examined by plotting the depths to secondary $CaCO_3$ and gypsum in units of yearly water penetration based on the AWC of each horizon (fig. 13).

The wetting depths to accumulations of secondary $CaCO_3$ in the Kane fan soils do not show a relation with soil age (fig. 13). As discussed above, the wetting depth to secondary $CaCO_3$ is probably controlled in these soils by the amount of secondary gypsum contained in the uppermost horizons. The measured depths to secondary $CaCO_3$ in the profiles (supplementary table 1) are only a few centimeters. Thus, the variable wetting depths to $CaCO_3$ in soils of various ages (fig. 13) may be related to slight erosion or deflation of fan surfaces.

Different depths to gypsum horizons in younger (F3) and older soils (F4-7, fig. 13) suggest a drier climate before 100 ka. Because temperature has little effect on gypsum solubility (Hardie, 1967), effects on the soils would probably be related to changes in effective moisture caused by changes in temperature or in the amount and seasonal distribution of precipitation. Gypsum horizons of fan 3 soils occur near the leaching depth calculated from the postulated climatic parameters (table 1) during glacial periods, but positions for soils on fans 2 and 4-7 cluster closely around the modern leaching index of 2.6 cm.

The soils on fans 2 and 3 have been subjected to the climates of the last glaciation and of the Holocene. Accumulation of silt and clay in the A and B horizons with time raises the soil AWC. If the accumulation of gypsum at a given wetting depth occurred prior to the accumulation of silt and clay above the gypsum, then the wetting depth to the gypsum measured at present will be greater than that

at which it accumulated. Therefore, greater depth to gypsum in fan 3 as opposed to fan 2 soils may be age-related rather than climate-related. Alternatively, the assumed age of 65,000 yr for fan 2 may be incorrect. If fan 2 is younger, perhaps dating to the end of the last glaciation, then it has developed only under the recent interglacial climate. In that case, the depth to gypsum in fan 2 could reflect the modern, shallow leaching depth, whereas gypsum depth in fan 3 soils mainly reflects the greater available moisture of the last glaciation.

Soils on fans 4 through 7 have developed through many glacial-interglacial cycles. The presence of secondary gypsum at depths well below the maximum concentration of gypsum demonstrates that greater available moisture during glacial episodes probably affected the soils. But the maximum gypsum horizons correspond to the modern interglacial wetting depth; this suggests that the positions of these horizons is controlled by the interglacial episodes.

The simplest hypothesis that explains gypsum depth in soils older than 100 ka invokes the hygroscopic qualities of gypsum. It is well known that salts have the ability to sorb larger amounts of moisture than mineral grains (Winkler, 1975; Dan and others, 1982). Experiments with brine-saturated bricks have shown that the volume percent of hygroscopic moisture content of a brick increases by a factor of 20 when the amount of salt (NaCl) in the brine increases from 0 to 4 percent (Winkler, 1975). Because the calculated AWCs are based on field texture, they probably underestimate the real AWCs of gypsum-rich soils. If gypsum has even 10 percent the water-holding capacity of NaCl, then a gypsic horizon with 5 percent gypsum can double the AWC of that horizon. Gypsum quantities in Kane fan soils approach 50 percent in some horizons, including gravel content. Estimated from field textures, the AWC of the uppermost gypsic horizons in fans 5, 6, and 7 is 2 cm in a 20-cm-thick, 1-cm^2 section. The gypsum in these horizons is probably sufficient to hold all of the estimated additional moisture of a glacial climate. The water-holding ability of the gypsum is further enhanced by the high porosity of the gypsic horizons: the bulk density of gypsic peds in some of these horizons is less than 1.0 g/cm^3, whereas the density of gypsum is 2.3 g/cm^3. When gypsum accumulates in a near-surface position over a lengthy interglacial, it can increase the soil AWC enough to hold the increased moisture of a glacial period within the gypsic and overlying A and B horizons. Thus, the gypsic horizon may prevent its own leaching.

Two other hypotheses could help account for shallow depth to gypsum in older soils. First, the rate of gypsum influx during glacial periods may have increased to levels that overwhelmed the ability of the downward flux of water to transport gypsum. Because loess deposition accompanies and closely follows glaciations, this hypothesis has some merit. But even with modern rainfall, the influx must increase by two orders of magnitude to allow gypsum to remain at shallow depths in the old soils. This hypothesis alone seems inadequate. Second, moisture during glacial periods may have actually decreased from modern levels, even though evapotranspiration was greatly reduced, because of the predominant northerly winds and the increased proportion of snow to rain. If no winter moisture was added to the soils due to the presence of frozen ground and wind deflation, summer precipitation must have decreased to half the present level to place the calculated glacial leaching index at the level of the gypsum horizons. Such a decrease is much larger than that previously postulated (Gates, 1976) but is within the realm of possibility.

In summary, the most likely hypothesis that accounts for the retention of gypsum near the surface of soils that have undergone glacial climates is the hygroscopic property of gypsum. This hypothesis is most simple because it does not require any changes external to the soils. It is also possible that increased dust flux and decreased moisture during glaciations may have played a part in the development of the Kane fan soils. In any case, because gypsum increases linearly with time, precipitation in the past 600,000 years has never been sufficient to flush gypsum completely from the soils.

SUMMARY

Field properties and gypsum contents of Kane fan soils change at statistically significant linear rates. These linear rates imply an external source for pedogenic materials. Total texture and pH increase with time in soils on fans 1-4, whereas pH appears to decrease in soils on fans 5-7. Rubification increases with time in all soils. The profile index increases with time, but the correlation is stronger if the index is calculated using only texture and rubification.

Evidence from dust traps indicates that the modern influx of aerosolic gypsum is sufficient to produce a large proportion of the observed amounts of pedogenic gypsum. Despite the presence of alkali springs and gypsum in bedrock units in the Cottonwood Creek drainage, gypsum occurs in very small quantities (less than 0.1 percent) in fan gravels at depth, and it does not concentrate in basal gravels over impermeable shale where ground water should concentrate.

Gradual accumulation of pedogenic gypsum strongly affects development of other soil properties. Gypsum causes rapid clast weathering and may cause reddening of the C horizons; it also reduces the solubility of $CaCO_3$ so much that redistribution of $CaCO_3$ has stopped in soils older than 300 ka. The small amounts of gypsum in the A and B horizons of most of the soils is apparently sufficient to prevent $CaCO_3$ from being carried in solution to depths greater than about 10 cm by the average yearly precipitation. Gypsum may also inhibit downward translocation of clay by flocculating clay particles, which would account for the lack of continuing increase in fines near the surface of older soils.

Large accumulations of gypsum can so increase the AWC of the soil that increased moisture during glacial episodes can be held at shallow depths. The positions of gypsic horizons should be related to available soil moisture, which was probably increased during past glacial periods. Gypsic horizons in soils older than 100 ka correspond to the modern average yearly wetting depth, which suggests that over a long period of time, depth to gypsum is controlled by soil

moisture available during interglacials. Gypsum that accumulates close to the surface in an interglacial climate can, by increasing soil AWC, hold the increased moisture available during a glacial period. Some younger soils have accumulations of gypsum deeper than older soils; this may be because younger soils reflect the climate of the last glaciation, when leaching depths were greater, or because the small amount of gypsum added to young soils can be easily moved to greater depths by large wetting events.

REFERENCES CITED

Allison, L. E., 1965, Organic carbon, in Black, C. A., ed., Methods of Soil Analysis, Part 2: American Society of Agronomy, Monograph Series no. 9, p. 1367-1378.

Andrews, D. A., Pierce, W. G., and Eargle, D. H., 1947, Geologic map of the Bighorn Basin, Wyoming and Montana, showing terrace deposits and physiographic features: U.S. Geological Survey Oil and Gas Investigations, Preliminary Map 71.

Arkley, R. J., 1963, Calculation of carbonate and water movement in soil from climatic data: Soil Science, v. 96, p. 239-248.

Bachman, G. O., and Machette, M. N., 1977, Calcic soils and calcretes in the southwestern United States: U.S. Geological Survey Open-file Report 77-794, 163 p.

Birdseye, R. U., 1980, A fluvial model based on climatic and base level controls: Geological Society of America Abstracts with Programs, v. 12, no. 1, p. 2.

——1983, Quaternary geology of the western Five Springs area, Big Horn County, Bighorn Basin, Wyoming: Wyoming Geological Association Guidebook, 34th Annual Field Conference, p. 209-215.

Birkeland, P. W., 1984, Soils and Geomorphology: New York, Oxford University Press, 372 p.

Blake, G. R., 1965, Bulk density, in Black, C. A., ed., Methods of Soil Analysis, Part 1: American Society of Agronomy, Monograph Series no. 9, p. 374-390.

Bockheim, J. G., 1980a, Properties and classification of some desert soils in coarse-textured glacial drift in the Arctic and Antarctic: Geoderma, v. 24, p. 45-69.

——1980b, Solution and use of chronofunctions in studying soil development: Geoderma, v. 24, p. 71-85.

Bower, C. A., and Huss, R. B., 1948, Rapid conductometric method for estimating gypsum in soils: Soil Science, v. 66, p. 199-204.

Brook, G. A., Folkoff, M. A., and Box, E. O., 1983, A world model of soil carbon dioxide: Earth Surface Processes and Landforms, v. 8, p. 79-88.

Bullock, J. M., and Wilson, W. H., 1969, Gypsum deposits in the Cody area, Park County, Wyoming: Geological Survey of Wyoming, Preliminary Report no. 9, 12 p.

Chapman, S. L., and Horn, M. E., 1968, Parent material uniformity and origin of silty soils in northwest Arkansas based on zirconium-titanium contents: Soil Science Society of America Proceedings, v. 32, p. 265-271.

Coleman, J. M., Gagliano, S. M., and Smith, W. G., 1966, Chemical and physical weathering on saline high tidal flats, northern Queensland, Australia: Geological Society of America Bulletin, v. 77, p. 205-206.

Colman, S. M., and Pierce, K. L., 1981, Weathering rinds on andesitic and basaltic stones as a Quaternary age indicator, western United States: U.S. Geological Survey Professional Paper 1210, 56 p.

Dan, J., Gerson, R., Koyumdjisky, H., and Yaalon, D. H., 1981, Aridic Soils of Israel: Properties, Genesis, and Management: Guidebook, International Conference on Aridic Soils, Jerusalem, Israel: Bet Dagan, Israel, Volcani Center, 353 p.

Dan, J., Yaalon, D. H., Moshe, R., and Nissim, S., 1982, Evolution of reg soils in southern Israel and Sinai: Geoderma, v. 28, p. 173-202.

Darton, N. H., 1906, Geology of the Bighorn Mountains: U.S. Geological Survey Professional Paper 51, 129 p.

Day, P. R., 1965, Particle fractionation and particle-size analysis, in Black, C. A., ed., Methods of Soil Analysis, Part 1, American Society of Agronomy Monograph Series no. 9, p. 545-567.

Deming, W. E., 1943, Statistical Adjustment of Data: New York, Wiley, 261 p.

Gardner, L. R., 1972, Origin of the Mormon Mesa caliche, Clark County, Nevada: Geological Society of America Bulletin, v. 83, p. 143-156.

Gates, W. L., 1976, Modeling the ice-age climate: Science, v. 191, p. 1138-1144.

Gilbert, B. M., Pearsall, D., and Boellstorff, J., 1980, Post-Sangamon record of vulcanism and climatic change at Natural Trap Cave, Wyoming: American Quaternary Association, Sixth Biennial Meeting, Abstracts and Program, p. 86.

Gile, L. H., and Grossman, R. B., 1979, The Desert Soil Project Monograph: U.S. Department of Agriculture, Soil Conservation Service, 984 p.

Gile, L. H., Hawley, J. W., and Grossman, R. B., 1981, Soils and geomorphology in the Basin and Range area of southern New Mexico--Guidebook to the Desert Project: New Mexico Bureau of Mines and Mineral Resources Memoir 39, 222 p.

Gile, L. H., Peterson, F. F., and Grossman, R. B., 1966, Morphological and genetic sequences of carbonate accumulation in desert soils: Soil Science, v. 101, p. 347-360.

Goss, D. W., Smith, S. J., and Stewart, B. A., 1973, Movement of added clay through calcareous materials: Geoderma, v. 9, p. 97-103.

Goudie, A. S., Cooke, R. U., and Doornkamp, J. C., 1979, The formation of silt from quartz dune sand by salt-weathering processes in deserts: Journal of Arid Environments, v. 2, p. 105-112.

Guccione, M. J. W., 1982, Stratigraphy, soil development and mineral weathering of Quaternary deposits, Midcontinent, U.S.A.: University of Colorado, Boulder, Ph.D. thesis, 302 p.

Harden, J. W., 1982a, A study of soil development using the geochronology of Merced River deposits, California: University of California at Berkeley, Ph.D. thesis, 195 p.

——1982b, A quantitative index of soil development

from field descriptions: Examples from a chronosequence in central California: Geoderma, v. 28, p. 1-28.

Harden, J. W., and Taylor, E. M., 1983, A quantitative comparison of soil development in four climatic regimes: Quaternary Research, v. 20, p. 342-359.

Hardie, L. A., 1967, The gypsum-anhydrite equilibrium at one atmosphere pressure: American Mineralogist, v. 52, p. 171-200.

Holliday, V. T., 1982, Morphological and chemical trends in Holocene soils at the Lubbock Lake archeological site, Texas: University of Colorado, Boulder, Ph.D. thesis, 285 p.

Izett, G. A., 1981, Volcanic ash beds: Recorders of Upper Cenozoic silicic pyroclastic volcanism in the western United States: Journal of Geophysical Research, v. 86, p. 10,200-10,222.

Izett, G. A., and Wilcox, R. E., 1982, Map showing localities and inferred distributions of the Huckleberry Ridge, Mesa Falls, and Lava Creek ash beds (Pearlette Family ash beds) of Pliocene and Pleistocene age in the western United States and southern Canada: U.S. Geological Survey Miscellaneous Investigations Map I-1325, scale 1:4,000,000.

Jackson, M. L., 1958, Soil Chemical Analysis: Englewood Cliffs, N.J., Prentice-Hall, 498 p.

Jenny, H., 1941, Factors of Soil Formation: New York, McGraw-Hill, 281 p.

Jenny, H., and Leonard, C. D., 1939, Functional relationships between soil properties and rainfall: Soil Science, v. 38, p. 368-381.

Johns, W. D., Grim, R. E., and Bradley, W. F., 1954, Quantitative estimations of clay minerals by diffraction methods: Journal of Sedimentary Petrology, v. 24, p. 242-251.

Krauskopf, K. B., 1967, Introduction to Geochemistry: New York, McGraw-Hill, 721 p.

Lamar, J. E., and Shrode, R. S., 1958, Water soluble salts in limestone and dolomite: Economic Geology, v. 48, p. 97-112.

Machette, M. N., 1978, Dating Quaternary faults in the southwestern United States by using buried calcic paleosols: U.S. Geological Survey Journal of Research, v. 6, p. 369-382.

——1985, Calcic soils and calcretes of the southwestern United States, in Weide, D. L., ed., Soils and Quaternary Geomorphology of the Southwestern United States: Geological Society of America Special Paper 203, p. 1-21.

Mackin, J. H., 1937, Erosional history of the Big Horn Basin, Wyoming: Geological Society of America Bulletin, v. 48, p. 813-894.

McFadden, L. D., and Tinsley, J. C., 1985, The rate and depth of pedogenic carbonate accumulation in soils: Formulation and testing of a compartment model, in Weide, D. L., ed., Soils and Quaternary Geomorphology of the Southwestern United States: Geological Society of America Special Paper 203, p. 23-41.

Mears, B., Jr., 1981, Periglacial wedges and the late Pleistocene environment of Wyoming's intermontane basins: Quaternary Research, v. 15, p. 171-198.

Moss, J. H., 1974, The relation of river terrace formation to glaciation in the Shoshone River basin, western Wyoming, in Coates, D., ed., Glacial Geomorphology: Binghamton, N. Y., Publications in Geomorphology, p. 293-314.

Moss, J. H., and Bonini, W. E., 1961, Seismic evidence supporting a new interpretation of the Cody terrace near Cody, Wyoming: Geological Society of America Bulletin, v. 72, p. 547-556.

Moss, J. H., and Whitney, J. H., 1971, Diversity of origin of the Cody and Powell terraces along the Shoshone River, Bighorn Basin, Wyoming: Geological Society of America Abstracts with Programs, v. 3, p. 652-653.

Muhs, D. R., 1982, A soil chronosequence on Quaternary marine terraces, San Clemente Island, California: Geoderma, v. 28, p. 257-283.

National Climatic Center, 1976, Climate of Lovell, Wyoming: National Oceanic and Atmospheric Administration, Climatography of the United States, no. 20.

Nelson, R. E., Klameth, L. C., and Nettleton, W. D., 1978, Determining soil gypsum content and expressing properties of gypsiferous soils: Soil Science Society of America Journal, v. 42, p. 659-661.

Nettleton, W. D., Flach, K. W., and Brasher, B. R., 1969, Argillic horizons without clay skins: Soil Science Society of America Proceedings, v. 33, p. 121-125.

Nettleton, W. D., Nelson, R. E., Brasher, B. R., and Derr, P. S., 1982, Gypsiferous soils in the western United States, in Kittrick, J. A., Fanning, D. S., and Hossner, L. R., eds., Acid Sulfate Weathering: Soil Science Society of America Special Publication no. 10, p. 147-168.

Page, W. D., 1972, The geological setting of the archeological site at Oued el Akarit and the paleoclimatic significance of gypsum soils, southern Tunisia: University of Colorado, Boulder, Ph.D. thesis, 111 p.

Palmquist, R. C., 1978, Ash dated terrace sequence in the eastern portion of the Big Horn Basin, Wyoming: Geological Society of America Abstracts with Programs, v. 10, p. 467.

——1979, Estimated ages of Quaternary terraces, northwestern Wyoming: Geological Society of America Abstracts with Programs, v. 11, no. 7, p. 491.

——1983, Terrace chronologies in the Bighorn Basin, Wyoming: Wyoming Geological Association Guidebook, 34th Annual Field Conference, p. 217-231.

Pierce, K. L., 1982, Glacial snowline changes: Effect of altitudinal precipitation gradients on paleotemperature calculations, western U. S.: Geological Society of America Abstracts with Programs, v. 14, no. 6, p. 345-346.

Pierce, K. L., Obradovitch, J. D., and Friedman, I., 1976, Obsidian hydration dating and correlation of Bull Lake and Pinedale glaciations near West Yellowstone, Montana: Geological Society of America Bulletin, v. 87, p. 702-710.

Pierce, W. G., 1978, Geologic map of the Cody $1^{\circ} \times 2^{\circ}$ quadrangle, northwestern Wyoming: U.S. Geological Survey Miscellaneous Field Studies Map MF-963, scale 1:250,000.

Reheis, M. C., 1984, Chronologic and climatic control

on soil development, northern Bighorn Basin, Wyoming and Montana: University of Colorado, Boulder, Ph.D. thesis, 346 p.
Reider, R. G., Kuniansky, N. J., Stiller, D. M., and Uhl, P. J., 1974, Preliminary investigation of comparative soil development on Pleistocene and Holocene geomorphic surfaces of the Laramie Basin, Wyoming, in Wilson, M., ed., Applied Geology and Archaeology: The Holocene History of Wyoming: Geological Survey of Wyoming Report of Investigations no. 10, p. 27-33.
Richmond, G. M., 1976, Pleistocene stratigraphy and chronology in the mountains of western Wyoming, in Mahaney, W. C., ed., Quaternary Stratigraphy of North America: Stroudsburg, Penn., Dowden, Hutchinson, and Ross, p. 353-379.
Rioux, R. L, 1958, Geology of the Spence-Kane area, Big Horn County, Wyoming: U.S. Geological Survey Open-File Report 58-84.
Ritter, D. F., and Kauffman, M. E., 1983, Terrace development in the Shoshone River vally near Powell, Wyoming, and speculations concerning the sub-Powell terrace: Wyoming Geological Association Guidebook, 34th Annual Field Conference, p. 197-203.
Salter, P. J., and Williams, J. B., 1967, The influence of texture on the moisture characteristics of soils, IV. A method of estimating the available-water capacities of profiles in the field: Journal of Soil Science, v. 18, p. 174-181.
Shackleton, N. J., and Opdyke, N. D., 1976, Oxygen-isotope and paleomagnetic stratigraphy of Pacific Core V28-239, late Pliocene to latest Pleistocene, in Cline, R. M., and Hays, J. D., eds., Investigation of Late Quaternary Paleoceanography and Paleoclimatology: Geological Society of America Memoir 145, p. 449-464.
Shlemon, R. J., 1978, Quaternary soil-geomorphic relationships, southeastern Mojave Desert, California and Arizona, in Mahaney, W. C., ed., Quaternary Soils: Norwich, England, Geoabstracts, p. 187-207.
Smeck, N. E., and Wilding, L. P., 1980, Quantitative evaluation of pedon formation in calcareous glacial deposits in Ohio: Geoderma, v. 24, p. 1-16.
Soil Survey Staff, 1975, Soil Taxonomy: U.S. Department of Agriculture, Soil Conservation Service, Agriculture Handbook 436, 754 p.
Stevens, R. E., and Carron, M. K., 1948, Simple field test for distinguishing minerals by abrasion pH: American Mineralogist, v. 33, p. 31-49.
Taggart, J. E., Jr., Lichte, F. E., and Wahlberg, J. S., 1981, Methods of analysis of samples using X-ray fluorescence and induction-coupled plasma spectroscopy, in Lipman, P. W., and Mullineaux, D. R., eds., The 1980 Eruptions of Mount St. Helens, Washington: U.S. Geological Survey Professional Paper 1250, p. 683-687.
Trembour, F. W., Friedman, L, Jurseka, F. J., and Smith, F. L., 1986, A simple device for integrating temperature, relative humidity and salinity over time: Journal of Climate and Applied Meteorology, v. 3, p. 186-190.
van Hylckama, T. E. A., 1959, A nomogram to determine monthly potential evapotranspiration: Monthly Weather Review, v. 87, p. 107-110.
Walker, D. N., 1982, A late Pleistocene Ovibos from southeastern Wyoming: Journal of Paleontology, v. 56, p. 486-491.
Watson, A., 1979, Gypsum crusts in deserts: Journal of Arid Environments, v. 2, p. 3-20.
Whittig, L. D., 1965, X-ray diffraction techniques for mineral identification and mineralogical composition, in Black, C. A., ed., Methods of Soil Analysis, Part 1, American Society of Agronomy, Monograph Series no. 9, p. 671-698.
Wilding, L. P., Drees, L. R., Smeck, N. E., and Hall, G. F., 1971, Mineral and elemental composition of Wisconsin-age till deposits in west-central Ohio, in Goldthwait, R. P., ed., Till—A Symposium: Columbus, Ohio State University Press, p. 290-317.
Winkler, E. M., 1975, Stone: Properties, Durability in Man's Environment: New York, Springer-Verlag, 230 p.

FIELD METHODS AND CALCULATIONS

Sampling and Description

Soils developed on the Kane fans were sampled in hand-dug holes or backhoe pits at sites that appeared least affected by erosion or deposition subsequent to abandonment of each fan surface (fig. 2 and supplementary table 1). These sites were supplemented by exposures in an ash pit (B-7) and a diversion ditch (B-6A). I sampled at least two soils on each fan, except fans 1 and 4, to assess soil variability. Four soils appear to have undergone slight truncation of the upper parts of the B horizons (supplementary tables 1 and 2). Humans probably truncated B-5, located near a parking area, and B-6A, on the sloping side of a diversion ditch. The surface of fan 7 is more bouldery and dissected than the others; thus, soils B-4 and B-19 may have been eroded. Alkali springs are just east of remnants of fans 4 and 5. In order to minimize possible groundwater effects, soils B-16, B-17, and B-7 were sampled as far away from the springs as possible. The surfaces of these fans at their westward ends are presently well above any potential groundwater influence, but earlier alteration could have occurred when the fans were less dissected.

Horizon nomenclature and soil property descriptions follow Soil Survey Staff (1975) usage, with the exception of texture modifiers describing gravel content. Field textural descriptions (determined by hand) in supplementary table 2 were not corrected using laboratory-determined carbonate-free particle-size data, because removal of carbonates prior to laboratory work resulted in removal of the limestone and dolomite parent material. Hand-determined field textures are influenced not only by carbonates, but also by the feel of gypsum crystals in gypsum-rich horizons. Moist and dry colors were obtained with a Munsell soil color chart. pH was determined in the laboratory with a pH meter. $CaCO_3$ stages follow those proposed by Bachman and Machette (1977). I adapted gypsum stages (fig. 6) from $CaCO_3$ stage descriptions as follows:

I—thin, discontinuous coatings on lower surfaces of stones

II—abundant gypsum pendants under stones;

gypsum crystals scattered through matrix or forming small, soft powdery nodules

III--gypsum continuous through matrix and forming large (up to 10 cm long) pendants under stones

IV--continuous gypsum-plugged fabric; stones and smaller debris float in gypsum matrix

Index of Soil Development

Soil field data, which are measured mainly on ordinal scales, were converted to ratio data using Harden's (1982a) index of soil development, in which a point system is used to quantify various field properties of soils. Points for each horizon are then normalized to give all properties equal weight and multiplied by the horizon thickness; the products are summed for each soil. Thus, individual properties can be examined with depth in one soil or compared between soils, or several properties can be combined to obtain a total profile-development index value for each soil. (See flow diagram in Harden and Taylor, 1983).

I have modified Harden's index for the Kane fans. The change of pH in the index is assessed in terms of pH lowering, and this works well in relatively moist environments. In the case of soils developed on the Kane fans, however, I believe that pH increases with soil age, because of the aridity and sparse vegetation of the area and because of the availability of $CaCO_3$. This phenomenon occurs in semiarid soils along Rock Creek, Mont. (Reheis, 1984). The change in pH for the Kane fans, therefore, was shown as a pH increase from the parent material state. A value of 1.5 was used as the normalization value for pH increase, because it was the maximum pH increase observed in soils of the northern Bighorn Basin (Reheis, 1984).

It is very difficult to assess parent-material pH for the Kane fan soils. The pH of basal C horizons of the young soils on fans 1-3 is about 8.4. If this value accurately reflects parent-material pH, then nearly all the soil horizons show decreases in pH (supplementary table 3). Such a trend is inconsistent with observations of calcareous soils made elsewhere (Reheis, 1984). In theory, the pH in calcareous soils is unlikely to decrease unless leaching is sufficient to remove a significant proportion of the exchangeable Ca^{+2} ions (Birkeland, 1984, p. 22-23). Thus, I believe that the pH of 8.4 representing the lowest depths sampled in young Kane fan soils is a pedogenic product; consequently the original pH is likely less than 8.4. The mean pH of leachate from limestone is about 7.9, whereas the mean pH of leachate from dolomite is about 8.5 (Lamar and Shrode, 1958). As limestone is slightly more soluble than dolomite, weathering of limestone probably dominates soil pH on the Kane fans. These considerations led me to select arbitrarily a value of 8.0 as the parent-material pH in order to calculate pH increase for these soils. Perhaps coincidentally, this pH value is the same as the mean pH of the calcareous A horizons of Kane fan soils.

Dust Traps

Dust traps were set out in three locations on the fans (fig. 2) to assess aerosolic additions to the soils. Plastic-lined aluminum trays, 29.5 x 29.5 x 6.5 cm in size, were filled with marbles and mounted on poles about 2 m above the ground (Gile and Grossman, 1979). After one year, two traps were removed (the third was destroyed by high winds), and the dust was collected by washing the traps and marbles with distilled water.

Water Movement

Arkley's (1963) method of calculating water movement in soils was used to examine the relationship of local climate to the depth of $CaCO_3$ or gypsum accumulation. Month-by-month precipitation data for the 24-year record at Lovell and average monthly potential evapotranspiration (using van Hylckama's method, 1959) were used to calculate monthly excesses of precipitation over evaporation—that is, the depth of water available to wet the soil in a given month. The average amount of water per year that passes any given depth in a soil can then be calculated. If the available water-holding capacity (AWC) of the various horizons is known or can be estimated, the amount of water can be plotted against actual soil depth. I estimated AWC of the Kane fan soils from field textural data using Salter and Williams' (1967) method. They state that their method has a mean error of ±17 percent using a 12 textural-class (field) system.

Depression of $CaCO_3$ Solubility by Gypsum

Solubilities of gypsum (Sg) and $CaCO_3$ (Sc) at 25°C are calculated from their solubility products (Kg, Kc) as follows (Krauskopf, 1967):

$$Kg = (Sg)^2 = (Ca^{2+})(SO_4^{2-}) = 2.51\times10^{-5} \text{ mol/L}$$

$$Sg = (2.51\times10^{-5})^{0.5} = 5.00\times10^{-3} \text{ mol/L}$$

$$Kc = (Sc)^2 = (Ca^{2+})(CO_3^{2-}) = 6.03\times10^{-9} \text{ mol/L}$$

$$Sc = (6.03\times10^{-9})^{0.5} = 7.76\times10^{-5} \text{ mol/L}$$

If a solution is saturated with respect to gypsum, the concentration of Ca^{2+} in solution is 5.0×10^{-3} mole/liter. Let $\underline{x}$ equal the solubility of $CaCO_3$ in this gypsum-saturated solution; then

$$Kc = (Ca^{2+})(CO_3^{2-}) = (\underline{x}+5.0\times10^{-3})\underline{x}$$
$$= \underline{x}^2+5.0\times10^{-3}\underline{x} = 6.03\times10^{-9} \text{ mol/L}$$

$\underline{x}$ will not be larger than the solubility of $CaCO_3$ in pure water, so the term $\underline{x}^2$ is small enough to be ignored. Then

$$5.0\times10^{-3}\underline{x} = 6.03\times10^{-9} \text{ mol/L}$$
$$\underline{x} = 1.21\times10^{-6} \text{ mol/L}$$

These calculations indicate that the solubility of $CaCO_3$ is depressed by a factor of 64 in the presence of a solution saturated with gypsum at 25°C.

SUPPLEMENTARY TABLES

Supplementary Table 1, Part 1. Sample locations and site conditions

Site	Geologic Unit	Elevation (ft)	Modern vegetation[1]	Modern land use	Type of excavation	Parent material texture[2]	Location (Montana Base Meridian)
B-21	Fan 1	3,735	cactus, sagebrush, grasses	grazing	hand-dug hole	gr/S,Si	SE/4,SE/4,NE/4, Sec. 4, T. 56 N., R. 94 W.
B-5	Fan 2	3,667	cactus, sagebrush, grasses	grazing	hand-dug hole	gr/S,Si	NW/4,SW/4,SE/4, Sec. 4, T. 56 N., R. 94 W.
B-15	Fan 2	3,735	cactus, sagebrush, grasses	grazing	backhoe pit	gr/S,Si	NE/4,NE/4,SE/4, Sec. 4, T. 56 N., R. 94 W.
B-6A	Fan 3	3,715	cactus, sagebrush, grasses	grazing	diversion ditch	gr/S,Si	NE/4,SW4,NE/4, Sec. 4, T. 56 N., R. 94 W.
B-14	Fan 3	3,725	cactus, sagebrush, grasses	grazing	backhoe pit	gr/S,Si	SW/4,SW/4,SW/4, Sec. 3, T. 56 N., R. 94 W.
B-16	Fan 4	3,920	cactus, sagebrush, grasses	grazing	backhoe pit	gr/S,Si	SW/4,NE/4,NE/4, Sec. 3, T. 56 N., R. 94 W.
B-17	Fan 5	3,945	cactus, sagebrush, grasses	grazing	backhoe pit	gr/S,Si	NW/4,NE/4,NE/4, Sec. 3, T. 56 N., R. 94 W.
B-7	Fan 5	3,970	cactus, sagebrush, grasses	grazing	hand-dug hole and ash pit	gr/S,Si	NW/4,NW/4,NW/4, Sec. 2, T. 56 N., R. 94 W.
B-3	Fan 6	4,205	cactus, sagebrush, grasses	grazing	hand-dug hole	gr,L	NE/4,NW/4,SW/4, Sec. 1, T. 56 N. R. 94 W.
B-18A	Fan 6	4,085	cactus, sagebrush, grasses	grazing	backhoe pit	gr,L	NW/4,NE/4,NW/4, Sec. 11, T. 56 N., R. 94 W.
B-18B	Fan 6	4,085	cactus, sagebrush, grasses	grazing	backhoe pit	gr,L	NW/4,NE/4,NW/4, Sec. 11, T. 56 N., R. 94 W.
B-4	Fan 7	4,145	cactus, sagebrush, grasses	grazing	hand-dug hole	gr,L	NE/4,SW/4,NE/4, Sec. 11, T. 56 N., R. 94 W.
B-19	Fan 7	4,180	cactus, sagebrush, grasses	grazing	backhoe pit	gr,L	NE/4,SE/4,NE/4, Sec. 11, T. 56 N., R. 94 W.

[1]Percent bare ground is 50 percent or greater at all sites.

[2]Textures: gr/S, gravel and sand; L, loam; Si, silt.

Supplementary Table 1, Part 2. Field descriptions

[--, not measured. Analyst: M. C. Reheis, U.S. Geological Survey]

No.	Sample Number	Horizon	Depth (cm)	Lower Boundary	Moist Color	Dry Color	Texture	Structure	Wet Consistence	Clay Films	pH	Assumed Parent Material (<2mm) Texture	Assumed Parent Material (<2mm) Wet Consistence	Stage $CaCO_3$	Stage Gypsum
						Fan 1, 5 ka									
1	B-21	A	0-6	c,w	7.5YR4/3.5	7.5YR5.5/3.5	gSL	1fpl,v	so,po	0	7.7	SL	so,po	0	0
2		2Btca	6-13	c,w	7.5YR4.5/4	7.5YR5.5/4	gSL-	1gr	so,po	0	8.0	LS	so,po	I	0
3		2Cca	13-33	c,s	7.5YR5/3	7.5YR6.5/3	vgSL	m	so,po	0	8.1	LS	so,po	I+	0
4		2Cn	33-73+	--	7.5YR5/3	7.5YR5.5/3	vgLS	m	so,po	0	8.4	LS	so,po	0	0
						Fan 2, 65 ka									
5	B-5	A	0-3	c,w	--	--	sgL	v	so,po	0	--	SL	so,po	0	0
6		B2tca	3-11	d	7.5YR4.5/6	7.5YR5.5/6	sgL	2mabk	ss,ps	0	8.6	SL	so,po	I	0
7		B3tca	11-20	a,s	7.5YR5/4	7.5YR6.5/5	sgSL+	1fsbk	ss,ps	0	8.4	SL	so,po	II	0
8		2C1ca	20-31	d	7.5YR6.5/4	7.5YR7/4	vgSL	m	ss,po	0	8.6	SL	so,po	I	0
9		2C2ca	31-46	d	7.5YR5/4	7.5YR6/4	vgSL	m	ss,po	0	8.9	SL	so,po	I	0
10		2C3ca	46-71+	--	7.5YR5/4	7.5YR6/5	vgLS	m	so,po	0	8.9	LS	so,po	I-	0
11	B-15	A	0-4	a,s	7.5YR4.5/4	8.25YR6/4	gSL	2fpl,v	so,po	0	8.3	SL	so,po	0	0
12		B1	4-12	g	7.5YR4.5/4	7.5YR4.5/4	sgfSL	1fsbk,1fpl	ss,ps	0	8.2	SL	so,po	0	0
13		B2tca	12-24	c,w	7.5YR4.5/4	7.5YR4.5/4	gfSL	1fsbk	ss,ps	0	8.1	SL	so,po	I	0
14		2B3tca	25-45	d	7.5YR5/4	7.5YR6/3	vgSL	1gr	ss,ps	0	8.1	LS	so,po	II-	0
15		2Cca	45-65	d	7.5YR4.5/3	7.5YR5/3	vgLS	sg,m	so,po	0	8.5	LS	so,po	I	I-
16		2Cn	65-165+	--	7.5YR4/3	8.25YR5/2.5	vgLS	m	so,po	0	8.4	LS	so,po	I-	I-
						Fan 3, 100 ka									
17	B-6A	A	0-4	a,s	7.5YR4.5/4	7.5YR5.5/3	gL	v	so,po	0	8.1	SL	so,po	0	0
18		B2tca	4-29	a,w	7.5YR4/4	7.5YR5/4	sgL	1fabk	ss,ps	0	8.1	SL	so,po	I	0
19		2B3tca	29-46	a,w	7.5YR5/3	7.5YR6/3	vgSCL	1gr	s,p	0	8.3	SL	so,po	II	0
20		2Cca	46-88	d	5YR5.5/4	5YR5.5/3.5	vgSL	m	ss,po	0	8.2	SL	so,po	I	I-
21		2C1csca	88-181	d	5YR5/5	5YR5.5/3.5	vgSL	m	ss,po	0	8.2	SL	so,po	I	I
22		2C2cs	181-242+	--	5YR5/4	5YR5.5/3	vgLS	m	so,po	0	8.1	LS	so,po	0	I-
23		base of fan 3		d	10YR6/4	7.5YR7/4	vgLS	m	so,po	0	8.5	LS	so,po	0	0
24	B-14	A11	0-4	c,s	7.5YR4/3	7.5YR5.5/3.5	sgSL	2mgr,1fpl	so,po	0	8.0	SL	so,po	0	0
25		A12	4-8	a,s	7.5YR4.5/4	7.5YR5.5/3	sgfSL	2fpl	so,po	0	8.0	SL	so,po	0	0
26		B1	8-17	a,s	7.5YR5/4	7.5YR5/3	sgL	1fsbk	ss,ps	0	8.0	SL	so,po	0	0
27		B21tca	17-28	c,i	7.5YR4.5/4	7.5YR5/4	sgL	1f-mabk,1mpr	ss,p	0	8.1	SL	so,po	I	0
28		B22tca	28-44	a,s	7.5YR4.5/4	7.5YR5/4	sgL	1f-mabk,1mpr	ss,ps	0	8.1	SL	so,po	I+	0
29		2B3tca	44-70	d	7.5YR5/4	7.5YR6/3	vgSL-	sg,1fabk	ss,po	0	8.4	LS	so,po	II	0
30		2Cca	70-123	d	7.5YR4.5/4	7.5YR5/3.5	vgLS	m	so,po	0	8.4	LS	so,po	I	I-
31		2Cnca	123-193+	--	7.5YR4/3	7.5YR5/3	vgLS	m	so,po	0	8.3	LS	so,po	I-	I-
						Fan 4, 315 ka									
31	B-16	A11	0-4	c,s	7.5YR4.5/4	7.5YR5.5/3	gSL	v	ss,po	0	8.0	SL	so,po	0	0
33		A12	4-9	c,s	6.25YR5/4	7.5YR5.5/3	gSL+	2gr,v	ss,ps	0	8.0	SL	so,po	0	0
34		Bt	9-12	a,s	--	--	gSL+	1fsbk,sg	ss,p	0	8.1	SL	so,po	0	0
35		Btca	12-28	g,w	7.5YR6/4	7.5YR6/3	gSL+	1fsbk,sg	ss,p	0	8.1	SL	so,po	I	0
36		Ccacs	28-75	d	7.5YR7/4	7.5YR7/3	gSCL	m	s,p	0	8.4	SL	ss,ps	II	II
37		2C1csca	75-137	d	5YR6/4	5YR6/3	vgSCL-	m	s,p	0	8.5	SL	ss,ps	I	II
38		2C2cs	137-237+	--	3.75YR5/6	2.5YR5.5/4	vgSCL-	m	s,p	0	8.6	SL	ss,ps	0	I+
						Fan 5, 410 ka									
39	B-7	A	0-6	a,s	7.5YR5/6	7.5YR6/6	gL	1gr,v	ss,ps	0	7.8	SL	so,po	0	0
40		C1csca	6-30	d	7.5YR7/6	7.5YR8/4	sgSL	m	so,po	0	8.0	LS	so,po	II	II+
41		2C2csca	30-50	d	5YR6/7	5YR8/6	gSL+	m	so,po	0	8.0	LS	so,po	II	III
42		2C3csca	50-83	g	5YR6/6	5YR7/4	gSL-	m	so,po	0	8.3	LS	so,po	I	II
43		2C4cs	83-198+	--	4YR5/6	4YR6/6	gSL-	m	so,po	0	8.5	LS	so,po	0	II
44	B-17	A11	0-4	c,s	7.5YR5/4	7.5YR6/3	gSL+	1fpl,v	ss,ps	0	8.1	SL	so,po	0	0
45		A12	4-10	a,w	7.5YR4.5/4	7.5YR5.5/3	sgL	1gr	ss,p	0	8.1	SL	so,po	0	0
46		Btca	10-19	c,w	5YR5.5/4	5YR5.5/3	gSCL	2msbk	s,p	0	8.0	SL	so,po	II	0
47		2C1csca	19-40	g	5YR6/4	5YR7/3	gSL	m	so,po	0	8.1	LS	so,po	I	IV
48		2C2csca	40-89	g	5YR2.5/6	2.5YR6/4	vgSL	m	so,po	0	8.1	LS	so,po	I	II+
49		2C3cs	89-179	d	5YR5.5/6	5YR6/4	vgSL-	m	so,po	0	8.5	LS	so,po	0	II
50		2C4cs	179-249+	--	5YR5/6	2.5YR6/4	vgSL-	m	so,po	0	8.3	LS	so,po	0	I+

Supplementary Table 1, Part 2. Field descriptions--Continued

No.	Sample Number	Horizon	Depth (cm)	Lower Boundary	Moist Color	Dry Color	Texture	Structure	Wet Consistence	Clay Films	pH	Assumed Parent Material (<2mm) Texture	Assumed Parent Material (<2mm) Wet Consistence	Stage $CaCO_3$	Stage Gypsum
						Fan 6, 505 ka									
51	B-3	A	0-4	c,s	--	--	gSL	v	so,po	0	--	SL	so,po	0	0
52		Btca	4-24	c,s	5YR5/6	7.5YR6/6	sgfSL	1fsbk	ss,p	0	8.0	SL	so,po	II	0
53		C1csca	24-42	g	7.5YR6/6	7.5YR7/4	sgSL	m	ss,ps	0	7.9	SL	so,po	I	IV
54		2C2cs	42-62	c,w	7.5YR5/6	7.5YR6/5	sgL	m	ss,p	0	8.0	L	ss,ps	0	II
55		2C3cs	62-67+	--	2.5YR5/8	5YR6/8	sgL	m	s,p	0	8.1	L	ss,ps	0	II
56	B-18A	A11	0-2	a,s	7.5YR4.5/4	7.5YR5.5/3	gL	1fpl,v	ss,ps	0	8.1	L	so,po	0	0
57		A12	2-5	a,s	7.5YR5/4	7.5YR6/3	sgL	1gr,1fpl	ss,ps	0	8.1	L	so,po	0	0
58		Btca	5-10	a,w	5YR5.5/4	6.25YR6/4	gSCL	1gr,1fsbk	s,p	0	8.0	L	so,po	I+	0
59		2C1csca	10-37	g	5YR6/4	5YR7/3	gSL	m	ss,po	0	8.2	SL	ss,ps	I	IV
60		2C2cs	37-46	d	5YR5.5/4	5YR6.5/3	gSCL-	m	s,ps	0	8.1	SL	ss,ps	0	II+
61		2C3cs	46-86+	--	3.25YR5/7	3.25YR5/6	vgSCL	m	s,p	0	8.1	SL	ss,ps	0	II
62	B-18B	A	0-6	c,s	--	--	gL	1fpl,v	so,po	0	--	SL	so,po	0	0
63		Btca	6-22	c,w	6.25YR4/5	6.25YR5/4	sgSCL	2msbk	s,p	0	7.9	SL	so,po	I	0
64		2C1csca	22-51	c,w	5YR5/5	5YR6.5/4	sgSL	m	so,po	0	8.0	SL	so,po	I	IV
65		2C2cs	51-75	c,w	5YR4/6	5YR5.5/3	sgSCL	m	s,p	0	8.2	SL	ss,ps	0	II+
66		2C3cs	75-130	a,s	5YR4/8	5YR5/4	vgSL+	m	ss,po	0	8.3	SL	so,po	0	II
67		2C4cs	130-255+	--	3.25YR4/6	3.25YR5/4	vgSCL	m	s,ps	0	8.3	SL	ss,ps	0	I
						Fan 7, 585 ka									
68	B-4	A	0-6	a,s	7.5YR5/4	7.5YR6/4	sgSiL	v	so,po	0	8.0	SL	so,po	0	0
69		B21tcacs	6-12	a,w	7.5YR5/5	7.5YR5.5/6	gSiCL	1msbk	ss,p	0	7.7	SL	so,po	II	I
70		B22tcsca	12-30	g	7.5YR5/6	5YR8/3	gSCL	1msbk,m	s,p	0	7.8	SL	so,po	I	III
71		2C1csca	30-55	d	7.5YR5/6	7.5YR6/6	gSL	m	so,po	0	7.9	SL	so,po	I	IV
72		2C2cs	55-75+	--	7.5YR5/6	7.5YR5/6	gL	m	ss,ps	0	8.0	SL	ss,ps	0	III
73	B-19	A	0-6	a,s	7.5YR4.5/6	7.5YR5.5/4	gL	1fpl,v	so,po	0	8.1	L	so,po	0	0
74		B21tca	6-14	a,i	7.5YR4.5/6	7.5YR5/5	gL+	1fsbk	ss,ps	0	8.0	L	so,po	I	0
75		B22tcsca	14-25	c,w	7.5YR5/5	7.5YR6/4	gL-	1gr	ss,ps	0	8.0	L	so,po	I	II
76		2C1csca	25-40	d	7.5YR5/4	7.5YR6/3	gSL	m	so,po	0	8.1	SL	so,po	0	IV
77		2C2cs	40-85	d	5YR5/6	5YR5.5/4	vgSCL	m	s,p	0	8.1	SL	so,po	0	III
78		2C3cs	85-137	d	5YR4/5	5YR5/4	gSL-	m	so,po	0	8.2	SL	so,po	0	II
79		3C4cs	137-262+	--	5YR4/6	5YR5/5	vgSL	m	so,po	0	8.2	SL	so,po	0	I

EXPLANATION[1]

SOIL STRUCTURE

Grade	Size	Type
m, massive	vf, very fine (v thin)	gr, granular
sg, single grained	f, fine (thin)	pl, platey
1, weak	m, medium	pr, prismatic
2, moderate	c, coarse (thick)	cpr, columnar
3, strong	vc, very coarse (very thick)	abk, angular blocky
		sbk, subangular blocky

If two structures, listed as primary and secondary

SOIL TEXTURE

vsg, very slightly gravelly (<5%)	co, coarse	S, sand	SCL, sandy clay loam
sg, slightly gravelly (5-20%)	f, fine	LS, loamy sand	CL, clay loam
g, gravelly (20-50%)	vf, very fine	SL, sandy loam	SiCL, silty clay loam
vg, very gravelly (>50%)		L, loam	SC, sandy clay
		SiL, silt loam	C, clay
		Si, silt	SiC, silty clay

SOIL CONSISTENCE

Wet	
so, nonsticky	po, nonplastic
ss, slightly sticky	ps, slightly plastic
s, sticky	p, plastic
vs, very sticky	vp, very plastic

HORIZON BOUNDARIES

Distinctness	Topography
va, very abrupt	s, smooth
a, abrupt	w, wavy
c, clear	i, irregular
g, gradual	b, broken
d, diffuse	

CLAY FILMS

Frequency	Thickness	Morphology
v_1, very few	n, thin	pf, ped face coatings
1, few	mk, moderately thick	br, bridging grains
2, common	k, thick	po, pore linings
3, many		(w, occurs as waves or lamellae)
4, continuous		co, coats on clasts

STAGES OF $CaCO_3$ AND GYPSUM[2]

Roman numerals indicate increasing content of $CaCO_3$ or gypsum

---

[1]For more detailed information, see Soil Survey Staff (1975) and Birkeland (1984).
[2]For more detailed information, see section on "Field Methods and Calculations", and Bachman and Machette (1977).

Supplementary Table 2. Physical properties

[--, not measured. Analyst: M. C. Reheis, U.S. Geological Survey]

Methods

Bulk density was determined by two different methods (Blake, 1965). Two to four paraffin-coated peds taken from relatively fine-textured horizons provided mean bulk densities for A, B, and some C horizons. Bulk density was measured on many gravelly C horizons in the field by weighing an excavated amount of soil and measuring the volume of the hole with water-filled plastic bags. For C horizons not measured by either of these methods, bulk density was estimated by comparison to horizons with similar gravel contents.

Gravel percent by volume was visually estimated for all horizons. Gravels were separated and weighed from bulk samples of finer textured horizons to obtain gravel weight percent as a check on the visual estimate.

Particle size of the <2-mm fraction was obtained by methods described in Day (1965). All samples were pretreated to remove organic matter by gentle heating in a weak solution of hydrogen peroxide. Gypsum and carbonates were removed from samples by gentle heating in a weak solution of sodium acetate. This method was time-consuming and required frequent washing and replacement of the solution. The sand fraction was separated by wet sieving; the dried sand was weighed and dry-sieved to obtain the various sand fractions. Silt and clay fractions were obtained by the pipette method, except for dust-trap samples, for which there was insufficient material after removal of gypsum and $CaCO_3$. Sand was removed from both dust-trap samples by wet sieving, and the remaining sediment was combined to determine silt and clay fractions using the 5000b Sedigraph Analyzer (analyses by R. Kihl, Institute of Arctic and Alpine Research, Boulder, Colo.).

No.	Sample No.	Horizon	Basal depth (cm)	>2mm (%)	percentage of <2-mm fraction: Total sand	vco sand	co sand	med sand	fi sand	vfi sand	Total silt	<2μ clay	<1μ clay	Bulk density (g/cm³)	percentage of <2-mm fraction: co silt	med silt	vfi silt	coclay (2-.5μ)	ficlay (<.5μ)
									Fan 1, 5 ka										
1	B-21	A	6	40	44.31	0.56	1.63	2.67	16.42	23.02	41.74	13.95	10.39	1.6	31.34	7.18	3.23	--	--
2	B-21	2Btca	13	80	31.74	0.12	1.12	2.36	11.54	16.60	41.14	27.12	22.46	2.0	30.00	7.21	3.94	--	--
3	B-21	2Cca	33	80	37.66	3.66	5.85	5.66	11.87	10.63	48.99	13.35	13.35	1.6	35.32	9.58	4.10	--	--
4	B-21	2Cn	+73	90	37.77	3.92	7.77	6.60	11.54	7.94	55.58	6.65	6.65	2.1	47.09	7.11	1.37	--	--
									Fan 2, 65 ka										
5	B-5	A	3	--	--	--	--	--	--	--	--	--	--	--	--	--	--	--	--
6	B-5	B2tca	11	15	29.19	0.39	0.28	2.26	5.79	20.47	47.40	--	--	--	37.61	6.16	3.63	6.58	16.83
7	B-5	B3tca	20	15	38.63	0.16	0.58	7.11	13.07	17.71	42.79	--	--	--	33.62	6.30	2.87	2.58	16.00
8	B-5	2C1ca	31	80	50.52	1.39	2.63	6.59	21.71	18.20	34.12	--	--	--	20.14	13.98	0.00	5.24	10.12
9	B-5	2C2ca	46	80	55.23	3.44	4.05	8.25	22.23	17.26	31.78	--	--	--	19.13	8.12	4.53	6.81	6.18
10	B-5	2C3ca	+71	80	67.40	3.53	5.87	13.86	30.28	13.86	21.46	--	--	--	14.80	6.07	0.59	2.82	8.32
11	B-15	A	4	30	33.98	0.25	0.56	0.96	12.31	19.91	50.66	15.36	9.46	1.6	35.96	8.83	5.87	--	--
12	B-15	B1	12	10	33.65	0.19	0.40	0.99	12.10	19.96	50.28	16.06	11.49	1.6	35.68	14.59	0.00	--	--
13	B-15	B2tca	24	10	26.94	0.33	0.57	1.57	10.28	14.19	52.38	20.68	18.45	1.5	39.10	8.24	5.03	--	--
14	B-15	2B3tca	45	80	36.89	3.42	3.27	3.42	15.52	11.25	47.53	15.58	12.69	1.5	34.06	9.88	3.58	--	--
15	B-15	2Cca	65	80	36.02	2.49	5.22	5.33	12.22	10.75	47.92	16.06	11.07	2.1	26.90	13.79	7.23	--	--
16	B-15	2Cn	+165	80	45.68	3.64	5.45	5.48	18.65	12.46	38.73	15.59	11.03	2.1	24.26	2.67	11.80	--	--
									Fan 3, 100 ka										
17	B-6A	A	4	20	37.82	0.50	1.04	2.22	14.51	19.54	46.21	15.97	11.22	1.6	31.28	8.61	6.32	--	--
18	B-6A	B2tca	29	10	38.37	0.17	0.75	2.44	15.77	19.25	43.40	18.22	14.59	1.5	33.94	6.22	3.25	--	--
19	B-6A	2B3tca	46	70	39.83	1.11	2.00	4.42	18.60	13.69	41.09	19.08	15.87	1.5	31.32	7.24	2.53	--	--
20	B-6A	2Cca	88	80	31.27	2.45	3.36	3.35	12.71	9.40	42.51	26.24	21.92	2.0	31.26	7.51	3.74	--	--
21	B-6A	2C1csca	181	80	34.93	8.56	6.35	4.49	10.03	5.51	32.61	32.46	26.15	2.1	17.70	8.61	6.30	--	--
22	B-6A	2C2cs	+242	80	37.56	4.11	4.27	4.25	14.17	10.76	38.19	24.25	21.35	2.1	26.99	7.11	4.09	--	--
23	B-6A	base of fan 3		80	51.82	3.66	2.93	4.32	23.28	17.63	35.24	12.94	10.83	2.0	27.31	5.90	2.03	--	--
24	B-14	A11	4	10	50.09	0.49	1.12	2.39	18.20	27.89	41.06	8.86	7.62	1.6	32.23	5.99	2.84	--	--
25	B-14	A12	8	10	38.12	0.37	0.61	1.47	13.07	22.61	45.70	16.18	11.95	1.5	33.37	7.39	4.94	--	--
26	B-14	B1	17	10	34.66	0.18	0.39	1.20	11.13	21.76	46.23	19.11	17.34	1.5	33.98	8.28	3.97	--	--
27	B-14	B21tca	28	10	30.90	0.13	0.66	1.67	9.87	18.57	51.83	17.27	15.45	1.5	38.82	8.36	4.64	--	--
28	B-14	B22tca	44	15	30.87	0.20	0.51	1.30	9.66	19.21	50.62	18.51	15.72	1.5	38.88	7.51	4.23	--	--
29	B-14	2B3tca	70	80	56.88	1.48	6.53	14.25	22.32	12.30	28.89	14.22	13.10	1.8	18.42	7.00	3.47	--	--
30	B-14	2Cca	123	80	53.65	4.26	7.72	9.55	21.43	10.69	31.13	15.22	15.22	2.1	19.03	7.95	4.15	--	--
31	B-14	2Cnca	+193	80	44.69	4.82	8.24	7.24	15.60	8.80	34.76	20.56	17.68	2.1	19.32	9.60	5.84	--	--
									Fan 4, 315 ka										
32	B-16	A11	4	30	20.12	0.89	0.57	0.58	7.26	10.82	57.04	22.84	17.29	1.7	37.84	12.13	7.07	--	--
33	B-16	A12	9	30	19.00	0.21	0.33	0.45	6.82	11.18	58.53	22.47	16.47	1.5	39.35	11.52	7.65	--	--
34	B-16	Bt	12	25	19.39	0.46	0.63	0.73	7.26	10.31	46.84	33.77	28.93	1.3	33.44	8.46	4.94	--	--
35	B-16	Btca	28	25	19.39	0.46	0.63	0.73	7.26	10.31	46.84	33.77	28.93	1.3	33.44	8.46	4.94	--	--
36	B-16	Ccacs	75	25	21.72	1.56	2.09	2.28	8.87	6.91	38.76	39.52	37.03	1.7	22.89	15.87	0.00	--	--
37	B-16	2C1csca	137	50	21.05	2.21	1.74	1.45	7.46	8.19	38.50	40.46	38.08	1.7	25.67	8.79	4.04	--	--
38	B-16	2C2cs	+237	80	20.23	1.56	2.32	2.06	8.61	5.69	33.24	46.52	44.85	2.1	19.47	8.04	5.73	--	--

Supplementary Table 2. Physical properties—Continued

No.	Sample No.	Horizon	Basal depth (cm)	>2mm (%)	percentage of <2-mm fraction: Total sand	vco sand	co sand	med sand	fi sand	vfi sand	Total silt	<2μ clay	<1μ clay	Bulk density (g/cm³)	percentage of <2-mm fraction: co silt	med silt	vfi silt	coclay (2-.5μ)	ficlay (<.5μ)
Fan 5, 410 ka																			
39	B-7	A	6	20	29.67	0.56	0.50	0.64	9.01	18.96	42.21	--	--	--	26.50	11.24	4.47	9.77	18.35
40	B-7	C1csca	30	15	28.28	1.41	2.28	2.46	10.50	11.63	33.53	--	--	--	15.36	10.06	8.11	13.01	25.18
41	B-7	2C2csca	50	30	21.44	1.31	1.16	1.49	6.68	10.80	51.87	--	--	--	25.54	15.22	11.11	10.40	16.29
42	B-7	2C3csca	83	40	28.38	2.33	2.10	2.59	9.86	11.50	41.41	--	--	--	26.23	7.59	7.59	12.87	17.34
43	B-7	2C4cs	+198	40	47.21	2.64	2.16	2.02	19.13	21.26	31.93	--	--	--	19.83	7.18	4.92	5.25	15.61
44	B-17	A11	4	10	24.22	--	--	--	--	--	55.00	20.78	15.03	1.7	35.03	12.31	7.66	--	--
45	B-17	A12	10	10	25.14	0.44	1.07	1.96	11.55	10.11	47.88	26.99	19.79	1.5	25.26	14.68	7.94	--	--
46	B-17	Btca	19	15	18.35	0.74	0.98	1.54	8.02	7.08	52.96	28.69	23.47	1.3	34.22	12.95	5.78	--	--
47	B-17	2C1csca	40	20	31.32	--	--	--	--	--	33.88	34.81	32.80	1.4	20.94	6.86	6.08	--	--
48	B-17	2C2csca	89	65	32.62	4.36	3.52	2.91	13.05	8.79	35.01	32.35	31.87	1.8	23.08	7.17	4.76	--	--
49	B-17	2C3cs	179	65	36.57	3.20	3.69	3.79	15.49	10.40	35.68	27.75	27.25	2.0	25.90	7.16	2.61	--	--
50	B-17	2C4cs	+249	80	32.61	4.64	3.44	2.63	12.22	9.68	42.23	25.16	22.23	2.1	30.01	7.78	4.44	--	--
Fan 6, 505 ka																			
51	B-3	A	4	--	--	--	--	--	--	--	--	--	--	--	--	--	--	--	--
52	B-3	Btca	24	15	27.86	0.88	0.53	0.68	9.17	16.60	41.88	--	--	--	25.12	10.94	5.82	8.76	21.50
53	B-3	C1csca	42	15	21.46	0.35	0.26	0.42	6.81	13.62	49.08	--	--	--	17.83	15.64	15.61	13.31	16.15
54	B-3	2C2cs	62	15	26.38	0.21	0.40	0.79	9.04	15.94	52.72	--	--	--	24.59	16.29	11.84	12.18	8.72
55	B-3	2C3cs	+67	10	21.67	0.66	1.31	1.76	8.67	9.27	44.79	--	--	--	26.42	4.95	13.42	10.14	23.40
56	B-18A	A11	2	20	28.45	1.04	0.84	1.92	12.16	12.48	50.47	21.07	15.00	1.7	35.01	10.82	4.64	--	--
57	B-18A	A12	5	10	24.60	0.72	0.65	1.50	10.87	10.86	50.70	24.70	17.89	1.5	33.83	11.20	5.67	--	--
58	B-18A	Btca	10	20	25.61	1.03	1.02	2.32	11.55	9.68	39.03	35.36	30.90	1.3	25.87	8.90	4.26	--	--
59	B-18A	2C1csca	37	20	36.78	2.68	1.72	3.42	19.47	9.49	39.94	23.28	17.50	1.5	22.28	9.25	8.41	--	--
60	B-18A	2C2cs	46	20	33.83	2.27	1.55	3.55	15.25	11.21	34.09	32.09	28.90	1.5	26.57	6.41	1.10	--	--
61	B-18A	2C3cs	+86	50	37.38	1.20	1.70	4.14	18.12	12.22	35.54	27.08	25.11	2.0	23.97	7.55	4.02	--	--
62	B-18B	A	6	20	--	--	--	--	--	--	--	--	--	--	--	--	--	--	--
63	B-18B	Btca	22	20	27.95	0.63	0.78	2.52	11.65	12.36	40.46	31.59	27.93	1.5	26.34	7.71	6.42	--	--
64	B-18B	2C1csca	51	25	28.61	0.60	0.85	2.75	15.33	9.08	31.65	39.74	35.81	1.7	24.27	4.89	2.49	--	--
65	B-18B	2C2cs	75	5	36.52	1.11	1.08	3.53	19.52	11.29	33.98	29.50	27.96	1.5	21.24	9.23	3.52	--	--
66	B-18B	2C3cs	130	60	42.30	6.06	4.85	6.61	16.16	8.62	31.54	26.15	22.28	2.0	20.15	8.54	2.86	--	--
67	B-18B	2C4cs	+255	70	35.68	3.23	3.01	5.18	15.25	9.01	37.86	26.46	23.56	2.1	24.12	8.75	4.99	--	--
Fan 7, 585 ka																			
68	B-4	A	6	15	28.74	1.32	0.77	1.65	11.05	13.95	45.23	--	--	--	26.02	12.99	6.22	9.30	16.73
69	B-4	B21tcacs	12	20	32.24	2.30	1.40	2.78	13.95	11.81	33.85	--	--	--	18.13	12.00	3.72	9.08	24.83
70	B-4	B22tcsca	30	25	29.61	2.92	2.05	3.42	12.60	8.62	28.14	--	--	--	13.39	8.37	6.38	11.81	30.44
71	B-4	2C1csca	55	40	37.97	3.17	2.42	3.46	11.75	17.17	25.99	--	--	--	14.88	6.97	4.14	7.84	28.20
72	B-4	2C2cs	+75	40	50.40	1.69	1.36	6.25	28.59	12.51	20.83	--	--	--	10.67	6.49	3.67	10.62	18.15
73	B-19	A	6	20	21.12	1.43	0.89	1.89	8.67	8.25	56.02	22.86	17.52	1.6	36.37	12.32	7.33	--	--
74	B-19	B21tca	14	60	22.53	0.42	0.52	2.26	10.86	8.47	43.74	33.73	30.58	1.4	25.31	13.09	5.34	--	--
75	B-19	B22tcsca	25	50	48.12	2.63	1.41	3.32	23.02	17.74	28.54	23.34	22.32	1.6	19.95	6.30	2.30	--	--
76	B-19	2C1csca	40	20	30.05	0.43	0.66	1.69	19.24	8.04	28.49	41.50	37.35	1.4	17.31	8.93	2.25	--	--
77	B-19	2C2cs	85	50	27.83	1.20	1.31	2.42	14.20	8.70	36.83	35.34	32.25	1.5	21.89	10.48	4.46	--	--
78	B-19	2C3cs	137	40	34.13	1.24	1.15	2.28	16.65	12.80	37.88	27.99	26.74	1.9	29.40	4.94	3.54	--	--
79	B-19	3C4cs	+262	80	34.89	4.40	2.36	3.35	14.86	9.91	40.70	24.41	22.49	2.1	25.66	10.55	4.56	--	--

Supplementary Table 3. Extractive chemical analyses

[--, not measured. Analyst, M. C. Reheis, U.S. Geological Survey]

Methods

Organic-carbon content measured using the Walkley-Black titration procedure (Allison, 1965), $CaCO_3$ with the Chittick apparatus (Bachman and Machette, 1977).

Several different methods of measuring gypsum content were evaluated. The most accurate method for samples containing <5% gypsum measures the conductivity of gypsum in solution (Bower and Huss, 1948; Jackson, 1958). Greater gypsum contents are more easily and accurately measured by the weight loss upon converting gypsum to anhydrite in a 100°C oven. This method has a standard error of estimate of ±1.8%, compared to the method which calculates gypsum from SO_4^{2-} concentration (Nelson and others, 1978). Early in this study, gypsum in some samples was measured by the weight loss caused by repeated washing of each sample in distilled water. This method is time-consuming and may also result in measurement error if any carbonate is present and is dissolved with the gypsum.

No.	Sample number	Horizon	Basal depth (cm)	percentage: Organic C	$CaCO_3$	Gypsum[1]	pH 1:1H_2O
			Fan 1, 5 ka				
1	B-21	A	6	0.55	23.2	0.08	7.7
2	B-21	2Btca	13	0.71	35.8	0.07	8.0
3	B-21	2Cca	33	0.37	59.7	0.09	8.1
4	B-21	2Cn	+73	0.22	53.6	0.08	8.4
			Fan 2, 65 ka				
5	B-5	A	3	--	--	--	--
6	B-5	B2tca	11	0.40	15.3	0.14	8.6
7	B-5	B3tca	20	0.35	29.8	0.09	8.4
8	B-5	2C1ca	31	0.42	59.0	0.36	8.6
9	B-5	2C2ca	46	0.43	57.5	0.50	8.9
10	B-5	2C3ca	+71	0.14	60.3	0.51	8.9
11	B-15	A	4	0.49	15.4	0.07	8.3
12	B-15	B1	12	0.55	12.8	0.10	8.2
13	B-15	B2tca	24	0.78	17.2	0.07	8.1
14	B-15	2B3tca	45	0.16	44.5	0.09	8.1
15	B-15	2Cca	65	0.29	66.8	0.44	8.5
16	B-15	2Cn	+165	0.15	63.2	0.73	8.4
			Fan 3, 100 ka				
17	B-6A	A	4	0.46	17.7	0.07	8.1
18	B-6A	B2tca	29	0.22	10.9	0.22	8.1
19	B-6A	2B3tca	46	0.32	52.0	0.15	8.3
20	B-6A	2Cca	88	0.26	68.7	0.70	8.2
21	B-6A	2C1csca	181	0.03	73.8	1.26	8.2
22	B-6A	2C2cs	+242	0.23	65.9	0.15	8.1
23	B-6A	base of fan 3		0.00	8.5	0.10	55.8
24	B-14	A11	4	0.44	19.7	0.06	8.0
25	B-14	A12	8	0.52	23.1	0.09	8.0
26	B-14	B1	17	0.61	13.1	0.12	8.0
27	B-14	B21tca	28	0.41	13.8	0.07	8.1
28	B-14	B22tca	44	0.40	12.3	0.07	8.1
29	B-14	2B3tca	70	0.40	46.0	0.11	8.4
30	B-14	2Cca	123	0.27	65.7	0.49	8.4
31	B-14	2Cnca	+193	0.26	60.3	0.81	8.3
32	B-16	A11	4	0.95	31.6	0.10	8.0
33	B-16	A12	9	0.51	25.1	0.07	8.0
34	B-16	Bt	12	0.50	49.8	0.23	8.1
35	B-16	Btca	28	0.50	49.8	0.23	8.1
36	B-16	Ccacs	75	0.09	48.4	[2]31.4	8.4
37	B-16	2C1csca	137	0.01	37.2	[2]43.8	8.5
38	B-16	2C2cs	+237	0.04	38.3	[2]29.6	8.6
			Fan 5, 410 ka				
39	B-7	A	6	0.83	37.3	0.49	7.8
40	B-7	C1csca	30	0.26	24.3	[3]58.8	8.0
41	B-7	2C2csca	50	0.31	26.4	[3]45.2	8.0
42	B-7	2C3csca	83	0.11	41.0	[3]42.8	8.3
43	B-7	2C4cs	+198	0.14	57.3	[3]14.1	8.5
44	B-17	A11	4	0.50	25.2	0.18	8.1
45	B-17	A12	10	0.54	30.3	0.11	8.1
46	B-17	Btca	19	0.59	42.1	0.29	8.0
47	B-17	2C1csca	40	0.55	14.1	[2]70.3	8.1
48	B-17	2C2csca	89	0.09	56.5	[2]28.0	8.1
49	B-17	2C3cs	179	0.08	39.6	[2]37.2	8.5
50	B-17	2C4cs	+249	0.11	49.7	[2]27.2	8.3
			Fan 6, 505 ka				
51	B-3	A	4	--	--	--	--
52	B-3	Btca	24	0.40	33.6	0.008	8.0
53	B-3	C1csca	42	0.43	13.3	[3]48.6	7.9
54	B-3	2C2cs	62	0.18	11.8	[3]42.5	8.0
55	B-3	2C3cs	+67	0.19	19.3	[3]33.5	8.1
56	B-18A	A11	2	0.34	33.2	0.21	8.1
57	B-18A	A12	5	0.42	36.0	0.16	8.1
58	B-18A	Btca	10	0.47	49.8	0.14	8.0
59	B-18A	2C1csca	37	0.13	20.4	[2]60.6	8.2
60	B-18A	2C2cs	46	0.11	43.1	[2]32.6	8.1
61	B-18A	2C3cs	+86	0.15	33.0	[2]23.1	8.1
62	B-18B	A	6	0.34	34.6	0.37	--
63	B-18B	Btca	22	0.65	24.6	0.12	7.9
64	B-18B	2C1csca	51	0.31	11.9	[2]58.8	8.0
65	B-18B	2C2cs	75	0.16	9.0	[2]32.6	8.2
66	B-18B	2C3cs	130	0.26	45.3	[2]14.1	8.3
67	B-18B	2C4cs	+255	0.19	44.2	[2]8.5	8.3
			Fan 7, 585 ka				
68	B-4	A	6	0.55	34.8	0.01	8.0
69	B-4	B21tcacs	12	0.55	44.8	2.77	7.7
70	B-4	B22tcsca	30	0.19	16.9	[3]51.4	7.8
71	B-4	2C1csca	55	0.18	24.3	[3]40.7	7.9
72	B-4	2C2cs	+75	0.12	12.8	[3]43.2	8.0
73	B-19	A	6	0.57	28.9	0.10	8.1
74	B-19	B21tca	14	0.68	29.7	0.11	8.0
75	B-19	B22tcsca	25	0.43	22.2	[2]20.2	8.0
76	B-19	2C1csca	40	0.18	20.0	[2]56.0	8.1
77	B-19	2C2cs	85	0.25	17.6	[2]41.3	8.1
78	B-19	2C3cs	137	0.08	23.4	[2]31.3	8.2
79	B-19	3C4cs	+262	0.08	31.4	[2]18.1	8.2

[1] Gypsum measured by electrical conductivity except where numbered.
[2] Values measured by weight loss due to heating.
[3] Values measured by weight loss from solution in distilled water.

Supplementary Table 4. Clay mineralogy by X-ray diffraction

[--, not measured. Analyst: M. C. Reheis, U.S. Geological Survey]

Methods

Samples of clay fractions were drawn from the settling tubes after particle-size analyses and were plated on ceramic tiles (Whittig, 1965). X-ray diffraction traces (CuK alpha radiation) were run on these oriented clays after each of the following treatments: air-dried, glycolated, and heated to 400°C and 550°C. At least five clay minerals were identified in the Kane fan soils, including kaolinite, mica, smectite, and palygorskite.

X-ray traces revealed an unknown mineral with a primary peak at 11.4 A in the air-dried state that shifts down to 10.6 A after glycolation. Gentle heating to about 80°C gives a peak at 8.66 A that does not shift upon subsequent glycolation. Heating to 400°C destroys the mineral peaks. This mineral concentrates in the coarse clay fraction, but is not found in the silt fraction. Peaks of the unknown mineral increase with age of the soil (suggesting a pedogenic origin) and are largest in gypsum-rich horizons. These peaks and their behavior during the various treatments do not coincide with those of any common clay mineral. The main peak and some of the minor ones roughly fit the zeolite mineral offretite (Chih-Chun Kao and G. W. Brindley, written commun., 1983), but zeolites should not be affected by glycolation or heating to 400°C (R. L. Hay and R. A. Sheppard, written communs., 1983). One additional candidate is the Ca-rich sepiolite-like mineral tubermorite, which is thought to be rare in nature but is commonly found in mortar and concrete (D. McGrath and B. L. Allen, oral communs., 1983). Microprobe analyses of the unknown mineral revealed no concentrations of elements uncommon in silicate clays.

A modification of the Illinois State Survey method was employed to estimate clay mineral percentages, in which peak heights are measured from a curvilinear baseline drawn on the glycolated trace. Heights of the 10 A peak (mica) and the 7 A peak (kaolinite) were multiplied by factors of 2 and 3 respectively, to adjust for intrinsic differences in ability of various clays to produce peaks in soils (Guccione, 1982; Johns and others, 1954). Prominent peaks for smectite (17 A), the unknown mineral (10.6 A), and palygorskite (10.4 A) were not adjusted. The resultant peak heights are summed and used to obtain clay-mineral percentages. This arbitrary treatment is not to be interpreted as indicating actual clay-mineral percentages, but only relative changes in the proportion of the various clay minerals present.

No.	Sample number	Horizon	Basal depth (cm)	percentage of clay mineral: Kaolinite	Mica	Smectite	Palygorskite	Unknown mineral
			Fan 1, 5 ka					
1	B-21	A	6	36	40	24	0	0
2	B-21	2Btca	13	35	42	23	0	0
3	B-21	2Cca	33	17	25	17	9	32
4	B-21	2Cn	+73	17	23	17	10	33
			Fan 2, 65 ka					
5	B-5	A	3	--	--	--	--	--
6	B-5	B2tca	11	--	--	--	--	--
7	B-5	B3tca	20	--	--	--	--	--
8	B-5	2C1ca	31	--	--	--	--	--
9	B-5	2C2ca	46	--	--	--	--	--
10	B-5	2C3ca	+71	--	--	--	--	--
11	B-15	A	4	31	37	32	0	0
12	B-15	B1	12	27	44	29	0	0
13	B-15	B2tca	24	27	41	32	0	0
14	B-15	2B3tca	45	28	21	30	6	15
15	B-15	2Cca	65	30	32	31	0	7
16	B-15	2Cn	+165	29	28	26	6	11
			Fan 3, 100 ka					
17	B-6A	A	4	32	33	35	0	0
18	B-6A	B2tca	29	27	34	39	0	0
19	B-6A	2B3tca	46	29	27	34	10	0
20	B-6A	2Cca	88	30	31	30	9	0
21	B-6A	2C1csca	181	37	37	20	6	0
22	B-6A	2C2cs	+242	36	39	25	0	0
23	B-6A	base of fan 3		27	34	30	0	9
24	B-14	A11	4	22	47	31	0	0
25	B-14	A12	8	30	41	29	0	0
26	B-14	B1	17	28	45	27	0	0
27	B-14	B21tca	28	28	34	38	0	0
28	B-14	B22tca	44	23	35	35	7	0
29	B-14	2B3tca	70	22	24	31	5	18
30	B-14	2Cca	123	28	30	31	0	11
31	B-14	2Cnca	+193	36	30	26	0	8
			Fan 4, 315 ka					
32	B-16	A11	4	22	45	33	0	0
33	B-16	A12	9	26	50	24	0	0
34	B-16	Bt	12	21	34	34	11	0
35	B-16	Btca	28	21	34	34	11	0
36	B-16	Ccacs	75	21	23	42	7	7
37	B-16	2C1csca	137	35	20	33	6	6
38	B-16	2C2cs	+237	34	17	37	6	6
			Fan 5, 410 ka					
39	B-7	A	6	--	--	--	--	--
40	B-7	C1csca	30	--	--	--	--	--
41	B-7	2C2csca	50	--	--	--	--	--
42	B-7	2C3csca	83	--	--	--	--	--
43	B-7	2C4cs	+198	--	--	--	--	--
44	B-17	A11	4	30	40	30	0	0
45	B-17	A12	10	23	39	25	13	0
46	B-17	Btca	19	16	25	21	8	30
47	B-17	2C1csca	40	9	25	13	9	44
48	B-17	2C2csca	89	28	26	28	9	9
49	B-17	2C3cs	179	21	30	30	10	9
50	B-17	2C4cs	+249	10	37	27	10	16
			Fan 6, 505 ka					
51	B-3	A	4	--	--	--	--	--
52	B-3	Btca	24	--	--	--	--	--
53	B-3	C1csca	42	--	--	--	--	--
54	B-3	2C2cs	62	--	--	--	--	--
55	B-3	2C3cs	+67	--	--	--	--	--
56	B-18A	A11	2	26	46	28	0	0
57	B-18A	A12	5	20	39	27	14	0
58	B-18A	Btca	10	31	25	28	8	8
59	B-18A	2C1csca	37	7	11	3	7	72
60	B-18A	2C2cs	46	29	20	26	13	12
61	B-18A	2C3cs	+86	24	21	38	7	10
62	B-18B	A	6	--	--	--	--	--
63	B-18B	Btca	22	27	32	29	12	0
64	B-18B	2C1csca	51	24	22	39	15	0
65	B-18B	2C2cs	75	14	8	44	4	30
66	B-18B	2C3cs	130	23	23	33	8	13
67	B-18B	2C4cs	+255	24	22	37	7	10
			Fan 7, 585 ka					
68	B-4	A	6	--	--	--	--	--
69	B-4	B21tcacs	12	--	--	--	--	--
70	B-4	B22tcsca	30	--	--	--	--	--
71	B-4	2C1csca	55	--	--	--	--	--
72	B-4	2C2cs	+75	--	--	--	--	--
73	B-19	A	6	30	24	38	8	0
74	B-19	B21tca	14	19	17	45	12	7
75	B-19	B22tcsca	25	19	16	50	11	4
76	B-19	2C1csca	40	18	18	41	6	17
77	B-19	2C2cs	85	17	13	28	5	37
78	B-19	2C3cs	137	28	16	39	5	12
79	B-19	3C4cs	+262	24	19	42	6	9

Supplementary Table 5. Total chemical analyses of the fine fraction by induction-coupled plasma spectroscopy

[--, not measured. Analyst: A. Bartel under J. E. Taggart, U.S. Geological Survey]

Methods

The less-than-2-mm and the silt-plus-clay fractions of selected soil profiles and dust-trap samples were analyzed for major elements and Zr by the Analytical Laboratories of the U.S. Geological Survey. To avoid chemical contamination in obtaining the silt-plus-clay fraction, soils were dispersed by shaking samples overnight in distilled water and then sonicating them in a water bath. Sand was removed by wet-sieving, and the silt-plus-clay fraction was dried and ground.

Oxides were determined by inductively coupled argon plasma emission spectroscopy (ICP). This method is noted for its high sensitivity to most elements once they are in solution (Taggart and others, 1981)(ICP accuracy is estimated at 3-5% and precision at 1-2%; J. E. Taggart, personal communication, 1982). X-ray fluorescence (XRF) is a more accurate method, but it is not sensitive to small amounts of such elements as Zr (there is less than 0.1% Zr in the silt-plus-clay fractions of soils in the study area). Because determination of Zr was critical to this study, all samples were run using ICP, with revised pretreatments that dissolved Zr. Selected samples were split and analyzed using both ICP and XRF as a check on the accuracy of ICP, and the separate analyses were in very close agreement on all samples (data not shown).

No.	Sample Number	Horizon	Basal depth (cm)	Percentage of silt-plus-clay fraction									
				SiO_2	Al_2O_3	Fe_2O_3	MgO	CaO	Na_2O	K_2O	TiO_2	MnO	ZrO_2
				Fan 1, 5 ka									
1	B-21	A	6	62	10.34	4.01	3.32	6.42	1.06	2.18	0.63	0.068	0.105
2	B-21	2Btca	13	48	10.98	4.18	3.91	12.8	0.59	2.29	0.55	0.043	0.049
3	B-21	2Cca	33	28	4.42	1.65	8.46	25.6	0.34	1.22	0.22	0.037	0.024
4	B-21	2Cn	+73	36	6.03	2.20	7.23	20.1	0.49	1.66	0.33	0.047	0.047
				Fan 2, 65 ka									
5	B-5	A	3	--	--	--	--	--	--	--	--	--	--
6	B-5	B2tca	11	--	--	--	--	--	--	--	--	--	--
7	B-5	B3tca	20	--	--	--	--	--	--	--	--	--	--
8	B-5	2C1ca	31	--	--	--	--	--	--	--	--	--	--
9	B-5	2C2ca	46	--	--	--	--	--	--	--	--	--	--
10	B-5	2C3ca	+71	--	--	--	--	--	--	--	--	--	--
11	B-15	A	4	59	12.14	4.75	3.83	6.00	1.02	2.53	0.72	0.076	0.092
12	B-15	B1	12	61	11.61	4.48	3.30	6.64	1.13	2.41	0.68	0.059	0.090
13	B-15	B2tca	24	58	12.04	4.58	3.55	8.06	1.09	2.41	0.65	0.053	0.074
14	B-15	2B3tca	45	39	7.18	2.66	5.56	20.8	0.80	1.57	0.43	0.035	0.050
15	B-15	2Cca	65	44	8.00	2.76	6.93	15.7	1.04	1.93	0.43	0.043	0.033
16	B-15	2Cn	+165	46	9.55	3.28	5.75	13.8	1.12	2.17	0.50	0.048	0.030
				Fan 3, 100 ka									
17	B-6A	A	4	--	--	--	--	--	--	--	--	--	--
18	B-6A	B2tca	29	--	--	--	--	--	--	--	--	--	--
19	B-6A	2B3tca	46	--	--	--	--	--	--	--	--	--	--
20	B-6A	2Cca	88	--	--	--	--	--	--	--	--	--	--
21	B-6A	2C1csca	181	--	--	--	--	--	--	--	--	--	--
22	B-6A	2C2cs	+242	--	--	--	--	--	--	--	--	--	--
23	B-6A	base of fan 3		--	--	--	--	--	--	--	--	--	--
24	B-14	A11	4	69	9.64	3.82	2.85	4.39	1.24	2.04	0.65	0.074	0.127
25	B-14	A12	8	54	9.00	3.38	2.44	3.92	0.90	1.88	0.52	0.057	0.081
26	B-14	B1	17	60	11.02	4.06	3.03	6.70	1.05	2.27	0.58	0.058	0.080
27	B-14	B21tca	28	64	10.72	3.93	2.75	6.43	1.25	2.12	0.60	0.052	0.073
28	B-14	B22tca	44	64	10.84	4.06	2.68	5.61	1.18	2.18	0.63	0.048	0.080
29	B-14	2B3tca	70	41	7.37	3.08	4.98	19.9	0.77	1.24	0.43	0.044	0.069
30	B-14	2Cca	123	41	7.84	3.25	7.28	15.5	1.11	1.43	0.43	0.066	0.057
31	B-14	2Cnca	+193	47	9.96	3.85	5.85	11.6	0.96	1.66	0.53	0.099	0.046

Supplementary Table 5. Total chemical analyses of the fine fraction by induction-coupled plasma spectroscopy--Continued

No.	Sample Number	Horizon	Basal depth (cm)	Percentage of silt-plus-clay fraction									
				SiO_2	Al_2O_3	Fe_2O_3	MgO	CaO	Na_2O	K_2O	TiO_2	MnO	ZrO_2
				Fan 4, 315 ka									
32	B-16	A11	4	58	10.68	4.01	3.62	8.78	1.13	2.29	0.63	0.061	0.079
33	B-16	A12	9	59	10.93	4.02	3.35	8.71	1.13	2.29	0.60	0.052	0.073
34	B-16	Bt	12	40	7.56	2.78	4.73	21.1	0.74	1.33	0.38	0.034	0.037
35	B-16	Btca	28	40	7.56	2.78	4.73	21.1	0.74	1.33	0.38	0.034	0.037
36	B-16	Ccacs	75	28	5.26	1.92	9.87	23.2	0.65	0.84	0.25	0.027	0.016
37	B-16	2C1csca	137	16	2.84	1.10	7.89	33.6	0.43	0.48	0.13	0.021	0.014
38	B-16	2C2cs	+237	40	9.40	3.42	8.77	14.0	0.88	1.69	0.40	0.043	0.019
				Fan 5, 410 ka									
39	B-7	A	6	--	--	--	--	--	--	--	--	--	--
40	B-7	C1csca	30	--	--	--	--	--	--	--	--	--	--
41	B-7	2C2csca	50	--	--	--	--	--	--	--	--	--	--
42	B-7	2C3csca	83	--	--	--	--	--	--	--	--	--	--
43	B-7	2C4cs	+198	--	--	--	--	--	--	--	--	--	--
44	B-17	A11	4	56	10.00	3.55	3.76	10.7	0.96	2.11	0.52	0.058	0.057
45	B-17	A12	10	51	9.55	3.39	3.85	12.3	0.88	1.98	0.47	0.053	0.051
46	B-17	Btca	19	35	6.99	2.58	5.87	21.3	0.51	1.33	0.37	0.032	0.034
47	B-17	2C1csca	40	19	3.82	1.39	5.11	25.7	0.22	0.63	0.18	0.022	0.018
48	B-17	2C2csca	89	21	3.67	1.56	11.38	25.3	0.27	0.73	0.18	0.039	0.019
49	B-17	2C3cs	179	34	6.37	2.42	8.82	18.6	0.54	1.22	0.32	0.050	0.027
50	B-17	2C4cs	+249	34	6.03	2.26	8.77	19.9	0.57	1.24	0.32	0.048	0.030
				Fan 6, 505 ka									
51	B-3	A	4	--	--	--	--	--	--	--	--	--	--
52	B-3	Btca	24	--	--	--	--	--	--	--	--	--	--
53	B-3	C1csca	42	--	--	--	--	--	--	--	--	--	--
54	B-3	2C2cs	62	--	--	--	--	--	--	--	--	--	--
55	B-3	2C3cs	+67	--	--	--	--	--	--	--	--	--	--
56	B-18A	A11	2	53	9.60	3.61	3.62	11.7	1.01	2.05	0.57	0.059	0.075
57	B-18A	A12	5	48	9.21	3.40	3.90	15.7	0.90	1.93	0.50	0.052	0.053
58	B-18A	Btca	10	--	--	--	--	--	--	--	--	--	--
59	B-18A	2C1csca	37	--	--	--	--	--	--	--	--	--	--
60	B-18A	2C2cs	46	--	--	--	--	--	--	--	--	--	--
61	B-18A	2C3cs	+86	--	--	--	--	--	--	--	--	--	--
62	B-18B	A	6	50	9.40	3.51	3.76	13.7	0.95	1.99	0.54	0.055	0.064
63	B-18B	Btca	22	55	10.34	3.89	3.90	9.82	0.92	1.93	0.55	0.045	0.062
64	B-18B	2C1csca	51	25	4.20	1.69	4.33	25.3	0.55	0.72	0.27	0.032	0.038
65	B-18B	2C2cs	75	43	7.83	3.02	4.68	14.1	0.80	1.20	0.45	0.069	0.049
66	B-18B	2C3cs	130	33	5.94	2.96	8.42	18.9	0.84	1.20	0.33	0.125	0.027
67	B-18B	2C4cs	+255	42	8.11	3.36	6.29	15.7	1.01	1.81	0.45	0.085	0.038
				Fan 7, 585 ka									
68	B-4	A	6	--	--	--	--	--	--	--	--	--	--
69	B-4	B21tcacs	12	--	--	--	--	--	--	--	--	--	--
70	B-4	B22tcsca	30	--	--	--	--	--	--	--	--	--	--
71	B-4	2C1csca	55	--	--	--	--	--	--	--	--	--	--
72	B-4	2C2cs	+75	--	--	--	--	--	--	--	--	--	--
73	B-19	A	6	56	9.55	3.65	3.58	10.1	0.85	1.93	0.50	0.089	0.055
74	B-19	B21tca	14	49	9.13	4.28	3.28	13.1	0.65	1.58	0.49	0.144	0.043
75	B-19	B22tcsca	25	41	6.43	2.47	3.32	19.3	0.44	1.12	0.33	0.062	0.047
76	B-19	2C1csca	40	28	5.03	2.05	7.71	23.1	0.32	0.77	0.25	0.107	0.022
77	B-19	2C2cs	85	41	7.64	3.10	7.40	14.8	0.46	1.20	0.38	0.092	0.036
78	B-19	2C3cs	137	43	7.58	3.29	7.18	13.9	0.55	1.39	0.40	0.134	0.036
79	B-19	3C4cs	+262	47	8.73	3.71	4.15	13.9	0.65	1.75	0.47	0.143	0.041

Supplementary Table 6. Total chemical analyses of the less-than-2-mm fraction by induction-coupled plasma spectroscopy

[--, not measured. Analyst: P. H. Briggs under L. R. Layman, U.S. Geological Survey]

Methods

Same methods as in supplementary table 5.

No.	Sample number	Horizon	Basal depth (cm)	Percentage of less-than-2mm fraction									
				SiO_2	Al_2O_3	Fe_2O_3	MgO	CaO	Na_2O	K_2O	TiO_2	MnO	ZrO_2
Fan 1, 5 ka													
1	B-21	A	6	60	7.90	2.98	3.33	10.0	1.09	1.81	0.43	0.057	0.056
2	B-21	2Btca	13	48	7.56	2.72	4.05	15.8	0.80	1.81	0.37	0.045	0.037
3	B-21	2Cca	33	22	2.68	1.13	8.28	29.2	0.38	0.84	0.12	0.031	0.011
4	B-21	2Cn	+73	21	2.33	1.24	8.59	30.1	0.39	0.84	0.10	0.034	0.009
Fan 2, 65 ka													
5	B-5	A	3	--	--	--	--	--	--	--	--	--	--
6	B-5	B2tca	11	--	--	--	--	--	--	--	--	--	--
7	B-5	B3tca	20	--	--	--	--	--	--	--	--	--	--
8	B-5	2C1ca	31	--	--	--	--	--	--	--	--	--	--
9	B-5	2C2ca	46	--	--	--	--	--	--	--	--	--	--
10	B-5	2C3ca	+71	--	--	--	--	--	--	--	--	--	--
11	B-15	A	4	63	8.77	3.32	3.30	8.21	1.08	1.93	0.50	0.061	0.067
12	B-15	B1	12	63	9.17	3.40	2.82	7.06	1.09	2.05	0.50	0.056	0.061
13	B-15	B2tca	24	60	9.24	3.39	3.30	9.79	1.08	1.93	0.47	0.050	0.056
14	B-15	2B3tca	45	37	4.46	1.86	6.24	24.8	0.55	1.08	0.25	0.043	0.026
15	B-15	2Cca	65	29	3.46	1.53	8.26	26.7	0.50	0.96	0.18	0.041	0.014
16	B-15	2Cn	+165	28	3.23	1.52	8.13	27.8	0.49	0.96	0.17	0.045	0.012
Fan 3, 100 ka													
17	B-6A	A	4	--	--	--	--	--	--	--	--	--	--
18	B-6A	B2tca	29	--	--	--	--	--	--	--	--	--	--
19	B-6A	2B3tca	46	--	--	--	--	--	--	--	--	--	--
20	B-6A	2Cca	88	--	--	--	--	--	--	--	--	--	--
21	B-6A	2C1csca	181	--	--	--	--	--	--	--	--	--	--
22	B-6A	2C2cs	+242	--	--	--	--	--	--	--	--	--	--
23	B-6A	base of fan 3		--	--	--	--	--	--	--	--	--	--
24	B-14	A11	4	62	7.45	2.69	3.18	8.41	1.21	1.69	0.42	0.059	0.058
25	B-14	A12	8	63	8.83	3.12	2.95	6.94	1.11	1.93	0.45	0.059	0.055
26	B-14	B1	17	63	9.47	3.35	2.79	6.81	1.13	2.17	0.48	0.052	0.050
27	B-14	B21tca	28	63	9.64	3.43	2.77	7.05	1.27	2.05	0.50	0.049	0.051
28	B-14	B22tca	44	64	9.75	3.49	2.67	6.32	1.21	2.05	0.52	0.053	0.048
29	B-14	2B3tca	70	37	4.61	1.95	5.79	21.0	0.75	0.96	0.23	0.039	0.023
30	B-14	2Cca	123	25	3.23	1.36	8.86	26.6	0.58	0.84	0.15	0.037	0.014
31	B-14	2Cnca	+193	29	4.12	1.86	8.14	24.6	0.62	0.96	0.20	0.077	0.015
Fan 4, 315 ka													
32	B-16	A11	4	53	8.09	2.89	3.98	14.3	0.96	1.81	0.43	0.050	0.046
33	B-16	A12	9	53	8.45	3.03	3.60	14.3	0.88	1.81	0.43	0.048	0.040
34	B-16	Bt	12	38	5.67	2.13	4.43	23.6	0.63	1.08	0.30	0.028	0.028
35	B-16	Btca	28	38	5.67	2.13	4.43	23.6	0.63	1.08	0.30	0.028	0.028
36	B-16	Ccacs	75	13	1.74	0.80	6.17	33.3	0.24	0.36	0.08	0.018	0.008
37	B-16	2C1csca	137	19	2.44	1.04	6.72	27.6	0.40	0.48	0.12	0.017	0.012
38	B-16	2C2cs	+237	45	5.44	2.23	3.35	14.0	0.59	0.96	0.30	0.070	0.033

Supplementary Table 6. Total chemical analyses of the less-than-2-mm fraction by induction-coupled plasma spectroscopy--Continued

No.	Sample number	Horizon	Basal depth (cm)	Percentage of less-than-2mm fraction									
				SiO_2	Al_2O_3	Fe_2O_3	MgO	CaO	Na_2O	K_2O	TiO_2	MnO	ZrO_2
				Fan 5, 410 ka									
39	B-7	A	6	--	--	--	--	--	--	--	--	--	--
40	B-7	C1csca	30	--	--	--	--	--	--	--	--	--	--
41	B-7	2C2csca	50	--	--	--	--	--	--	--	--	--	--
42	B-7	2C3csca	83	--	--	--	--	--	--	--	--	--	--
43	B-7	2C4cs	+198	--	--	--	--	--	--	--	--	--	--
44	B-17	A11	4	56	8.96	3.13	3.62	11.1	1.05	2.05	0.47	0.057	0.049
45	B-17	A12	10	51	8.37	2.88	3.83	13.8	0.93	1.93	0.40	0.045	0.035
46	B-17	Btca	19	36	5.95	2.09	5.94	22.5	0.58	1.20	0.28	0.031	0.021
47	B-17	2C1csca	40	9	1.19	0.46	2.31	29.5	0.19	0.24	0.05	0.006	0.004
48	B-17	2C2csca	89	16	2.04	1.09	9.67	27.4	0.23	0.48	0.12	0.024	0.008
49	B-17	2C3cs	179	23	3.35	1.43	7.96	23.9	0.38	0.72	0.18	0.030	0.014
50	B-17	2C4cs	+249	24	3.25	1.32	7.89	25.6	0.38	0.72	0.17	0.028	0.017
				Fan 6, 505 ka									
51	B-3	A	4	--	--	--	--	--	--	--	--	--	--
52	B-3	Btca	24	--	--	--	--	--	--	--	--	--	--
53	B-3	C1csca	42	--	--	--	--	--	--	--	--	--	--
54	B-3	2C2cs	62	--	--	--	--	--	--	--	--	--	--
55	B-3	2C3cs	+67	--	--	--	--	--	--	--	--	--	--
56	B-18A	A11	2	55	7.54	2.85	3.45	13.9	0.93	1.69	0.40	0.074	0.042
57	B-18A	A12	5	51	7.64	2.92	3.75	15.9	0.82	1.57	0.40	0.071	0.042
58	B-18A	Btca	10	--	--	--	--	--	--	--	--	--	--
59	B-18A	2C1csca	37	--	--	--	--	--	--	--	--	--	--
60	B-18A	2C2cs	46	--	--	--	--	--	--	--	--	--	--
61	B-18A	2C3cs	+86	--	--	--	--	--	--	--	--	--	--
62	B-18B	A	6	53	7.59	2.89	3.60	14.9	0.87	1.63	0.40	0.072	0.042
63	B-18B	Btca	22	56	8.39	3.23	3.90	11.0	0.84	1.57	0.42	0.063	0.039
64	B-18B	2C1csca	51	24	2.89	1.27	3.25	23.5	0.38	0.60	0.17	0.031	0.019
65	B-18B	2C2cs	75	25	4.20	1.63	7.55	23.1	0.49	0.84	0.18	0.026	0.013
66	B-18B	2C3cs	130	32	3.72	3.08	6.57	22.5	0.53	0.84	0.20	0.193	0.019
67	B-18B	2C4cs	+255	41	4.88	2.58	5.24	20.3	0.65	1.20	0.27	0.094	0.025
				Fan 7, 585 ka									
68	B-4	A	6	--	--	--	--	--	--	--	--	--	--
69	B-4	B21tcacs	12	--	--	--	--	--	--	--	--	--	--
70	B-4	B22tcsca	30	--	--	--	--	--	--	--	--	--	--
71	B-4	2C1csca	55	--	--	--	--	--	--	--	--	--	--
72	B-4	2C2cs	+75	--	--	--	--	--	--	--	--	--	--
73	B-19	A	6	58	8.51	3.42	3.22	10.8	0.84	1.81	0.45	0.106	0.044
74	B-19	B21tca	14	51	7.50	3.72	2.82	14.4	0.59	1.45	0.38	0.152	0.029
75	B-19	B22tcsca	25	47	4.10	1.63	2.32	18.0	0.36	0.84	0.22	0.050	0.028
76	B-19	2C1csca	40	20	2.63	1.19	4.15	24.2	0.26	0.48	0.13	0.066	0.011
77	B-19	2C2cs	85	33	4.39	2.05	4.38	19.2	0.35	0.84	0.23	0.079	0.018
78	B-19	2C3cs	137	42	5.14	2.56	5.01	16.2	0.49	1.08	0.27	0.114	0.024
79	B-19	3C4cs	+262	44	5.63	3.33	3.57	18.0	0.54	1.33	0.32	0.170	0.025

Supplementary Table 7, Part 1. Horizon weights of sand, silt, clay, carbon, $CaCO_3$, gypsum, and clay minerals

[--, not measured. Analyst: Marith C. Reheis, U.S. Geological Survey]

Methods

Profile weights of soil properties (g/cm^2/column of soil) are calculated from the property percentage, bulk density, and texture of each horizon. The pedogenic increase from the amount of the property in the parent material is calculated by estimating the property percentage, bulk density, and texture in the original deposit (method modified from Machette, 1978, and Machette, 1985). Weights are calculated for each horizon, summed to give the total profile weight in a soil, and standardized to 250 cm depth to eliminate bias caused by different depths of sampling (backhoe pits vs. hand-dug holes).

Two basic equations are used to calculate pedogenic increase for clay, silt, $CaCO_3$, and gypsum. Equation 1 is used to calculate pedogenic increase in horizon weight of clay and silt (substitute appropriate silt percentages when calculating silt weights):

1. $$g\ clay = \left(\left(\frac{clay\%}{100}\right)(BDf)\left(\frac{100 - salts\%}{100}\right)(H)\right) - \left(\left(\frac{i\ clay\%}{100}\right)(i\ BDf)\left(\frac{100 - i\ salts\%}{100}\right)(H)\right)$$

where BDf is bulk density of the <2-mm fraction, H is horizon thickness, salts include organic matter, $CaCO_3$, and gypsum, and the letter i designates an estimate of the parent material state. This equation includes a factor to account for salts and organic matter because particle size is measured on an organic-free and salt-free basis. Equation 2 is used to calculate pedogenic weights of gypsum and $CaCO_3$ (again, substitute $CaCO_3$ percentages in place of gypsum percentages when calculating $CaCO_3$ weights):

2. $$g\ gypsum = \left(\left(\frac{gypsum\%}{100}\right)(BDf)(H)\right) - \left(\left(\frac{i\ gypsum\%}{100}\right)(i\ BDf)(H)\right)$$

Profile weights for sand, carbon, clay minerals, and major oxides are not corrected for the estimated parent material contents. Values for sand are calculated using the first term of equation 1 above, substituting the appropriate sand percentages for clay percentages. Values for carbon and major oxides (Supplementary Table 7, Part 2) are calculated using the first term of equation 2 above, substituting the appropriate property percentages for gypsum percentage. Horizon weights for clay minerals are calculated by equation 3:

3. $$g\ clay\ mineral = \left(\frac{clay\ mineral\%}{100}\right)\left(\frac{clay\%}{100}\right)(H)(BDf)\left(\frac{100 - salts\%}{100}\right)$$

No.	Sample number	Horizon	Basal depth (cm)	Weight (g/cm^2/horizon column) Sand	Silt[1]	Clay[1]	Carbon	$CaCO_3$[1]	Gypsum[1]	Kaolinite	Mica	Smectite	Palygorskite	Unknown mineral
				Fan 1, 5 ka										
1	B-21	A	6	1.02	0	0.18	0.017	-1.61	-0.0005	0.11	0.13	0.077	0	0
2	B-21	2Btca	13	0.57	0.16	0.41	0.020	-0.38	0.0002	0.17	0.20	0.11	0	0
3	B-21	2Cca	33	0.97	-0.20	0.13	0.024	0.30	0.0012	0	0	0.059	0.031	0.11
4	B-21	2Cn	+73	1.47	0.26	0	0.018	0	0.0008	0.044	0.064	0.044	0.026	0.082
				Fan 2, 65 ka										
5	B-5	A	3	--	--	--	--	--	--	--	--	--	--	--
6	B-5	B2tca	11	--	--	--	--	--	--	--	--	--	--	--
7	B-5	B3tca	20	--	--	--	--	--	--	--	--	--	--	--
8	B-5	2C1ca	31	--	--	--	--	--	--	--	--	--	--	--
9	B-5	2C2ca	46	--	--	--	--	--	--	--	--	--	--	--
10	B-5	2C3ca	+71	--	--	--	--	--	--	--	--	--	--	--
11	B-15	A	4	0.89	0.88	0.24	0.015	-1.24	0	0.13	0.15	0.13	0	0
12	B-15	B1	12	3.10	3.42	1.03	0.059	-3.26	0.0048	0.40	0.65	0.43	0	0
13	B-15	B2tca	24	3.27	4.51	1.82	0.115	-4.39	0.0015	0.68	1.03	0.81	0	0
14	B-15	2B3tca	45	1.29	0.59	0.14	0.010	-1.35	0.0004	0.15	0.11	0.16	0.033	0.082
15	B-15	2Cca	65	0.99	0.12	0	0.024	0.99	0.0311	0.13	0.14	0.14	0	0.031
16	B-15	2Cn	+165	6.92	0	0	0.063	3.44	0.277	0.69	0.71	0.61	0.14	0.26
				Fan 3, 100 ka										
17	B-6A	A	4	1.31	1.02	0.31	0.019	-2.18	-0.0008	0.18	0.18	0.19	0	0
18	B-6A	B2tca	29	10.45	8.27	3.44	0.068	-14.9	0.0444	1.34	1.68	1.93	0	0
19	B-6A	2B3tca	46	1.46	0.47	0.25	0.025	-1.35	0.0047	0.20	0.19	0.24	0.070	0
20	B-6A	2Cca	88	1.61	0.39	0.07	0.044	2.30	0.106	0.40	0.42	0.40	0.12	0
21	B-6A	2C1csca	181	3.40	0	0.23	0.012	7.34	0.465	1.17	1.17	0.63	0.19	0
22	B-6A	2C2cs	+242	3.27	0	0.17	0.059	2.79	0.0205	0.76	0.82	0.53	0	0
23	B-6A	base of fan 3		--	--	--	--	--	--	--	--	--	--	--
24	B-14	A11	4	2.13	1.09	0.06	0.023	-1.88	-0.0005	0.083	0.18	0.12	0	0
25	B-14	A12	8	1.43	1.06	0.40	0.026	-1.79	0.0007	0.18	0.25	0.18	0	0
26	B-14	B1	17	3.32	2.93	1.09	0.068	-5.13	0.0049	0.51	0.82	0.49	0	0
27	B-14	B21tca	28	3.59	4.24	1.12	0.056	-6.18	-0.0008	0.56	0.68	0.76	0	0
28	B-14	B22tca	44	4.71	5.37	1.66	0.070	-8.33	-0.0011	0.65	0.99	0.99	0.20	0
29	B-14	2B3tca	70	2.87	0.32	0.15	0.037	-0.84	0.0037	0.16	0.17	0.22	0.036	0.13
30	B-14	2Cca	123	4.03	0	0	0.060	2.38	0.0935	0.32	0.34	0.36	0	0.13
31	B-14	2Cnca	193	5.11	0	0	0.076	1.56	0.218	0.85	0.71	0.61	0	0.19

Supplementary Table 7, Part 1. Horizon weights of sand, silt, clay, carbon, $CaCO_3$, gypsum, and clay minerals--Continued

No.	Sample number	Horizon	Basal depth (cm)	Weight (g/cm^2/horizon column) Sand	Silt[1]	Clay[1]	Carbon	$CaCO_3$[1]	Gypsum[1]	Kaolinite	Mica	Smectite	Palygorskite	Unknown mineral
				Fan 4, 315 ka										
32	B-16	A11	4	0.48	0.83	0.18	0.033	-0.82	0.0011	0.12	0.25	0.13	0	0
33	B-16	A12	9	0.48	0.85	0.12	0.017	-1.57	-0.0007	0.15	0.28	0.14	0	0
34	B-16	Bt	12	0.18	0	0.01	0.009	-0.75	0.0021	0.065	0.11	0.11	0.034	0
35	B-16	Btca	28	0.95	-0.03	0	0.049	-4.03	0.0111	0.35	0.56	0.56	0.18	0
36	B-16	Ccacs	75	2.09	0.92	1.78	0.043	11.9	14.9	0.80	0.87	1.60	0.27	0.27
37	B-16	2C1csca	137	0.81	0	-1.08	0.002	-7.05	8.94	0.54	0.31	0.51	0.093	0.093
38	B-16	2C2cs	+237	2.72	0	2.05	0.017	-7.01	12.4	2.13	1.07	2.32	0.38	0.38
				Fan 5, 410 ka										
39	B-7	A	6	--	--	--	--	--	--	--	--	--	--	--
40	B-7	C1csca	30	--	--	--	--	--	--	--	--	--	--	--
41	B-7	2C2csca	50	--	--	--	--	--	--	--	--	--	--	--
42	B-7	2C3csca	83	--	--	--	--	--	--	--	--	--	--	--
43	B-7	2C4cs	+198	--	--	--	--	--	--	--	--	--	--	--
44	B-17	A11	4	1.03	1.84	0.54	0.029	-1.48	0.0066	0.27	0.35	0.27	0	0
45	B-17	A12	10	1.28	1.72	0.86	0.040	-2.15	0.0025	0.32	0.54	0.35	0.18	0
46	B-17	Btca	19	0.84	1.46	0.63	0.047	-2.52	0.0157	0.21	0.33	0.28	0.11	0.40
47	B-17	2C1csca	40	0.87	0.11	0.36	0.098	-2.45	12.5	0.087	0.24	0.13	0.087	0.43
48	B-17	2C2csca	89	0.027	-0.37	0.03	0.024	3.63	7.39	0.008	0.007	0.008	0.003	0.003
49	B-17	2C3cs	179	1.16	0.38	0.51	0.036	-2.97	16.7	0.19	0.26	0.26	0.09	0.08
50	B-17	2C4cs	249	2.21	0	0	0.032	-1.56	7.98	0.17	0.63	0.46	0.17	0.27
				Fan 6, 505 ka										
51	B-3	A	4	--	--	--	--	--	--	--	--	--	--	--
52	B-3	Btca	24	--	--	--	--	--	--	--	--	--	--	--
53	B-3	C1csca	42	--	--	--	--	--	--	--	--	--	--	--
54	B-3	2C2cs	62	--	--	--	--	--	--	--	--	--	--	--
55	B-3	2C3cs	+67	--	--	--	--	--	--	--	--	--	--	--
56	B-18a	A11	2	0.44	0.47	0.11	0.008	-0.39	0.0119	0.084	0.15	0.090	0	0
57	B-18a	A12	5	0.58	0.62	0.18	0.016	-0.87	0.0031	0.12	0.23	0.16	0.081	0
58	B-18a	Btca	10	0.48	-0.21	-0.01	0.018	-1.79	0.0023	0.21	0.17	0.19	0.053	0.053
59	B-18a	2C1csca	37	1.79	0.32	-0.02	0.033	-1.15	15.5	0.079	0.13	0.034	0.079	0.82
60	B-18a	2C2cs	46	0.70	0	0.09	0.007	0.51	1.99	0.19	0.13	0.17	0.087	0.080
61	B-18a	2C3cs	+86	4.11	0	0.44	0.038	-5.54	5.80	0.71	0.63	1.13	0.23	0.30
62	B-18b	A	6	1.17	1.30	0.30	0.021	-1.29	0.0189	0.25*	0.45*	0.27*	0*	0*
63	B-18b	Btca	22	3.20	2.54	1.88	0.099	-5.50	0.0065	0.98	1.16	1.05	0.43	0
64	B-18b	2C1csca	51	2.46	1.20	2.13	0.091	-3.37	17.2	0.82	0.75	1.33	0.51	0
65	B-18b	2C2cs	75	6.97	5.25	4.59	0.052	-2.74	10.6	0.79	0.45	2.48	0.23	1.69
66	B-18b	2C3cs	130	3.31	0.29	0.22	0.114	-4.27	6.17	0.47	0.47	0.67	0.16	0.27
67	B-18b	2C4cs	+255	13.3	3.00	1.93	0.150	-8.51	6.64	2.37	2.17	3.65	0.69	0.99
				Fan 7, 585 ka										
68	B-4	A	6	--	--	--	--	--	--	--	--	--	--	--
69	B-4	B21tcacs	12	--	--	--	--	--	--	--	--	--	--	--
70	B-4	B22tcsca	30	--	--	--	--	--	--	--	--	--	--	--
71	B-4	2C1csca	55	--	--	--	--	--	--	--	--	--	--	--
72	B-4	2C2cs	+75	--	--	--	--	--	--	--	--	--	--	--
73	B-19	A	6	0.94	1.48	0.30	0.036	-1.64	0.0019	0.31	0.25	0.38	0.082	0
74	B-19	B21tca	14	-0.32	0.39	0.36	0.031	-2.01	0.0007	-0.09	-0.08	-0.21	-0.057	-0.033
75	B-19	B22tcsca	25	0.69	-0.03	0.02	0.011	-0.95	0.509	0.063	0.053	0.17	0.037	0.013
76	B-19	2C1csca	40	0.92	-0.93	-0.03	0.023	-3.72	7.13	0.23	0.23	0.52	0.076	0.22
77	B-19	2C2cs	85	0.64	1.00	1.95	0.084	-6.19	13.9	0.14	0.11	0.23	0.033	0.30
78	B-19	2C3cs	137	6.43	2.81	2.18	0.033	-5.42	13.0	1.48	0.84	2.06	0.26	0.63
79	B-19	3C4cs	+262	9.25	2.50	0.54	0.042	-12.4	9.47	1.55	1.23	2.72	0.39	0.58

[1] Pedogenic weights, estimated parent material amount subtracted.
* Estimated by comparison to A horizons of soil B-18a.

Supplementary Table 7, Part 2. Horizon weights of major oxides plus zirconium

[--, not measured. Analyst: M. C. Reheis, U.S. Geological Survey]

Methods

Horizon weights for element oxides are calculated using the first term in equation 2 given in Supplementary Table 7, Part 1.

No.	Sample number	Horizon	Basal depth (cm)	Weight (g/cm^2/horizon column) of oxide in less-than-2mm fraction									
				SiO_2	Al_2O_3	Fe_2O_3	MgO	CaO	Na_2O	K_2O	TiO_2	MnO	ZrO_2
				Fan 1, 5 ka									
1	B-21	A	6	1.8	0.24	0.089	0.10	0.30	0.033	0.054	0.013	0.0017	0.0017
2	B-21	2Btca	13	1.3	0.21	0.076	0.11	0.44	0.022	0.051	0.010	0.0013	0.0010
3	B-21	2Cca	33	1.4	0.17	0.072	0.53	1.9	0.024	0.054	0.0077	0.0020	0.0007
4	B-21	2Cn	73	1.8	0.20	0.10	0.72	2.5	0.033	0.071	0.0084	0.0028	0.0007
				Fan 2, 65 ka									
5	B-5	A	3	--	--	--	--	--	--	--	--	--	--
6	B-5	B2tca	11	--	--	--	--	--	--	--	--	--	--
7	B-5	B3tca	20	--	--	--	--	--	--	--	--	--	--
8	B-5	2C1ca	31	--	--	--	--	--	--	--	--	--	--
9	B-5	2C2ca	46	--	--	--	--	--	--	--	--	--	--
10	B-5	2C3ca	+71	--	--	--	--	--	--	--	--	--	--
11	B-15	A	4	2.0	0.27	0.10	0.10	0.26	0.034	0.060	0.016	0.0019	0.0021
12	B-15	B1	12	6.7	0.98	0.36	0.30	0.75	0.12	0.22	0.053	0.0060	0.0065
13	B-15	B2tca	24	8.9	1.4	0.50	0.49	1.4	0.16	0.28	0.069	0.0074	0.0083
14	B-15	2B3tca	45	2.3	0.28	0.12	0.39	1.6	0.035	0.068	0.016	0.0027	0.0016
15	B-15	2Cca	65	2.4	0.29	0.13	0.69	2.2	0.042	0.081	0.015	0.0034	0.0012
16	B-15	2Cn	+165	12.	1.4	0.64	3.4	12.	0.21	0.40	0.071	0.019	0.0050
				Fan 3, 100 ka									
17	B-6A	A	4	--	--	--	--	--	--	--	--	--	--
18	B-6A	B2tca	29	--	--	--	--	--	--	--	--	--	--
19	B-6A	2B3tca	46	--	--	--	--	--	--	--	--	--	--
20	B-6A	2Cca	88	--	--	--	--	--	--	--	--	--	--
21	B-6A	2C1csca	181	--	--	--	--	--	--	--	--	--	--
22	B-6A	2C2cs	+242	--	--	--	--	--	--	--	--	--	--
23	B-6A	base of fan 3		--	--	--	--	--	--	--	--	--	--
24	B-14	A11	4	3.3	0.40	0.14	0.17	0.45	0.064	0.090	0.022	0.0031	0.0031
25	B-14	A12	8	3.1	0.43	0.15	0.15	0.34	0.055	0.095	0.022	0.0029	0.0027
26	B-14	B1	17	7.0	1.0	0.37	0.31	0.75	0.13	0.24	0.053	0.0058	0.0055
27	B-14	B21tca	28	8.5	1.3	0.46	0.37	0.95	0.17	0.28	0.068	0.0066	0.0069
28	B-14	B22tca	44	11.	1.7	0.61	0.47	1.1	0.21	0.36	0.091	0.0092	0.0084
29	B-14	2B3tca	70	3.5	0.43	0.18	0.54	2.0	0.070	0.090	0.022	0.0037	0.0022
30	B-14	2Cca	123	5.6	0.72	0.30	2.0	5.9	0.13	0.19	0.033	0.0082	0.0031
31	B-14	2Cnca	193	8.5	1.2	0.55	2.4	7.2	0.18	0.28	0.059	0.023	0.0044
				Fan 4, 315 ka									
32	B-16	A11	4	1.9	0.28	0.10	0.14	0.50	0.034	0.064	0.015	0.0018	0.0016
33	B-16	A12	9	1.8	0.29	0.10	0.12	0.49	0.030	0.062	0.015	0.0016	0.0014
34	B-16	Bt	12	0.70	0.10	0.039	0.081	0.43	0.012	0.020	0.0055	0.0005	0.0005
35	B-16	Btca	28	3.7	0.55	0.21	0.43	2.3	0.062	0.11	0.029	0.0027	0.0027
36	B-16	Ccacs	75	6.2	0.83	0.38	2.9	16.	0.11	0.17	0.038	0.0085	0.0038
37	B-16	2C1csca	137	3.9	0.50	0.21	1.4	5.6	0.082	0.98	0.025	0.0035	0.0025
38	B-16	2C2cs	+237	19.	2.3	0.94	1.4	5.9	0.25	0.40	0.13	0.029	0.014

Supplementary Table 7, Part 2. Horizon weights of major oxides plus zirconium—Continued

No.	Sample number	Horizon	Basal depth (cm)	Weight (g/cm^2/horizon column) of oxide in less-than-2mm fraction									
				SiO_2	Al_2O_3	Fe_2O_3	MgO	CaO	Na_2O	K_2O	TiO_2	MnO	ZrO_2
				Fan 5, 410 ka									
39	B-7	A	6	--	--	--	--	--	--	--	--	--	--
40	B-7	C1csca	30	--	--	--	--	--	--	--	--	--	--
41	B-7	2C2csca	50	--	--	--	--	--	--	--	--	--	--
42	B-7	2C3csca	83	--	--	--	--	--	--	--	--	--	--
43	B-7	2C4cs	+198	--	--	--	--	--	--	--	--	--	--
44	B-17	A11	4	3.2	0.51	0.18	0.21	0.63	0.06	0.12	0.027	0.0033	0.0028
45	B-17	A12	10	3.8	0.62	0.21	0.28	1.0	0.069	0.14	0.030	0.0033	0.0026
46	B-17	Btca	19	2.9	0.48	0.17	0.48	1.8	0.047	0.096	0.022	0.0025	0.0017
47	B-17	2C1csca	40	1.6	0.21	0.082	0.41	5.3	0.034	0.043	0.0089	0.0011	0.0007
48	B-17	2C2csca	89	4.2	0.54	0.29	2.6	7.3	0.061	0.13	0.032	0.0064	0.0021
49	B-17	2C3cs	179	10.	1.5	0.64	3.6	11.	0.17	0.32	0.081	0.014	0.0063
50	B-17	2C4cs	249	7.1	0.96	0.39	2.3	7.5	0.11	0.21	0.050	0.0082	0.0049
				Fan 6, 505 ka									
51	B-3	A	4	--	--	--	--	--	--	--	--	--	--
52	B-3	Btca	24	--	--	--	--	--	--	--	--	--	--
53	B-3	C1csca	42	--	--	--	--	--	--	--	--	--	--
54	B-3	2C2cs	62	--	--	--	--	--	--	--	--	--	--
55	B-3	2C3cs	+67	--	--	--	--	--	--	--	--	--	--
56	B-18A	A11	2	1.3	0.17	0.066	0.079	0.32	0.021	0.039	0.0092	0.0017	0.0010
57	B-18A	A12	5	1.9	0.28	0.11	0.14	0.59	0.030	0.058	0.015	0.0026	0.0015
58	B-18A	Btca	10	--	--	--	--	--	--	--	--	--	--
59	B-18A	2C1csca	37	--	--	--	--	--	--	--	--	--	--
60	B-18A	2C2cs	46	--	--	--	--	--	--	--	--	--	--
61	B-18A	2C3cs	+86	--	--	--	--	--	--	--	--	--	--
62	B-18B	A	6	3.3	0.48	0.18	0.23	0.94	0.55	0.10	0.025	0.0045	0.0026
63	B-18B	Btca	22	8.5	1.3	0.49	0.59	1.7	0.13	0.24	0.064	0.0096	0.0059
64	B-18B	2C1csca	51	7.0	0.85	0.37	0.95	6.9	0.11	0.18	0.050	0.0091	0.0056
65	B-18B	2C2cs	75	8.2	1.4	0.53	2.5	7.5	0.16	0.27	0.059	0.0085	0.0042
66	B-18B	2C3cs	130	14.	1.6	1.4	2.9	9.9	0.23	0.37	0.088	0.085	0.0084
67	B-18B	2C4cs	+255	32.	3.8	2.0	4.1	16.	0.51	0.95	0.21	0.074	0.020
				Fan 7, 585 ka									
68	B-4	A	6	--	--	--	--	--	--	--	--	--	--
69	B-4	B21tcacs	12	--	--	--	--	--	--	--	--	--	--
70	B-4	B22tcsca	30	--	--	--	--	--	--	--	--	--	--
71	B-4	2C1csca	55	--	--	--	--	--	--	--	--	--	--
72	B-4	2C2cs	+75	--	--	--	--	--	--	--	--	--	--
73	B-19	A	6	3.7	0.54	0.22	0.20	0.68	0.053	0.11	0.028	0.0068	0.0028
74	B-19	B21tca	14	2.3	0.34	0.17	0.13	0.65	0.026	0.065	0.017	0.0068	0.0013
75	B-19	B22tcsca	25	1.2	0.10	0.041	0.059	0.46	0.0091	0.021	0.0056	0.0013	0.0007
76	B-19	2C1csca	40	2.6	0.34	0.15	0.53	3.1	0.033	0.061	0.017	0.0084	0.0014
77	B-19	2C2cs	85	11.	1.5	0.69	1.5	6.5	0.12	0.28	0.078	0.027	0.0061
78	B-19	2C3cs	137	17.	2.1	1.1	2.1	6.7	0.20	0.45	0.11	0.047	0.010
79	B-19	3C4cs	262	23.	3.0	1.7	1.9	9.5	0.28	0.70	0.17	0.089	0.013

GPO 785-048/48023


U.S. DEPARTMENT OF THE INTERIOR
March 3, 1849